MPI in event generators

Klaus Werner

The term “Multiple Parton Interactions” applies to several quite different phenomena.

A recent book titled “Multiple Parton Interactions at the LHC“ (World Scientific, Dec 2018) contains actually two chapters:

- □ Hard MPI: The Double Parton Scattering (DPS),
- □ Soft MPI: Phenomenology and Description in MC Generators.

The second one will be discussed in this lecture, essentially Multiple scattering (understand high multiplicity pp phenomena)

Contents

1 Introduction

Before 2010:

Proton-proton scattering:

elementary, understood in terms of pQCD

Heavy ion collisions:

Collective effects, formation of a (flowing) quark-gluon-plasma, macroscopic description

Since 2010: Incredibly interesting and unexpected pp and pPb results at the LHC (collective effect also in pp?)

Collective effects means

- **Primary interactions at t = 0**
  Crucial : Multiple scattering

- **Secondary interactions**
  formation of “matter” which expands collectively, like a fluid

1.1 Example: space-time evolution in pp

In the following:

An example of a EPOS simulation

of expanding matter in pp scattering

pp @ 7TeV EPOS 3.119

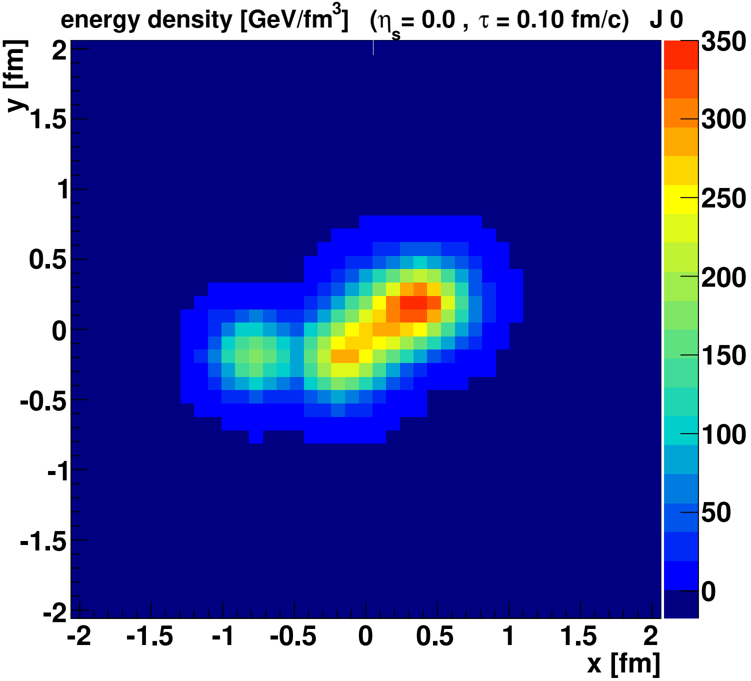

pp @ 7TeV EPOS 3.119

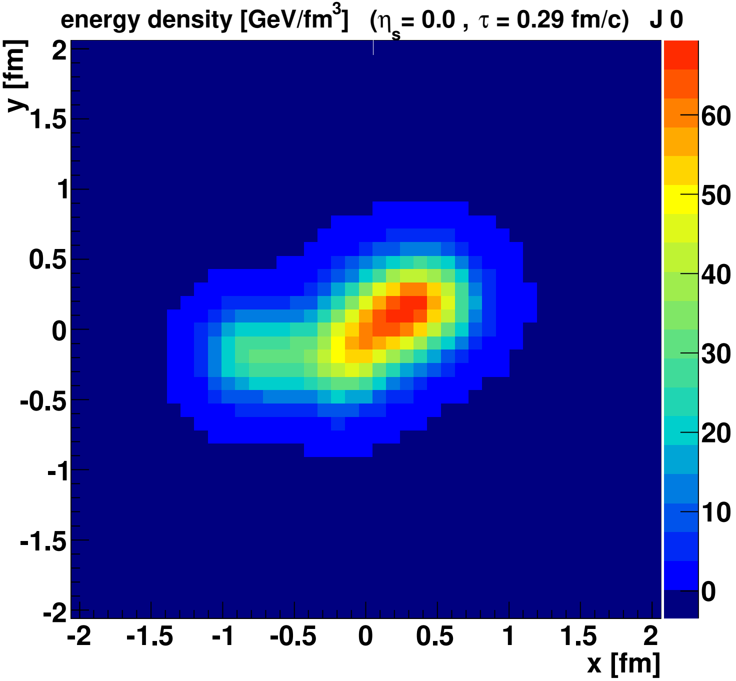

pp @ 7TeV EPOS 3.119

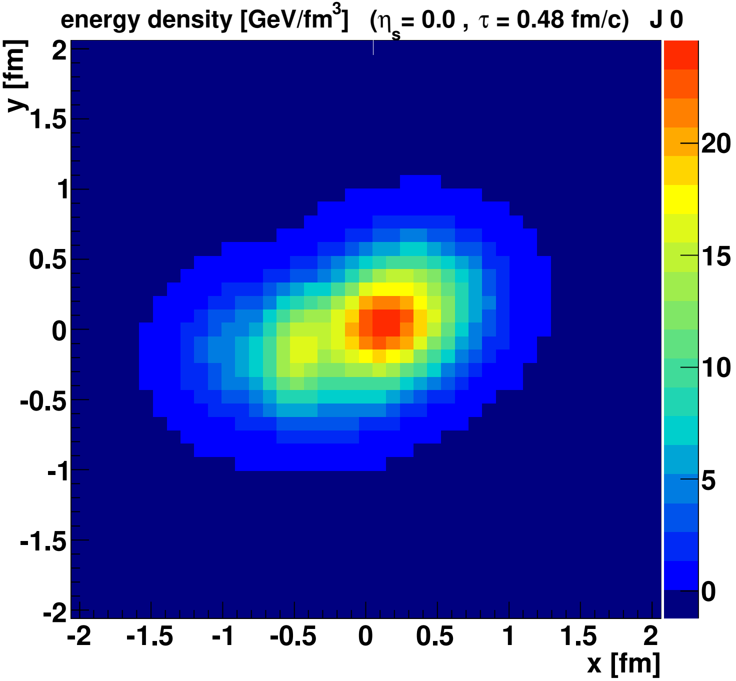

pp @ 7TeV EPOS 3.119

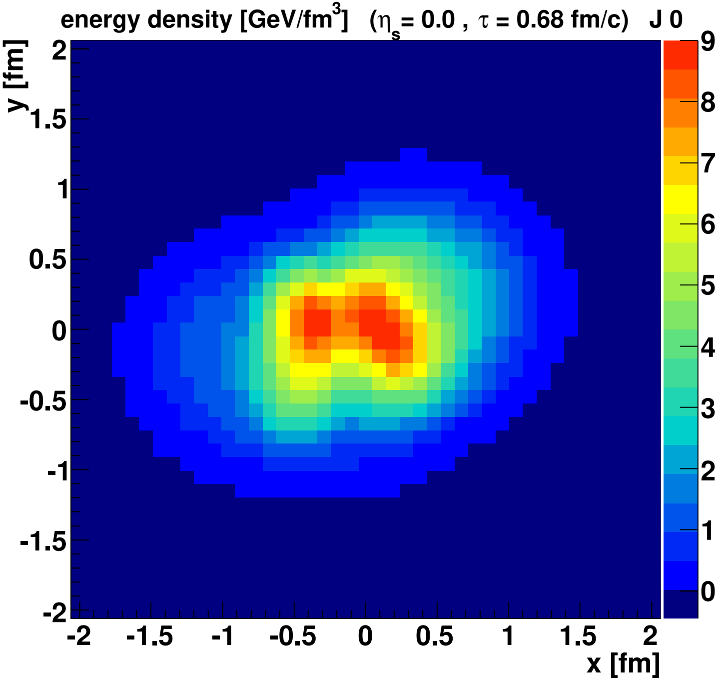

pp @ 7TeV EPOS 3.119

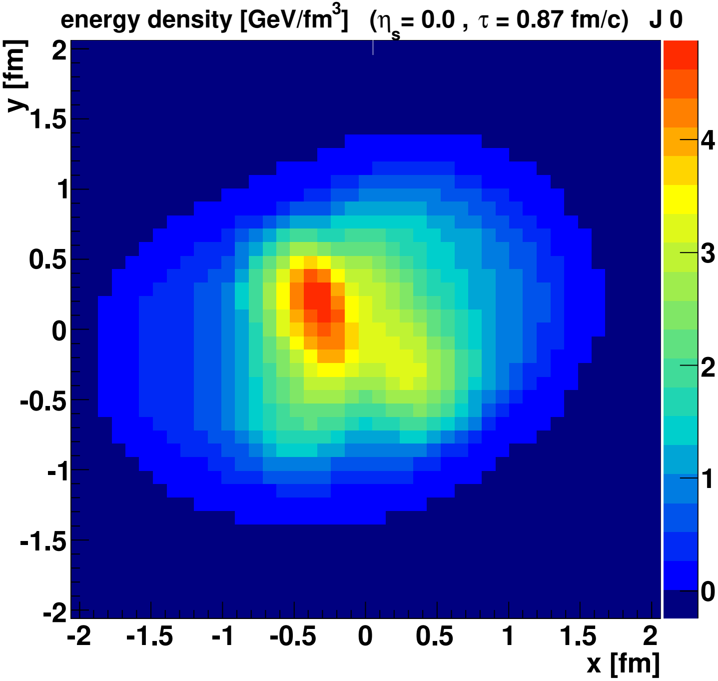

pp @ 7TeV EPOS 3.119

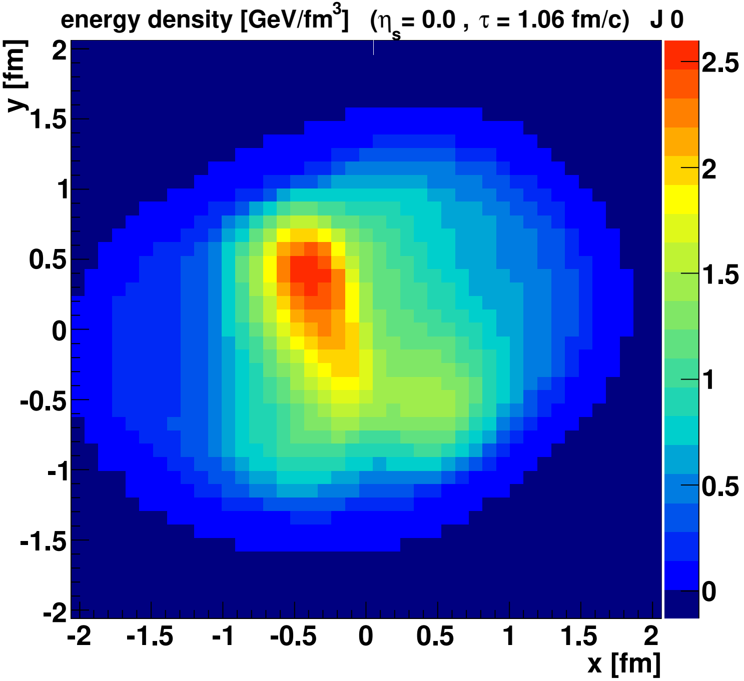

pp @ 7TeV EPOS 3.119

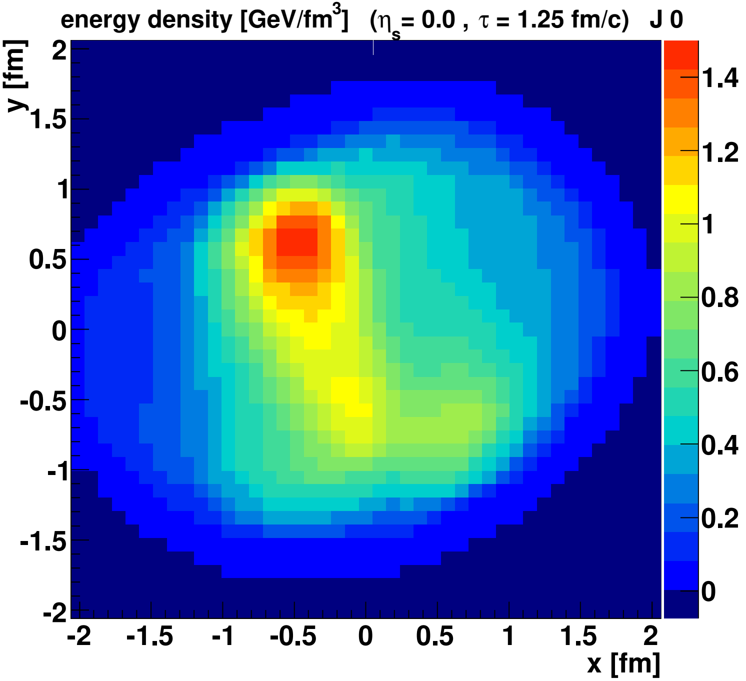

pp @ 7TeV EPOS 3.119

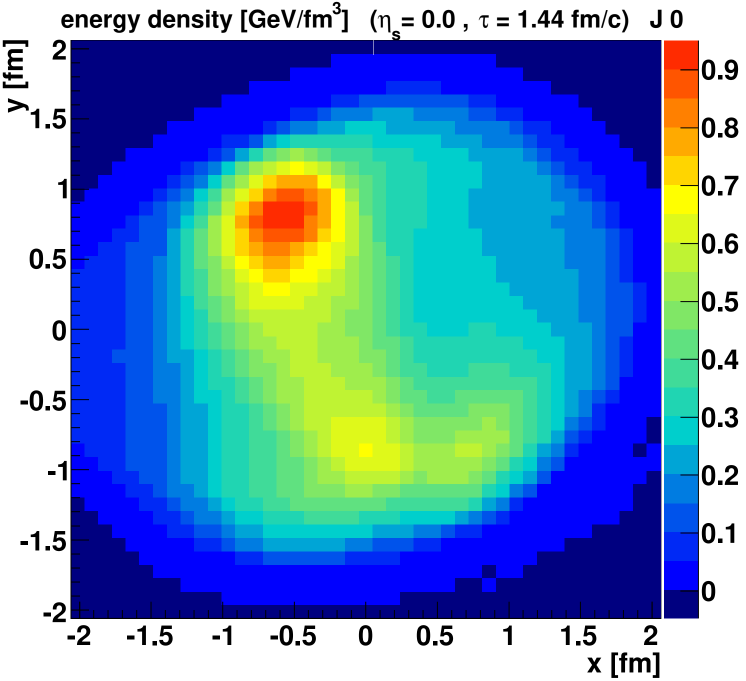

pp @ 7TeV EPOS 3.119

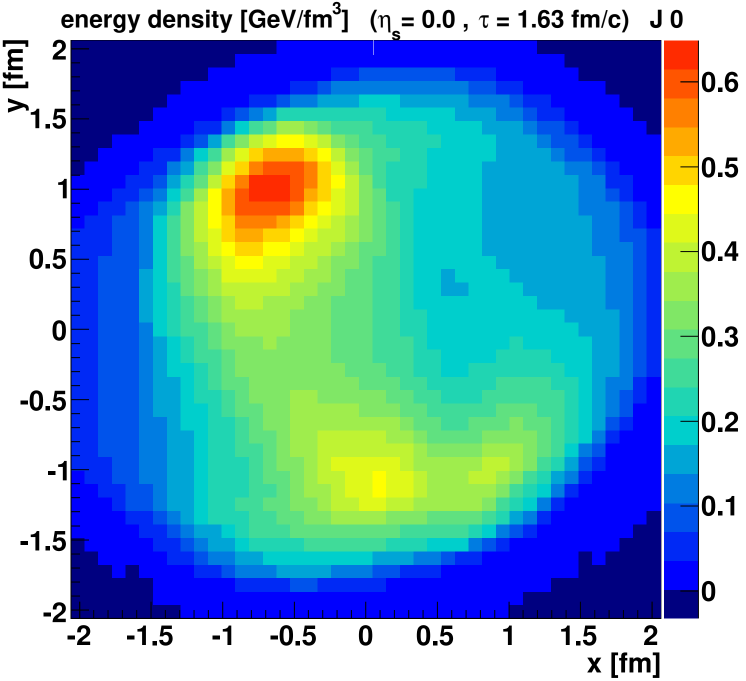

pp @ 7TeV EPOS 3.119

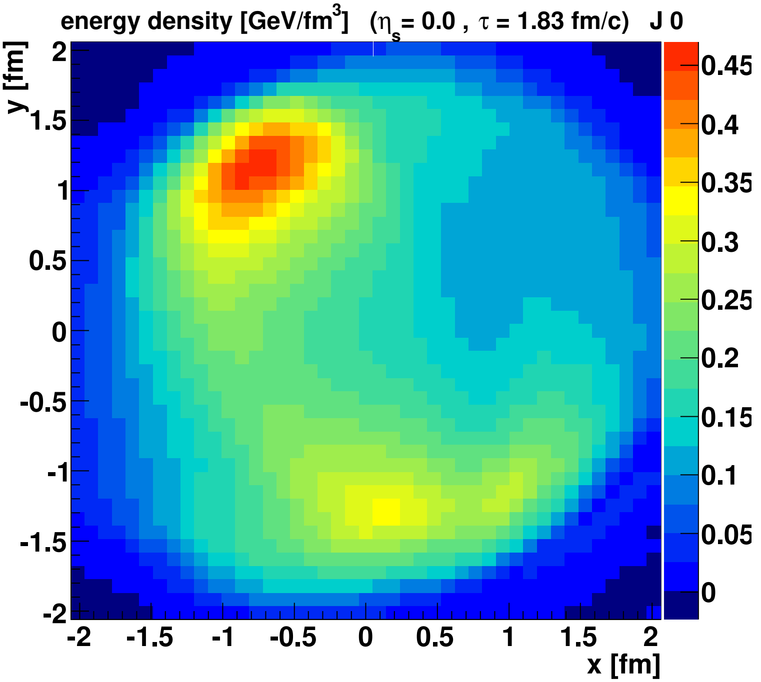

pp @ 7TeV EPOS 3.119

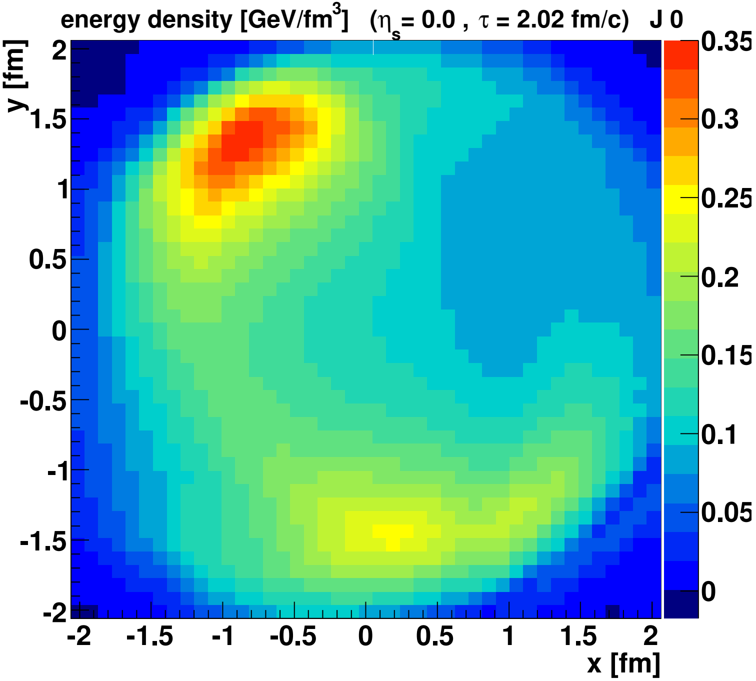

pp @ 7TeV EPOS 3.119

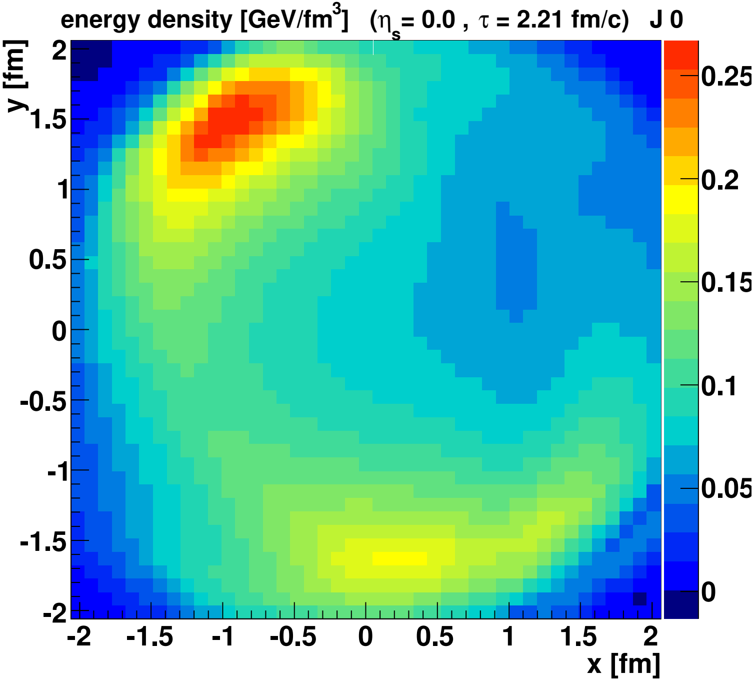

pp @ 7TeV EPOS 3.119

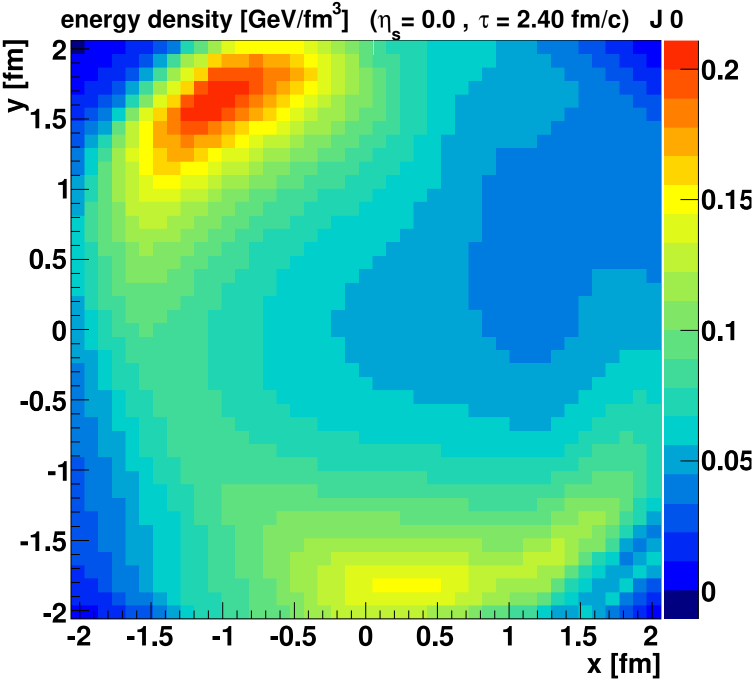

pp @ 7TeV EPOS 3.119

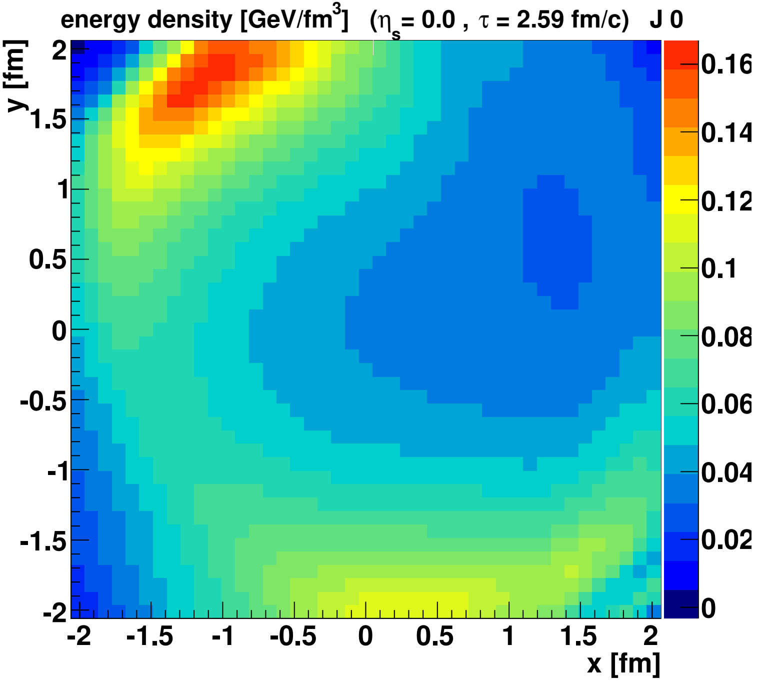

1.2 Radial flow visible in particle distributions

Particle spectra affected by radial flow

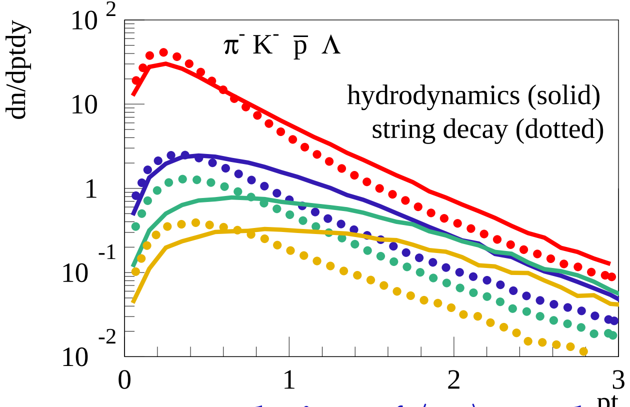

=> mass ordering of $\langle p_t \rangle$, lambda/K increase

pPb at 5TeV

CMS, arXiv:1307.3442

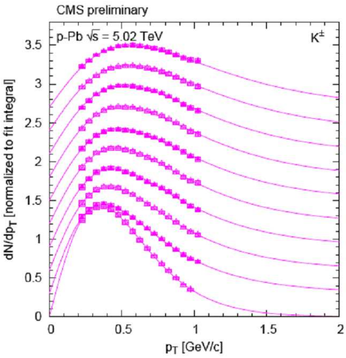

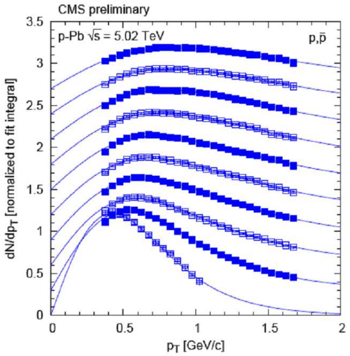

Strong variation of shape with multiplicity

for kaon and even more for proton pt spectra

(flow like)

Λ / K_s versus pT (high compared to low multiplicity) in pPb (left) similar to PbPb (right)

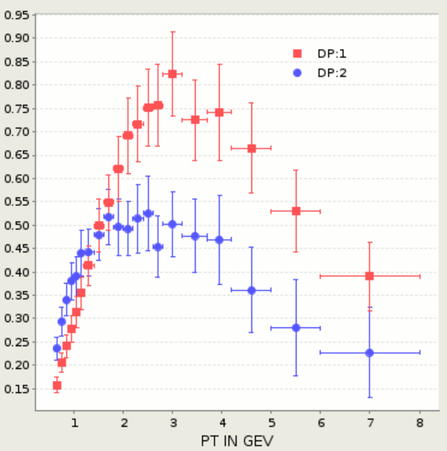

ALICE (**2013**) arXiv:1307.6796

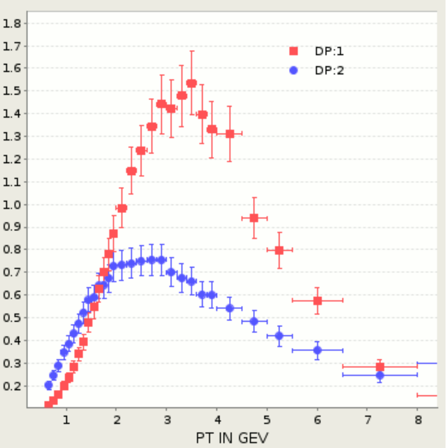

ALICE (**2013**) arXiv:1307.5530
Phys. Rev. Lett. 111, 222301 (2013)

In AA: partially due to flow

1.3 Ridges & flow harmonics

Ridges appear in

$$R = \frac{1}{N_{\text{trigg}}} \frac{dn}{d\Delta\phi\Delta\eta}$$

due to initial azimuthal anisotropies

(longitudinally invariant)

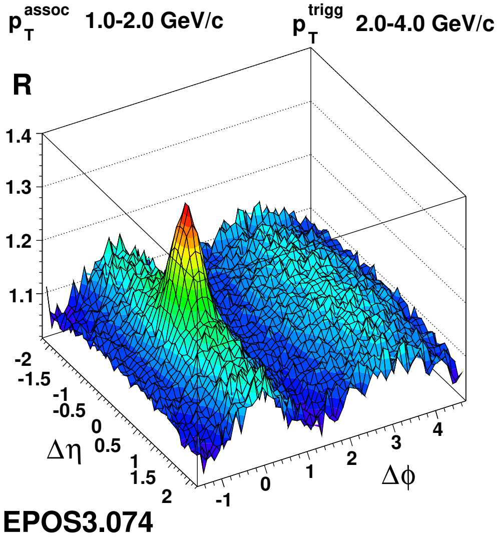

Initial "elliptical" matter distribution:

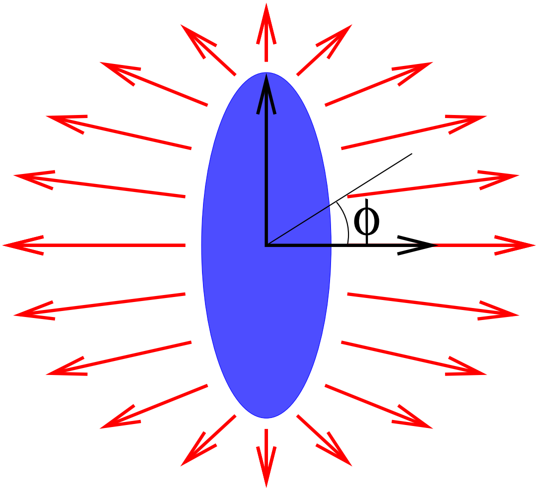

Preferred expansion
along $\phi = 0$
and $\phi = \pi$

η_s-invariance
same form at any η_s
$\eta_s = \frac{1}{2}\ln\frac{t+z}{t-z}$

Particle distribution:
Preferred directions
$\phi = 0$ and $\phi = \pi$

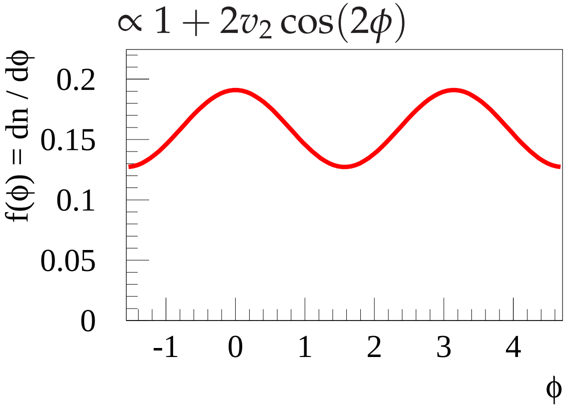

Dihadrons:
preferred $\Delta\phi = 0$ and $\Delta\phi = \pi$ (even for big $\Delta\eta$)

Initial "triangular" matter distribution:

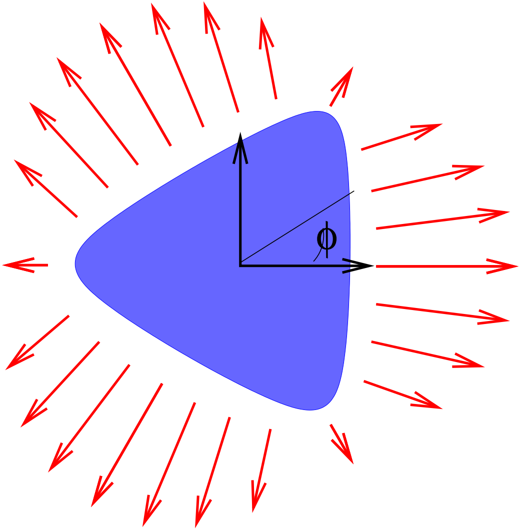

Preferred expansion along $\phi = 0$, $\phi = \frac{2}{3}\pi$, and $\phi = \frac{4}{3}\pi$

η_s-invariance

Particle distribution: Preferred directions $\phi = 0$, $\phi = \frac{2}{3}\pi$, and $\phi = \frac{4}{3}\pi$

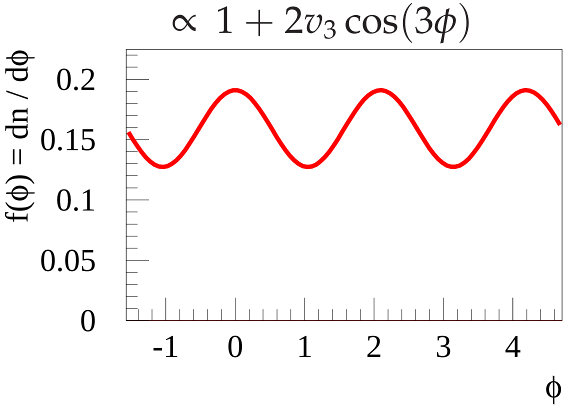

Dihadrons:
preferred $\Delta\phi = 0$, and $\Delta\phi = \frac{2}{3}\pi$, and $\Delta\phi = \frac{4}{3}\pi$
(even for large $\Delta\eta$)

In general, superposition of several eccentricities ε_n,

$$\varepsilon_n e^{in\psi_n^{PP}} = -\frac{\int dxdy\, r^2 e^{in\phi} e(x,y)}{\int dxdy\, r^2 e(x,y)}$$

Particle distribution characterized by harmonic flow coefficients

$$v_n e^{in\psi_n^{EP}} = \int d\phi\, e^{in\phi} f(\phi)$$

At $\phi = 0$:
The **ridge**

(extended in η)

Awayside peak may originate from jets, not the ridge (for large $\Delta\eta$)

Here, v_2 and v_3 non-zero
$\propto 1 + 2v_2 \cos(2\phi) + 2v_3 \cos(3\phi)$

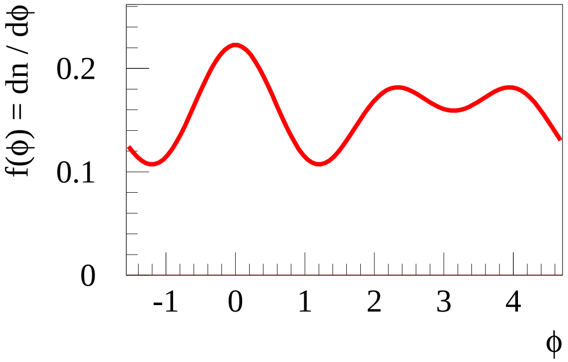

CMS: Ridges (in dihadron correlation functions) also seen in pp (left) and pPb (right)

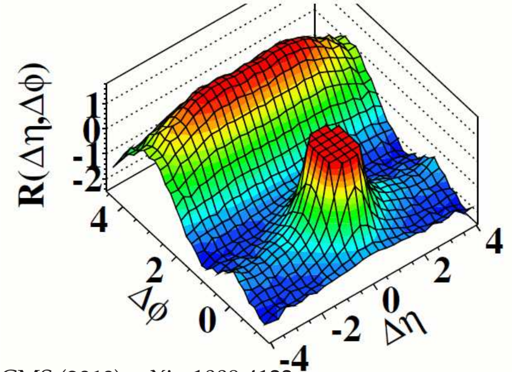

CMS (**2010**) arXiv:1009.4122
JHEP 1009:091,2010

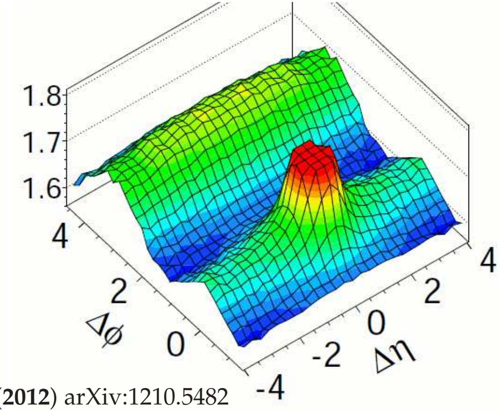

CMS (**2012**) arXiv:1210.5482
Phys. Lett. B 718 (2013) 795

Looks like flow !

1.4 Flow harmonics, identified particles

Flow shifts particles to higher p_t

Effect increases with mass

Also true for v_2 vs p_t

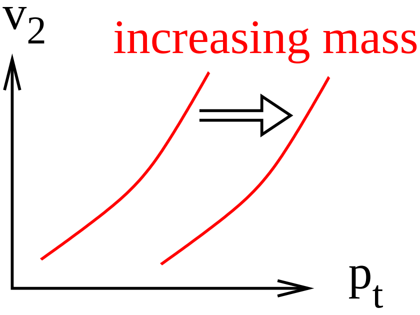

ALICE: v2 versus pT: mass splitting (π, K, p) in pPb (left) similar to PbPb (right)

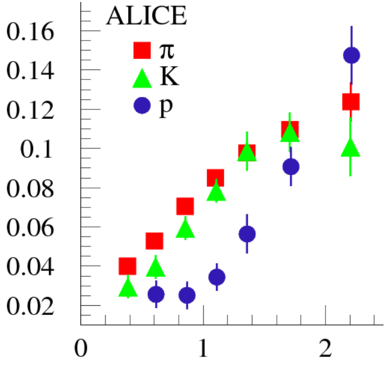

ALICE (**2013**) arXiv:1307.3237

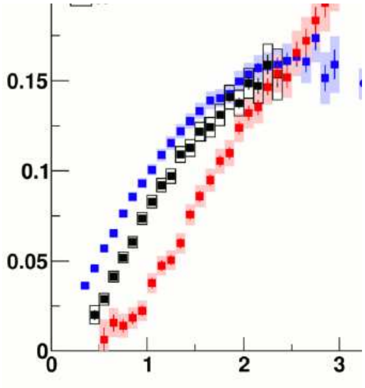

ALICE (**2012**) F. Noferini QM2012

Typical flow result!

So : “Flow-like phenomena” are also seen in pp and pA, therefore:

Heavy ion approach

= primary (multiple) scattering
+ subsequent fluid evolution

becomes interesting for pp and pA

2 Multiple scattering: Theory

concerning primary interactions

providing initial conditions
for secondary interactions

2.1 Poles and branch cuts

Even functions $f(x)$ of a **real variable** x
may need to be **continued into the complex plane,**
to understand their properties.

Example
$$f(x) = \sum_{n=0}^{\infty} a_n x^n = \sum_{n=0}^{\infty} \left(\frac{x}{2i}\right)^n .$$

The radius of convergence is

$$\rho = \lim_{n\to\infty} |a_n|^{-1/n} = 2$$

Which is obvious, since f considered as function of a complex variable z, writes

$$f(z) = \frac{1}{1 - z/(2i)}$$

having a **pole** at $z = 2i$,

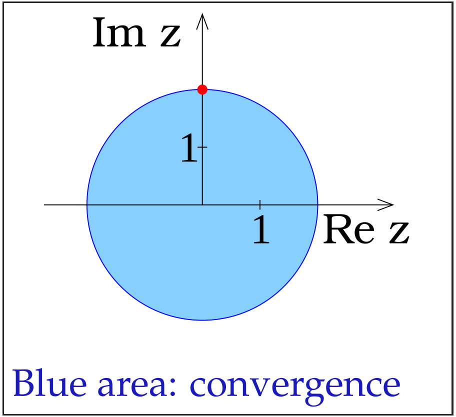

whereas $f(x)$ has no singularity (for $x \in \mathbb{R}$)

Branch cuts

An example: The logarithm.

The exponential function defines a mapping M

$$M: \quad \begin{array}{l} \mathbb{C} \to \mathbb{C} \\ w \to z \quad = \exp(w) \end{array}$$

which is well defined in the whole complex plane.

Consider $w = x + iy$, with x fixed and y going from $-\pi$ to π.

(Trajectory γ going from $w_1 = x - i\pi$ to $w_2 = x + i\pi$)

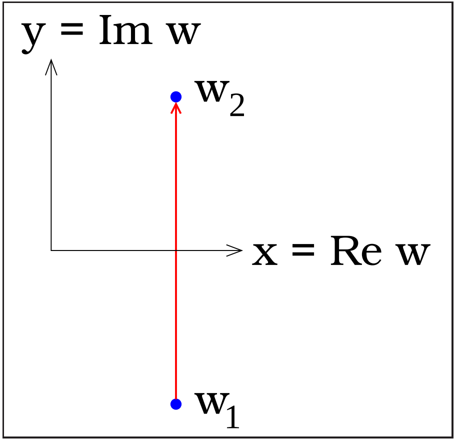

The mapped trajectory $\gamma' = M(\gamma)$ is given as

$$z = \exp(w) = \exp(x)\exp(iy)$$

=> A circle with start and end point $z_1 = z_2 = -e^x$

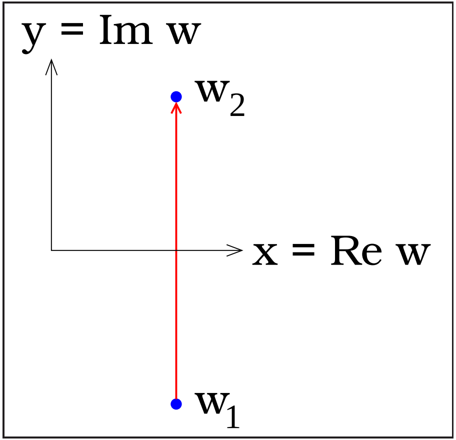

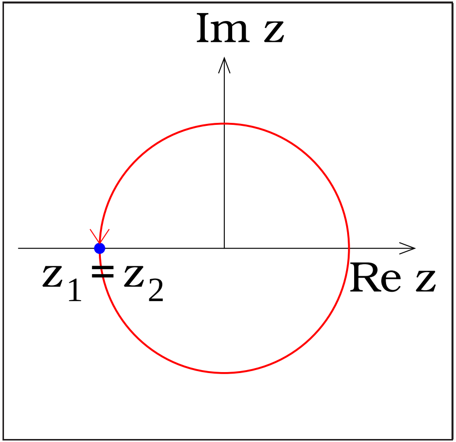

Doing the inverse mapping

$$M^{-1}:\ z \to w = \log(z),$$

we get for $z_1 = z_2$ two different values w_1 and w_2 !!

One has to define **log** in $\mathbb{C} - \mathbb{R}_{\leq \mathbf{0}}$ (branch).
The negative real axis is called branch cut.

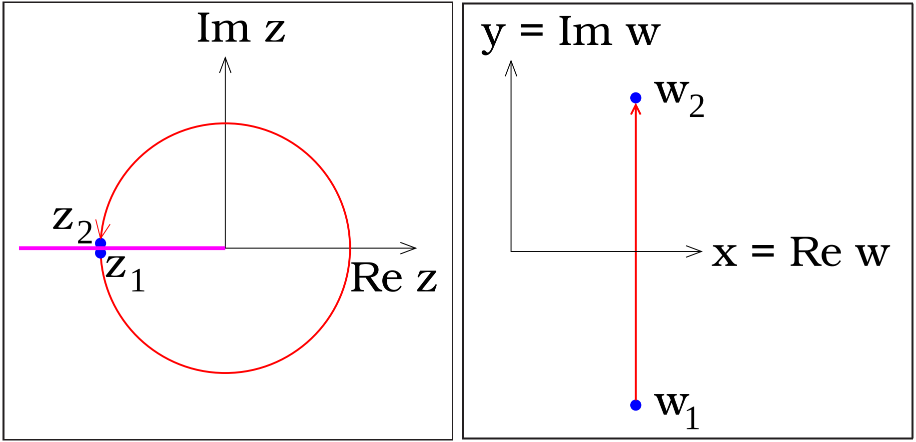

The discontinuity at $z = -e^x$:

$$\log(z + i\epsilon) - \log(z - i\epsilon) = 2\pi i$$

2.2 Cut diagrams

The scattering operator $\hat{S}$ is defined via

$$|\psi(t=+\infty)\rangle = \hat{S}\,|\psi(t=-\infty)\rangle$$

Unitarity relation $\hat{S}^{\dagger}\hat{S} = 1$ gives (considering a discrete Hilbert space)

$$\begin{aligned} 1 &= \langle i|\,\hat{S}^{\dagger}\hat{S}\,|i\rangle \\ &= \sum_f \langle i|\,\hat{S}^{\dagger}\,|f\rangle\,\langle f|\,\hat{S}\,|i\rangle \\ &= \sum_f \langle f|\,\hat{S}\,|i\rangle^{*}\,\langle f|\,\hat{S}\,|i\rangle \end{aligned}$$

Expressed in terms of the S-matrix:

$$1 = \sum_f S_{fi}^* S_{fi}$$

Using $$S_{fi} = \delta_{fi} + i(2\pi)^4 \delta(p_f - p_i) T_{fi}$$

dividing by $i(2\pi)^4\delta(0)$:

$$\begin{aligned} \frac{1}{i}\left(T_{ii} - T_{ii}^*\right) &= \sum_f (2\pi)^4 \delta(p_f - p_i) \left|T_{fi}\right|^2 \\ &= 2s\,\sigma_{\mathrm{tot}} \quad \text{for } s \to \infty \end{aligned}$$

(see next page)

Be ϕ le current of incoming particles hitting a target of surface A containing N particles. The transsition rate τ is

$$\tau = \phi A \,\frac{\sigma N}{A} = \phi\,\sigma\,N,$$

The cross section is
$$\sigma = \frac{\tau}{N\phi} = \frac{\tau}{V\,\phi\,\rho} = \frac{W}{TV\,\phi\,\rho} \equiv \frac{W}{TV\,w}.$$

The transition probability $W = |S_{fi}|^2$ is

$$\left((2\pi)^4\delta^4(p_f - p_i)\right)^2 |T_{fi}|^2 = TV\,(2\pi)^4\delta^4(p_f - p_i)|T_{fi}|^2.$$

The cross section is then
$$\sigma = \frac{1}{w}|T_{fi}|^2\,(2\pi)^4\delta^4(p_f - p_i).$$

with $w = 2E_1 v_1 2E_2$. We need a covariant form of $f = E_1 v_1 E_2$. In the lab frame, we have $f^2 = |\vec{p}_1|^2 m_2^2 = (E_1^2 - m_1^2)m_2^2$, which gives the invariant form $f = \sqrt{(p_1 p_2)^2 - m_1^2 m_2^2}$. With $2p_1 p_2 = s - m_1^2 - m_2^2$, we get $2f = \sqrt{(s - m_1^2 - m_2^2)^2 - 4m_1^2 m_2^2}$, and thus

$$w = 4f = 2\sqrt{\left(s - (m_1 + m_2)^2\right)\left(s - (m_1 - m_2)^2\right)} \to 2s \text{ for } s \to \infty$$

Using

$$\frac{1}{i}\left(T_{ii}-T_{ii}^{*}\right)=2\mathrm{Im}T_{ii}\,,$$

we get the optical theorem

$$2\mathrm{Im}T_{ii} \;=\; \sum_{f}(2\pi)^{4}\delta(p_{f}-p_{i})\left|T_{fi}\right|^{2}=2s\,\sigma_{\mathrm{tot}}$$

Assume:

- □ T_{ii} is Lorentz invariant $\rightarrow$ use s, t
- □ $T_{ii}(s,t)$ is an analytic function of s, with s considered as a complex variable
  (Hermitean analyticity)
- □ $T_{ii}(s,t)$ is real on some part of the real axis

Using the Schwarz reflection principle, $T_{ii}(s,t)$ first defined for $\mathrm{Im}s \geq 0$ can be continued in a unique fashion via $T_{ii}(s^*,t) = T_{ii}(s,t)^*$.

So:

$$\frac{1}{i}\left(T_{ii}(s,t) - T_{ii}(s,t)^*\right) = \frac{1}{i}\left(T_{ii}(s,t) - T_{ii}(s^*,t)\right)$$

Def:

$$\operatorname{disc} T = T_{ii}(s+i\epsilon,t) - T_{ii}(s-i\epsilon,t)$$

We have finally

$$\frac{1}{\mathrm{i}}\mathrm{disc}\, T \;=\; (2\pi)^4\delta(p_f - p_i)\sum_f \left|T_{fi}\right|^2 = 2s\,\sigma_{\mathrm{tot}}$$

Interpretation: $\frac{1}{\mathrm{i}}\mathrm{disc}\, T$ can be seen as a so-called "cut diagram", with modified Feynman rules, the "intermediate particles" are on mass shell.

Modified Feynman rules :

- Draw a dashed line from top to bottom

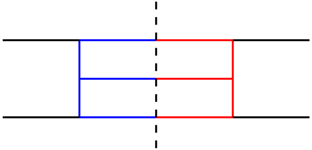

- Use “normal” Feynman rules to the left
- Use the complex conjugate expressions to the right
- For lines crossing the cut: Replace propagators by mass shell conditions $2\pi\theta(p^0)\delta(p^2 - m^2)$

Cutting a diagram representing **elastic** scattering

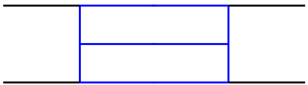

corresponds to **inelastic** scattering

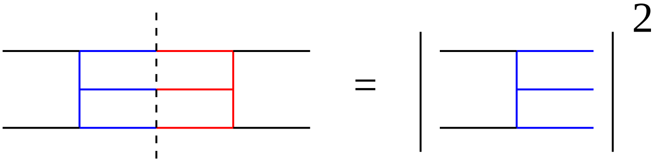

Cutting diagrams is useful in case of substructures:

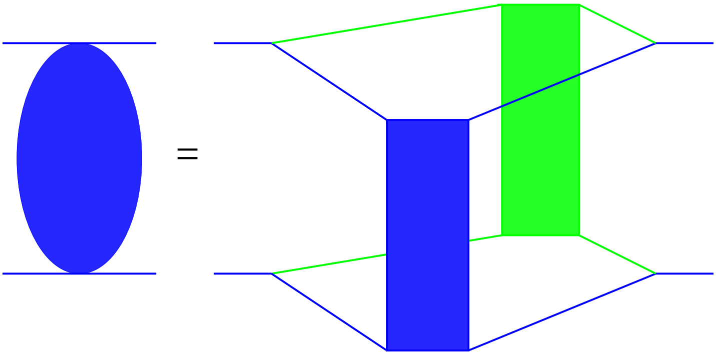

Precisely the multiple scattering structure in EPOS

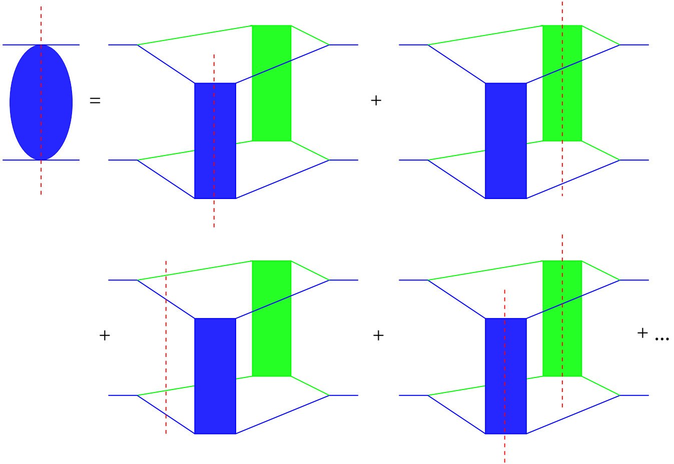

Cut diagram

= sum of products of cut/uncut subdiagrams

=> Gribov-Regge approach of multiple scattering

2.3 Parton evolution

A fast moving proton

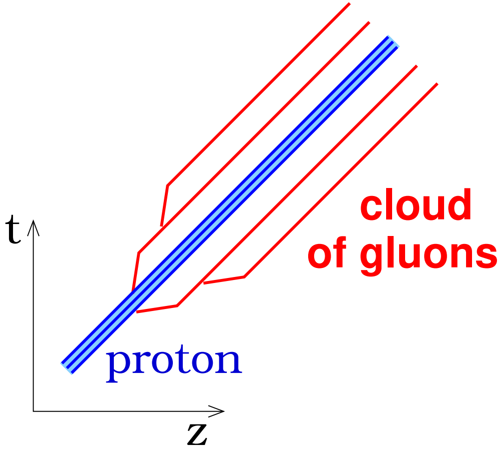

emits successively partons (mainly gluons), quasi-real (large gamma factors)

... which can be probed by a virtual photon
(emitted from an electron)

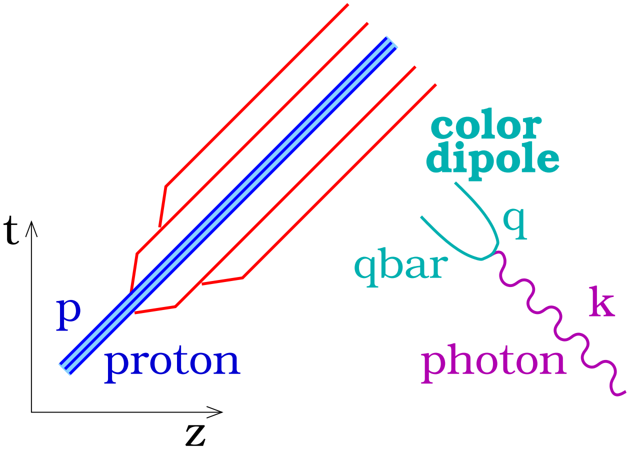

photon splits into q-qbar

→ Color dipole

p and *k* are proton and photon momentum

What precisely the photon “sees” depends on two kinematic variables,

the **virtuality**

$$Q^2 = -k^2$$

and the **Bjorken variable**

$$x = \frac{Q^2}{2pk}$$

which probes partons with momentum fraction x.
It determines also the **approximation scheme** to compute the parton cloud.

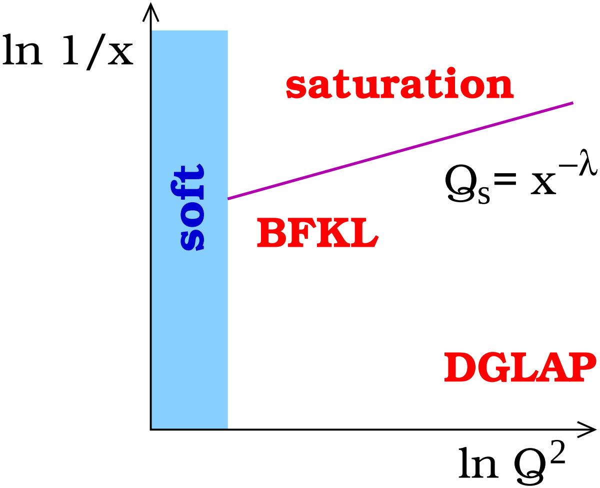

DGLAP: summing to all orders of $\alpha_s \ln Q^2$

BFKL: summing to all orders of $\alpha_s \ln \frac{1}{x}$

Linear equations

BFKL (Balitsky, Fadin, Kuraev, and Lipatov):

$$\frac{\partial\varphi(x,\boldsymbol{q})}{\partial\ln\frac{1}{x}}\;\frac{\alpha_s N_c}{\pi^2}\int d^2k\,K(\boldsymbol{q},\boldsymbol{k})\,\varphi(x,\boldsymbol{k})$$

$$\text{with } xg(x,Q^2)=\int_0^{Q^2}\frac{d^2k}{k^2}\varphi(x,\boldsymbol{k}),$$

DGLAP (Dokshitzer, Gribov, Lipatov, Altarelli and Parisi):

$$\frac{\partial g(x,Q^2)}{\partial\ln q^2}=\int_x^1\frac{dz}{z}\,\frac{\alpha_s}{2\pi}P(z)\,g\!\left(\frac{x}{z},Q^2\right)$$

Very large $\ln 1/x$: Saturation domain

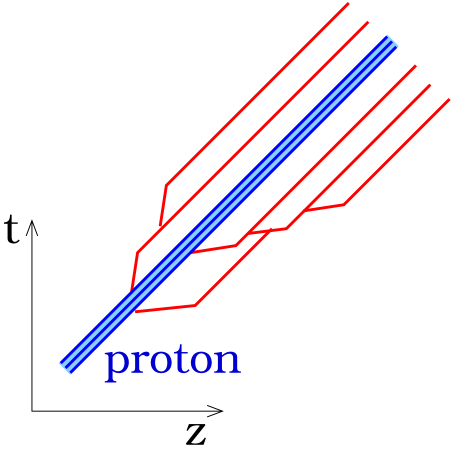

Non-linear effects

Gluon from one cascade is absorbed by another one

2.4 pp scattering (linear domain)

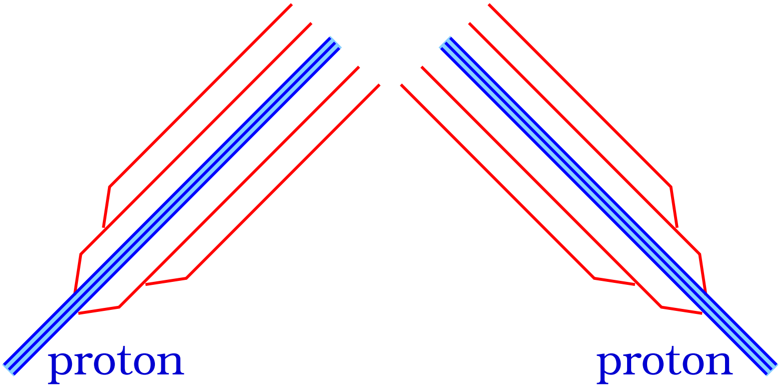

Same evolution as in proton-photon (causality)

Different way of plotting the same reaction

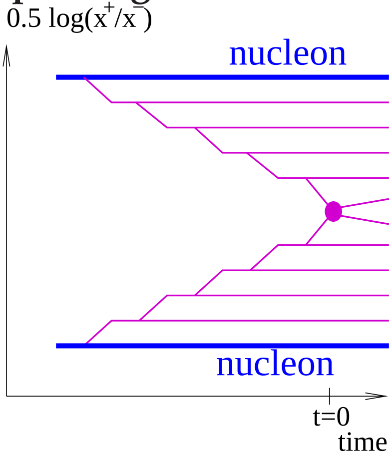

inelastic scattering diagram

Corresponding cut diagram

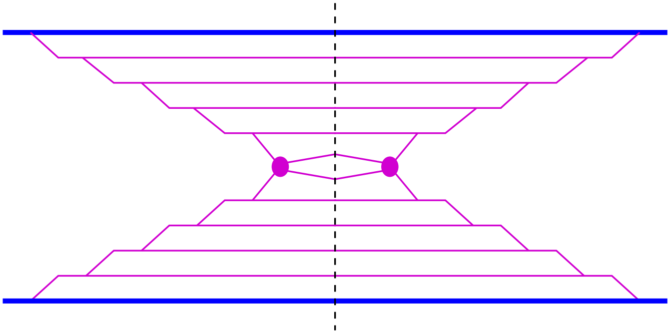

referred to as “cut parton ladder”
= amplitude squared of the inelastic diagram

Corresponding elastic diagram

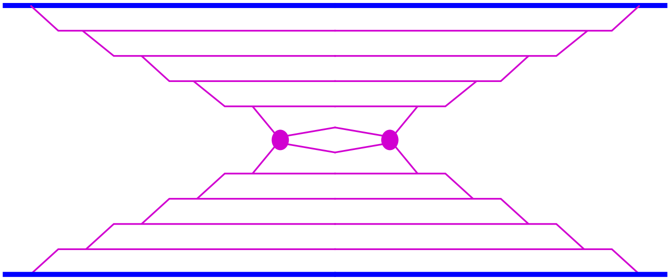

referred to as “(uncut) parton ladder”

2.5 Soft domain

Very small $\ln Q^2$: No perturbative treatment!

But one may use again the hypothesis of **Lorentz invariance** and **analyticity** of the T-matrix. One starts with a partial wave expansion of the T-matrix (Watson-Sommerfeld transform) :

$$T(t,s) = \sum_{j=0}^{\infty}(2j+1)\mathcal{T}(j,s)P_j(z)$$

with $t \propto z-1$, $z = \cos\vartheta$, P_j: Legendre polynomials.

With $\alpha(s)$ being the right-most pole of $\mathcal{T}(j,s)$ one gets for $t \to \infty$:

$$T(t,s) \propto t^{\alpha(s)}$$

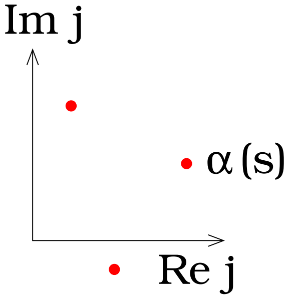

and assuming crossing symmetry one gets the famous asymptotic result

$$T(s,t) \propto s^{\alpha(t)}$$

with the "Regge pole"

$$\alpha(t) = \alpha(0) + \alpha' t$$

Perturbative:
Parton ladder

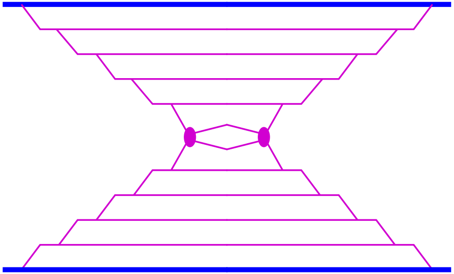

T-matrix computed
(DGLAP)

Soft:
Soft Pomeron

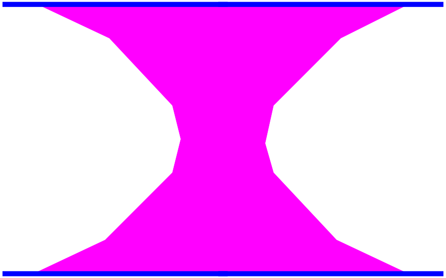

gluon fields

T-matrix parametrized

Formulas (see Phys.Rept. 350 (2001) 93-289):

$$T_{\mathrm{soft}}(\hat{s},t) \;=\; 8\pi s_0\, i\, \gamma^2_{\mathrm{Pom-parton}} \left(\frac{\hat{s}}{s_0}\right)^{\alpha_{\mathrm{soft}}(0)} \times \exp(\lambda_{\mathrm{soft}}\, t)\,,$$

with

$$\lambda_{\mathrm{soft}} = 2R^2_{\mathrm{Pom-parton}} + \alpha'_{\mathrm{soft}} \ln\frac{\hat{s}}{s_0}.$$

Cut soft Pomeron (Schwarz reflection principle):

$$\frac{1}{i}\mathrm{disc}\, T_{\mathrm{soft}}(\hat{s},t)$$

$$= \frac{1}{i}\left[T_{\mathrm{soft}}(\hat{s}+i0,t) - T_{\mathrm{soft}}(\hat{s}-i0,t)\right]$$

$$= 2\mathrm{Im}\, T_{\mathrm{soft}}(\hat{s},t)$$

Interaction cross section,

$$\sigma_{\mathrm{soft}}(\hat{s}) = \frac{1}{2\hat{s}} 2\mathrm{Im}\, T_{\mathrm{soft}}(\hat{s}, 0)\,,$$

$$= 8\pi\gamma_{\mathrm{part}}^{2} \left(\frac{\hat{s}}{s_0}\right)^{\alpha_{\mathrm{soft}}(0)-1}\,,$$

using the optical theorem (with $t = 0$),

which grows faster than data

2.6 Semihard Pomeron

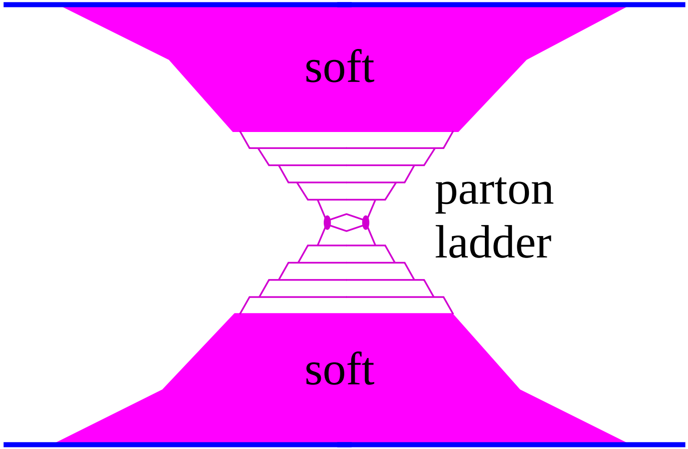

Space-time picture of semihard Pomeron

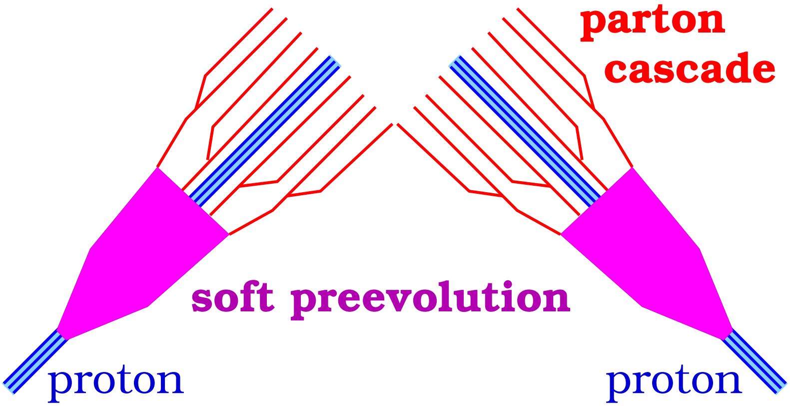

Hard cross section and amplitude (see Phys.Rept. 350 (2001) 93-289):

$$\sigma^{jk}_{\mathrm{hard}}(\hat{s},Q_0^2) = \frac{1}{2\hat{s}} 2\mathrm{Im}\, T^{jk}_{\mathrm{hard}}(\hat{s},t=0)$$

$$= K \sum_{ml} \int dx_B^+ dx_B^- dp_\perp^2 \frac{d\sigma^{ml}_{\mathrm{Born}}}{dp_\perp^2}(x_B^+ x_B^- \hat{s}, p_\perp^2)$$

$$\times E^{jm}_{\mathrm{QCD}}(x_B^+, Q_0^2, M_F^2)\, E^{kl}_{\mathrm{QCD}}(x_B^-, Q_0^2, M_F^2)\theta\left(M_F^2 - Q_0^2\right),$$

One knows (Lipativ, 86): amplitude is imaginary, and nearly independent on t => (with $R^2_{\mathrm{hard}} \simeq 0$) :

$$T^{jk}_{\mathrm{hard}}(\hat{s},t) = i\hat{s}\,\sigma^{jk}_{\mathrm{hard}}(\hat{s},Q_0^2)\ \exp\left(R^2_{\mathrm{hard}}\, t\right)$$

Semihard amplitude :

$$iT_{\mathrm{semihard}}(\hat{s},t) = \sum_{jk} \int_0^1 \frac{dz^+}{z^+}\frac{dz^-}{z^-}$$

$$\times \mathrm{Im}\, T^j_{\mathrm{soft}}\Big(\frac{s_0}{z^+},t\Big)\ \mathrm{Im}\, T^k_{\mathrm{soft}}\Big(\frac{s_0}{z^-},t\Big)\ iT^{jk}_{\mathrm{hard}}(z^+z^-\hat{s},t)$$

(valid for $s \to \infty$ and small parton virtualities except for the ones in the ladder)

2.7 Cross sections

(a) Exclusive : $a + b \longrightarrow c + d$

(b) Total : $a+b \longrightarrow X$ (sum of (a))

(c) Inclusive : $a + b \longrightarrow c + X$ (weighted sum of (a))

There are simple formulas for inclusive cross sections (AGK cancellations), but one needs to go beyond when studying high multiplicity pp.

Consider multiple scattering amplitude

$$iT = \prod iT_{\mathrm{P}}$$

cross section: sum over all cuts.

For each cut Pom:

$$\frac{1}{i}\mathrm{disc}T_{\mathrm{P}} = 2\mathrm{Im}T_{\mathrm{P}} \equiv G$$

For each uncut one:

$$iT_{\mathrm{P}} + \{iT_{\mathrm{P}}\}^* = i\,(i\,\mathrm{Im}T_{\mathrm{P}}) + \{i\,(i\,\mathrm{Im}T_{\mathrm{P}})\}^* = -2\mathrm{Im}T_{\mathrm{P}} \equiv -G$$

Inclusive cross section: weighted sum over all cuts: The multiplicity for k cut Pomerons is kN, if N is the multiplicity per cut Pomeron.

Contribution to the inclusive cross section for n Pomerons:

$$\sigma_{\mathrm{incl}}^{(n)} \propto \sum_{k=0}^{n} kN\, G^k \,(-G)^{n-k} \left(\begin{array}{c} n \\ k \end{array} \right) = 0 \text{ for } n > 1$$

Only n=1 contributes (single Pomeron) !!

AGK cancellations for n>1

simple diagram even in case of multiple scattering

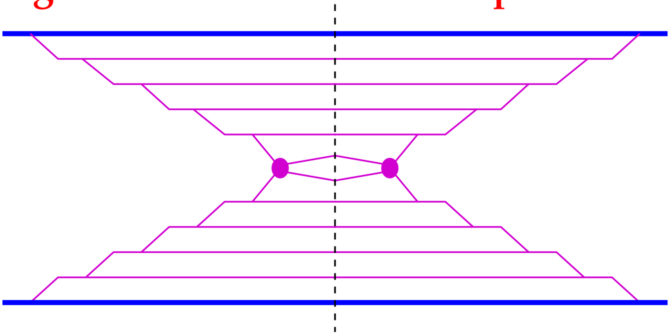

corresponds to factorization:

$$\sigma_{\mathrm{incl}} = F \otimes \sigma_{\mathrm{elem}} \otimes F$$

Kind of obvious that **factorization** should hold for inclusive cross sections, so

$$\sigma_{\mathbf{incl}} = F \otimes \sigma_{\mathbf{elem}} \otimes F$$

may be used as starting point, with F taken from DIS (photon-proton).

3 Multiple scattering: Model overview

with contributions from T. Pierog, S. Ostapchenko, C. Bierlich, F. Riehn, P. Tribedy, A. Fedynitch

Models for min bias and high multiplicity pp

model	Gribov Regge	Dipole	Facto risation	used for CR	authors
QGSJETII	X			X	Ostapchenko
EPOSLHC	X			X	Pierog, Werner
EPOS3	X				Werner, Pierog
DIPSY		X			Lönnblad, Bierlich
IP-Glasma		X			Tribedy, Schenke
SIBYLL			X	X	Engel, Riehn
DPMJETIII			X	X	Engel, Fedynitch
PYTHIA			X		Sjostrand, Skands
HERWIG			X		Marchesini, Webber

Models for high multipl pp, pA, AA

including collective effects

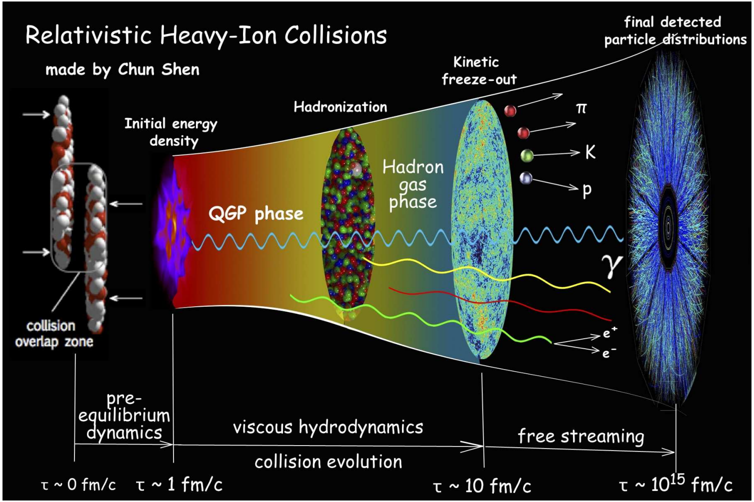

ohttp://u.osu.edu/vishnu/2014/08/06/sketch-of-relativistic-heavy-ion-collisions/

model	primary scatterings	secondary interactions	
EPOS	Gribov Regge	viscous hydrodynamical expansion of QGP	hadronic cascade
IP-Glasma	Dipole model	"	
AMPT	Minijets from Pythia	partonic cascade	"
Plus many hydro models with assumed initial conditions			

Cascade means:

Successive scatterings $a + b \to c + d$ according to known cross sections

3.1 Gribov-Regge multiple scattering approach

EPOS, QGSJETII

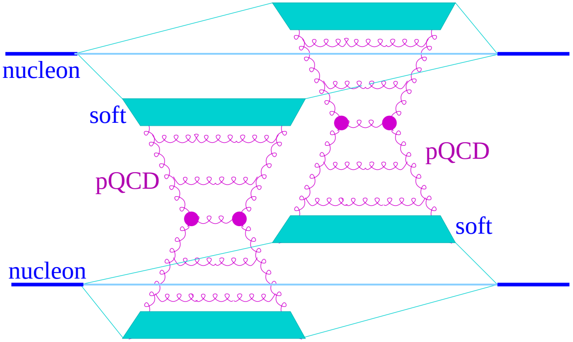

S-Matrix based on Pomerons

Pomerons :
Parton ladders (initial and final state radiation, DGLAP) + soft

Cutting rules to get inelastic cross sections.

Same principle for pp, pA, AA

more details later

Nonlinear effects in QGSJET

Pomeron-Pomeron coupling

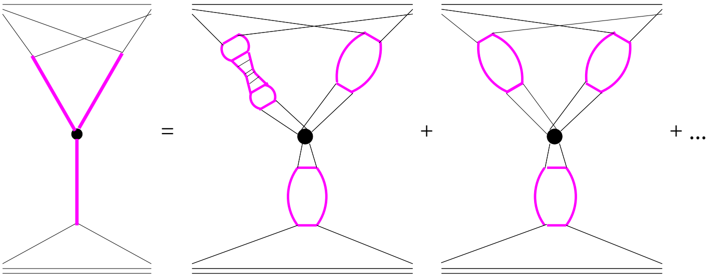

- ☐ Summing of **all orders**
- ☐ No energy conservation
- ☐ (in EPOS full energy conservation, but effective treatment of nonlinear effects)

Nonlinear effects in EPOS

Nonlinear effects (gluon fusion) taken care of via a saturation scale Q_s

Saturation scale depends on Pomeron energy ($\sqrt{x^+x^-s}$) and the environment

Selfconsistent procedure within multiple scattering framework (more later)

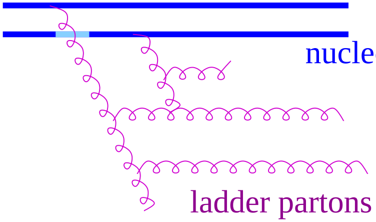

3.2 Dipole approach

Initial state radiation in DIPSY (from Christian Bierlich)

Initial nucleon: Three dipoles

LL BFKL in b-space + corrections: A dipole $(\vec{x}, \vec{y})$ can emit a gluon at position $\vec{z}$ with probability (P) per unit rapidity (Y)

$$\frac{dP}{dY} = \frac{\bar{\alpha}}{2\pi} d^2\vec{z} \frac{(\vec{x}-\vec{y})^2}{(\vec{x}-\vec{z})^2(\vec{z}-\vec{y})^2}$$

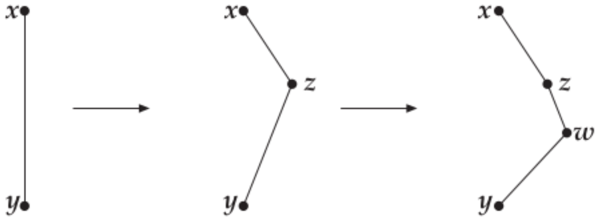

Multiple scattering

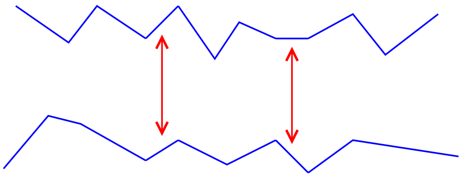

Multiple color exchange between dipoles *i* and *j* with probabilities

$$\frac{\alpha_s^2}{4}\left[\log\left(\frac{(\vec{x}_i-\vec{y}_j)^2(\vec{y}_i-\vec{x}_j)^2}{(\vec{x}_i-\vec{x}_j)^2(\vec{y}_i-\vec{y}_j)^2}\right)\right]^2$$

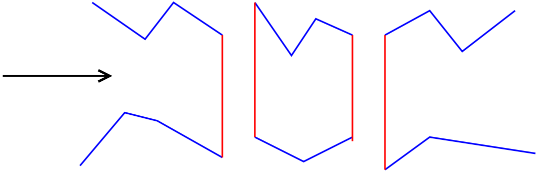

-> kinky strings

- ☐ **Two “leading“ strings**
- ☐ **Additional strings from loops**
- ☐ **No Remnants**

Many strings:
Lund strings may overlap

=> color ropes
(Larger eff. string tension)

Initial state in IP-Glasma (from Prithwish Tribedy)

IP-Sat dipole model ($r_\perp$ =dipole size):

$$\frac{d\sigma}{d^2b} = 2\left[1 - \exp\left(-F(r_\perp, x, b)\right)\right], \; F \propto r_\perp^2 \alpha_s(\mu^2) xg(x, \mu^2) T(b)$$

$T(b)$: Gaussian profile, $\mu^2 = 4/r_\perp^2 + \mu_0^2$, xg : DGLAP evolution

Saturation scale Q_s defined via

$$F\left(r_\perp, x = \frac{2}{Q_s^2}, b\right) = \frac{1}{2}$$

IP-Glasma: Color charge squared for projectile A and target B :

$g^2\mu_A^2 = \sum_{nucleons} g^2\mu_i^2$, with $g^2\mu_i^2 \propto Q_s^2$ with Q_s^2 from IP-Sat model.

Multiple Scattering

Color charge density $\rho_{A/B}$ generated from Gaussian distribution with variance $g^2\mu_A^2$ (contains DGLAP, saturation)

Current
$J^\nu = \delta^{\nu\pm}\rho_{A/B}(x^\mp, x_\perp)$

Field from $[D_\mu, F^{\mu\nu}] = J^\nu$
Numerical (lattice) solution, fields can be expressed in terms of initial ones:
$A^i = A^i_A + A^i_B,$
$A^\eta = \frac{ig}{2}[A^i_A, A^i_B]$

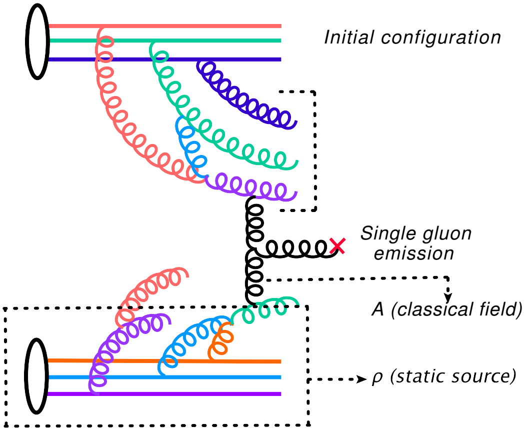

Multiple scattering:
Nonlinearity in terms of A:
Infinite number of $g + g \to g$ processes

Fields→Gluons→Pythia strings

3.3 Models based on factorization

$$\sigma_{\mathrm{jet}} = \int dx_1 dx_2 \int dp_t^2 \sum f_i(x_1, p_t^2)\, f_j(x_2, p_t^2)\, \frac{d\sigma_{ij}}{dp_t^2}(\hat{s}, \hat{t}) \quad (A)$$

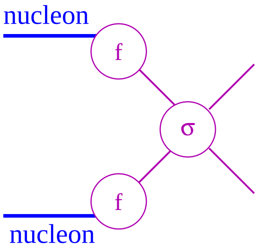

PYTHIA

HERWIG

SIBYLL

DPMJETIII

First step: σ_{jet} according to (A)

Second step: Multiple scattering scheme via eikonal formula

$$prob(n) = \frac{\left[\sigma_{\mathrm{jet}}(s)\, T(s,b)\right]^n}{n!} \exp\left(-\sigma_{\mathrm{jet}}(s)\, T(s,b)\right)$$

Multiple scattering in SIBYLL

From F. Riehn

Multiple scattering via eikonal model with soft and hard component

☐ No Remnants

☐ Main scattering
=> qq-q strings

☐ Further scatterings
=> strings between gluon pairs

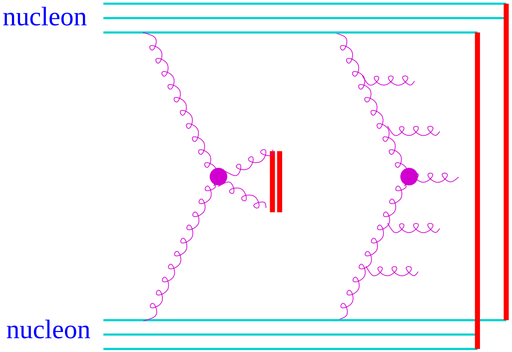

Saturation scale from

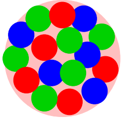

$$\frac{\alpha_s N_c}{Q^2} \times \frac{1}{N_c^2-1} \frac{xG}{\pi R^2} = 1$$

Multiple scattering in Pythia

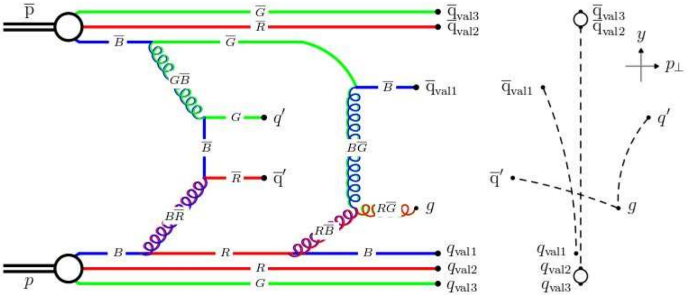

arXiv:1101.2599

Color reconnections

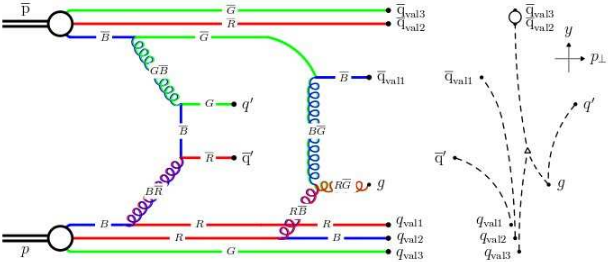

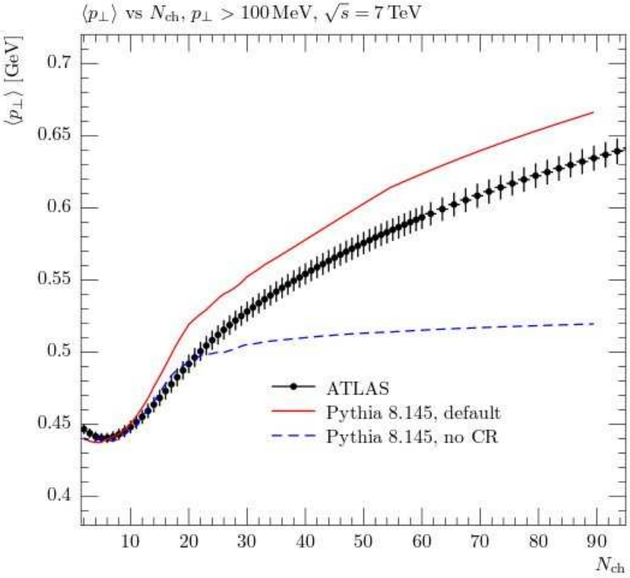

$\langle p_\perp \rangle$ vs N_{ch}, $p_\perp > 100$ MeV, $\sqrt{s} = 7$ TeV
$\langle p_\perp \rangle$ [GeV]
0.7
0.65
0.6
0.55
0.5
0.45
0.4
10
20
30
40
50
60
70
80
90
N_{ch}
ATLAS
Pythia 8.145, default
Pythia 8.145, no CR

4 Multiple scattering in EPOS

in collaboration with T. Pierog, S. Ostapchenko,
B. Guiot, G. Sophys, , M. Stefaniak

Parton based Gribov-Regge theory. By H.J. Drescher, M. Hladik, S. Ostapchenko, T. Pierog, K. Werner. hep-ph/0007198. Published in Phys.Rept. 350 (2001) 93-289.

4.1 Single scattering
(single Pomeron)

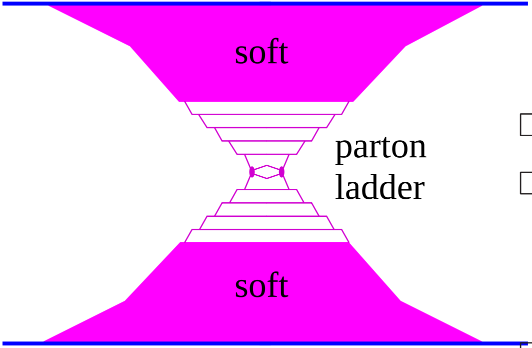

- **Parton emission starts long before the actual interaction** (partons are very long-lived due to a large γ).
- **Soft pre-evolution**
- Subsequent parton emissions towards smaller x-values and larger virtualities (from both sides).
- The final partons from either nucleon interact ("hard" collision).

4.2 Multiple scattering

Be T the elastic (pp,pA,AA) scattering T-matrix =>

$$2s\,\sigma_{\mathrm{tot}} = \frac{1}{\mathrm{i}}\mathrm{disc}\,T$$

Basic assumption : Multiple "Pomerons"

$$iT = \sum_k \frac{1}{k!}\left\{iT_{\mathrm{Pom}} \times \ldots \times iT_{\mathrm{Pom}}\right\}$$

Example: 2 “Pomerons”

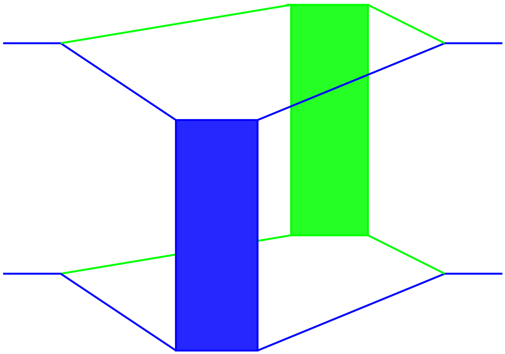

Evaluate

$$\frac{1}{i}\mathrm{disc}\,\{iT_{\mathrm{Pom}}\times\ldots\times iT_{\mathrm{Pom}}\}$$

using "cutting rules" :

A "cut" multi-Pomeron diagram amounts to the sum of all possible cuts

Example of two Pomerons

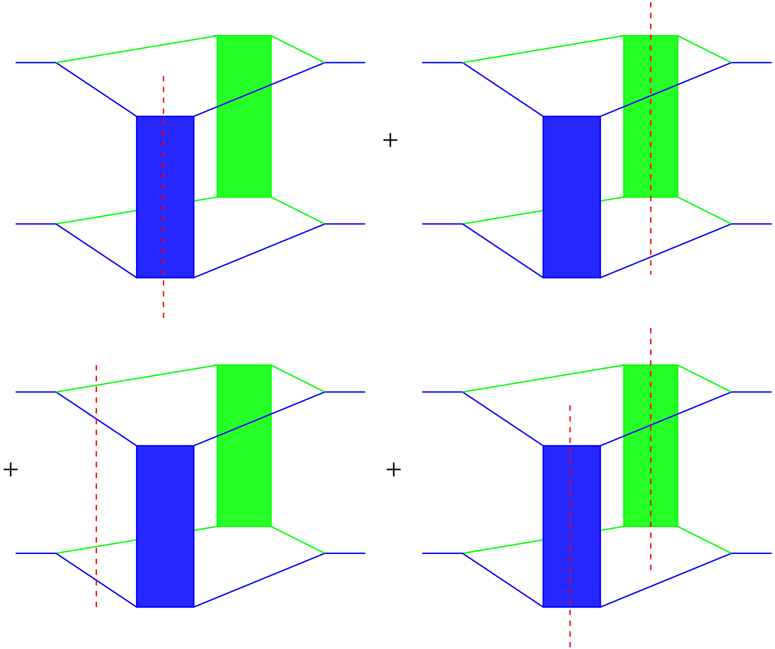

Using “Pomeron = parton ladder + soft”, we have (first diagram)

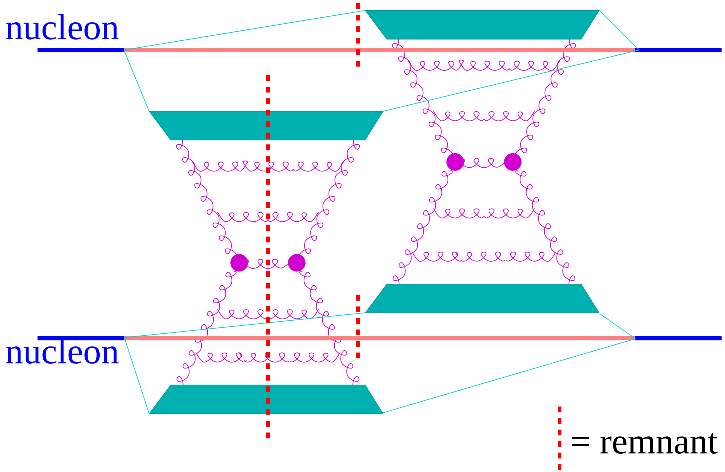

Using a simplified notation
for “cut” and “uncut” Pomeron

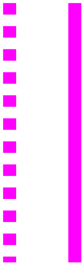

one gets ...

4.3 Complete result

(Drescher, Hladik, Ostapchenko, Pierog, and Werner, Phys. Rept. 350, 2001)

For pp, pA, AA:

$$\sigma^{\mathrm{tot}} = \sum_{\mathrm{cut\,P}} \int \sum_{\mathrm{uncut\,P}} \int$$

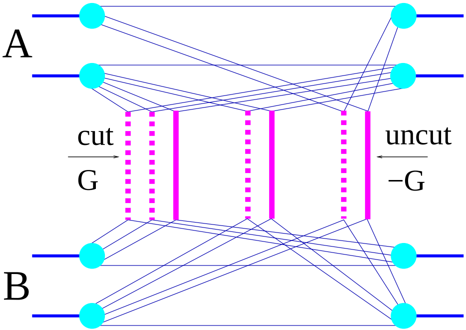

partial cross section σ_K

Dotted lines : Cut Pomerons (parton ladders)

$$
\begin{aligned}
\sigma^{\mathrm{tot}} = \int d^2b \int \prod_{i=1}^{A} d^2b_i^A \, dz_i^A \, \rho_A\Big(\sqrt{(b_i^A)^2 + (z_i^A)^2}\Big) \\
\prod_{j=1}^{B} d^2b_j^B \, dz_j^B \, \rho_B\Big(\sqrt{(b_j^B)^2 + (z_j^B)^2}\Big) \\
\sum_{m_1 l_1} \ldots \sum_{m_{AB} l_{AB}} (1 - \delta_{0\Sigma m_k}) \int \prod_{k=1}^{AB} \left(\prod_{\mu=1}^{m_k} dx_{k,\mu}^{+} dx_{k,\mu}^{-} \prod_{\lambda=1}^{l_k} d\tilde{x}_{k,\lambda}^{+} d\tilde{x}_{k,\lambda}^{-} \right) \Bigg\{ \\
\prod_{k=1}^{AB} \left(\frac{1}{m_k!} \frac{1}{l_k!} \prod_{\mu=1}^{m_k} G(x_{k,\mu}^{+}, x_{k,\mu}^{-}, s, |\vec{b} + \vec{b}_{\pi(k)}^{A} - \vec{b}_{\tau(k)}^{B}|) \right. \\
\left. \prod_{\lambda=1}^{l_k} -G(\tilde{x}_{k,\lambda}^{+}, \tilde{x}_{k,\lambda}^{-}, s, |\vec{b} + \vec{b}_{\pi(k)}^{A} - \vec{b}_{\tau(k)}^{B}|) \right) \\
\prod_{i=1}^{A} \left(1 - \sum_{\pi(k)=i} x_{k,\mu,}^{+} - \sum_{\pi(k)=i} \tilde{x}_{k,\lambda}^{+} \right)^{\alpha} \prod_{j=1}^{B} \left(1 - \sum_{\tau(k)=j} x_{k,\mu}^{-} - \sum_{\tau(k)=j} \tilde{x}_{k,\lambda}^{-} \right)^{\alpha} \Bigg\}
\end{aligned}
$$

- **Complicated due to strict energy sharing**

  => 10,000,000-dimensional intergrals, not separable

- **but doable**

  - **Parameterizations for $G(x^+, x^-, s, b)$**
  - **Analytical integrations**
  - **Employing Markov chain techniques**

Step 1:

- We compute **partial cross sections** σ_K for particular configurations K via analytical integration

- K is a multi-dimensional variable
  for example for double scattering in pp with two Pomerons involved: $K = \{x_1^+, x_1^-, \vec{p}_{t1}, x_2^+, x_2^-, \vec{p}_{t2}\}$

- Configurations K in AA scattering may be quite complex

Step 2:

The partial cross sections σ_K can be

- interpreted as **probability distributions**,

- enabling us to use Monte Carlo techniques to **generate configurations** K

Since we are dealing with multidimensional probability distributions, we have to employ very sophisticated

Markov chain techniques

to generate configurations according to Ω.

4.4 Configurations via Markov chains

(the heart of EPOS, see Phys. Rept. 350, 2001)

Consider a sequence of multidimensional random numbers (or better random configurations)

$$x_1\,,\; x_2\,,\;\; x_3, \ldots$$

with f_t being the law for x_t.

A homogeneous Markov chain is defined as

$$f_t(x) = \sum_{x'} f_{t-1}(x')p(x' \to x).$$

with $p(x' \to x)$ being the transition probability (or matrix).
Normalization : $\sum_x p(x' \to x) = 1.$

Let f be the law for x_t. The law for x_{t+1} is

$$\sum_a f(a)\, p(a \to b)\,.$$

One defines an operator T (comme Translation)

$$Tf(b) = \sum_a f(a)\, p(a \to b)\,.$$

So Tf is the law for x_{t+1} when f is the law for x_t.

A law is called stationary if $Tf = f$.

> Theorem: If a stationary law $Tf = f$ exists, then $T^k f_1$ converges towards f (which is unique) for any f_1.

So to generate random configurations according to some (given) law f,

- □ one constructs a T such that $Tf = f$
- □ and then considers $f_1 \to Tf_1 \to T^2 f_1$...
- □ and constructs the corresponding random configurations

One needs, for a given law f,
to **find a transition matrix p such that $Tf = f$**

Sufficient condition (detailed balance):

$$f(a)\,p(a \to b) = f(b)\,p(b \to a)\,,$$

Proof :

$$\begin{aligned} Tf(b) &= \sum_a f(a)\,p(a \to b) \\ &= \sum_a f(b)\,p(b \to a) \\ &= f(b) \sum_a p(b \to a) \\ &= f(b)\,. \end{aligned}$$

4.5 Metropolis alorithm

Definitions:

$$\begin{aligned} p_{ab} &= p(a \to b)\,, \\ f_a &= f(a)\,. \end{aligned}$$

Take

$$p_{ab} = w_{ab}\, u_{ab}\,. \qquad (a \neq b)\,.$$

with

w_{ab} : proposal matrix ($\sum_b w_{ab} = 1$)

u_{ab} : acceptance matrix ($u_{ab} \leq 1$)

This is NOT the simple acceptance-rejection method!!

Detailed balance:

$$f_a\, p_{ab} = f_b\, p_{ba}$$

amounts to

$$f_a\, w_{ab}\, u_{ab} = f_b\, w_{ba}\, u_{ba}\,,$$

or

$$\frac{u_{ab}}{u_{ba}} = \frac{f_b}{f_a}\,\frac{w_{ba}}{w_{ab}}\,.$$

$$\frac{u_{ab}}{u_{ba}} = \frac{f_b}{f_a}\,\frac{w_{ba}}{w_{ab}}\,.$$

is solved by

$$u_{ab} = F\left(\frac{f_b}{f_a}\,\frac{w_{ba}}{w_{ab}}\right),$$

with a function F with

$$\frac{F(z)}{F(\frac{1}{z})} = z\,.$$

$$\text{Proof : With } z \equiv \frac{f_b}{f_a}\,\frac{w_{ba}}{w_{ab}} \text{ one finds : } \frac{u_{ab}}{u_{ba}} = \frac{F(z)}{F(\frac{1}{z})} = z = \frac{f_b}{f_a}\,\frac{w_{ba}}{w_{ab}}.$$

The F according to Metropolis is

$$F(z) = \min(z, 1) \, .$$

One finds indeed

$$\frac{F(z)}{F(\frac{1}{z})} = \frac{\min(z,1)}{\min(\frac{1}{z},1)} = \left\{ \begin{array}{lll} z/1 & \text{pour} & z \leq 1 \\ 1/\frac{1}{z} & \text{pour} & z > 1 \end{array} \right\} = z \, .$$

So one proposes for each iteration a new configuation b according to some w_{ab}, and accepts it with probability

$$u_{ab} = \min \left(\frac{f_b}{f_a} \frac{w_{ba}}{w_{ab}}, 1 \right) .$$

Configuration lattice, define w_{ab} such that b changes w.r.t. a only on one lattice site (like Ising model Metropolis)

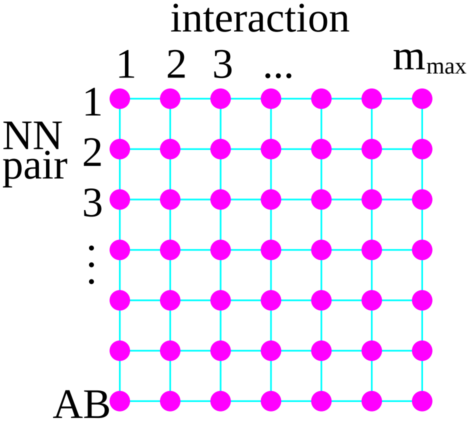

Long iterations, but allows to generate very complex configurations according to very complex laws.

4.6 Particle production

Generating "configurations" is only half the story:

> **How do we obtain the corresponding partons which "make" the ladder, and finally the hadrons?**

for a **given ladder**, **given momenta** and **given flavors** at the endpoints

For particle production, only the cut Pomerons play a role

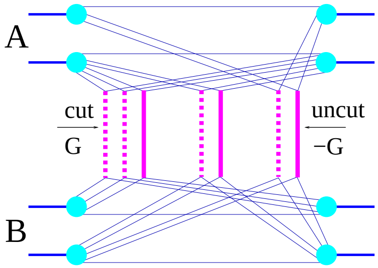

the uncut ones have been summed over

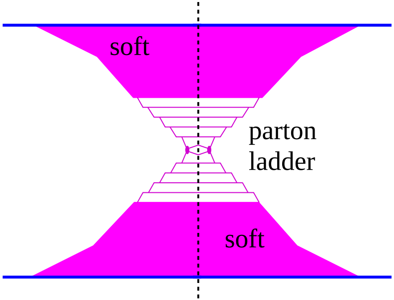

Reminder: in order to compute the contribution of a cut Pomeron to a partial cross section, we sum over emitted partons, integrate over all momenta.

Consistency requires to use these same formulas to obtain probability distributions for the parton emissions (what we do).

First : Get the **end partons** types (i and j) and their momenta of the hard part (parton ladder)

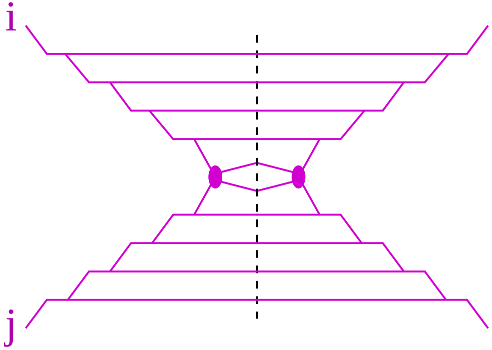

Prob. distribution proportional to the cross section

$$\sigma^{ij}_{\mathrm{hard}}(\hat{s}, Q_1^2, Q_2^2)$$

Realization:

- □ big tables with pre-calculated cross sections,
- □ to be used via interpolation

- □ to generate partons using rejection methods

Having the end partons i, j, how to get the intermediate ones (like m, k etc)?

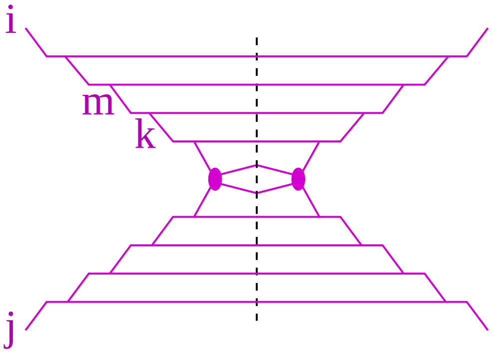

Actually the diagram k to j correponds to $\sigma_{\mathrm{hard}}^{kj}(\hat{s}, Q_1^2, Q_2^2)$,

the same σ_{hard} as used for the end partons, just with a different limit for Q_1

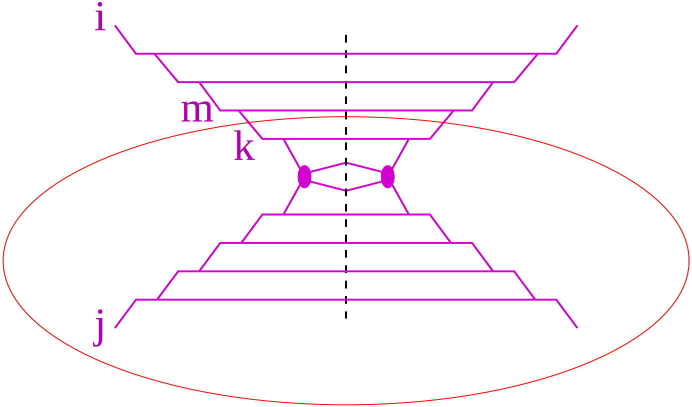

Probability of single emission $m \to k$:

$$prob(\xi, Q^2) = d\xi \frac{dQ^2}{Q^2} \, \Delta^m(Q_1^2, Q^2) \, \frac{\alpha_s}{2\pi} \, P_m^k(\xi) \, \sigma_{\mathrm{hard}}^{kj}(\xi\hat{s}, Q^2, Q_2^2)$$

with a given parton j on the other end.

Attention: emission on one side depends on existing parton the the other end!

4.7 Considering charm and botton

(recent development)

Notation:

q = light quark (u,d,s)

Q = heavy quark (c,b)

Heavy quark production in EPOS multiple scattering framework

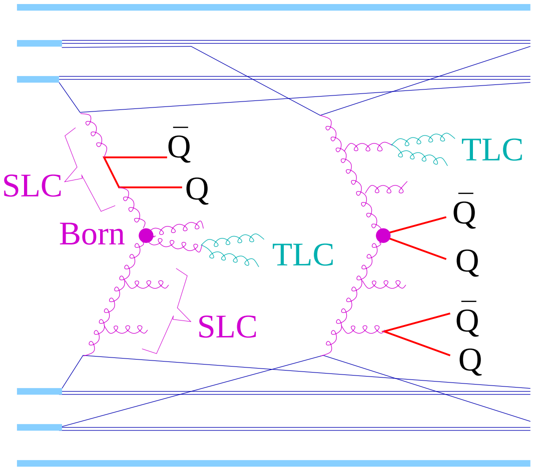

as light quark production

In any of the ladders

- ☐ **during SLC**
  (space-like cascade)
- ☐ **during TLC**
  (time-like cascade)
- ☐ **in Born**

but m_Q non-zero

$(m_c = 1.3,\ m_b = 4.2)$

Remarks

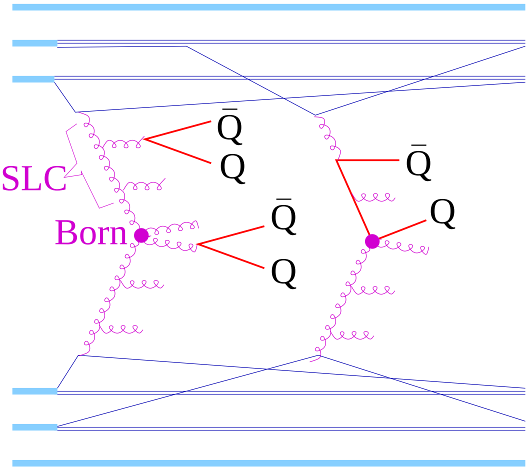

- TLC may be initiated by a parton
  - from Born process
  - from SLC
- Splittings in SLC may provide Q or $\bar{Q}$ in Born

Heavy quark masses play a role

- **in matrix elements**

- **as condition in TLC splitting:**

  $g \to Q\bar{Q}$ **requires** $Q^2 > (2m_Q)^2$

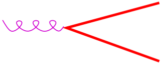

HQ pair

(Q^2= virtuality of mother)

- **as condition in SLC splitting:**

4−momenta:

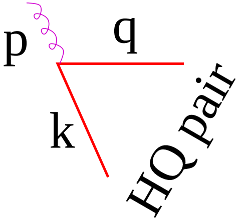

Energy-momentum conservation:
$q = p - k$

Technicalities:
We suppose

$$p = (E, 0, 0, E).$$

We define

$$\begin{aligned} n &= (1/2E, 0, 0, -1/2E), \\ k_t &= (0, k_x, k_y, 0). \end{aligned}$$

We get

$$p^2 = n^2 = pk_t = nk_t = 0, \; pn = 1.$$

$$\rightarrow k = xp + \frac{k^2 - k_t^2}{2x} n + k_t.$$

We define $Q^2 = -k^2$.

The virtuality of the TL parton is assumed to be m_Q^2, so

$$q^2 = k^2 - 2pk = -Q^2 + \frac{Q^2 + k_t^2}{x} = m_Q^2 \; (\mathrm{using}\, \mathrm{Q}^2 = -\mathrm{k}^2)$$

$$\to -k_t^2 = Q^2 - xQ^2 - xm_Q^2 > 0$$

which implies

$$\boxed{x < \frac{Q^2}{Q^2 + m_Q^2},}$$

suppressing large x.

As starting virtuality of the TLC, we use

$$Q_{\mathrm{ini}}^2 = (\alpha p_t)^2$$

with a coefficient α in the range 1-2.

Our favorite value is

$$\alpha = 2$$

In particular B-meson data in pp favor $\alpha = 2$, otherwise there is little production during the TLC, and spectra are too low compared to data.

Note: Contrary to the light quarks, there appear no HQs

- ☐ **initially in the in colliding hadrons**
- ☐ **in string fragmentation**
- ☐ **in QGP hadronization**

Only very recently: **Completely consistent treatment of HQ in the SL cascade** , with generation of partons ($m \to k$) according to

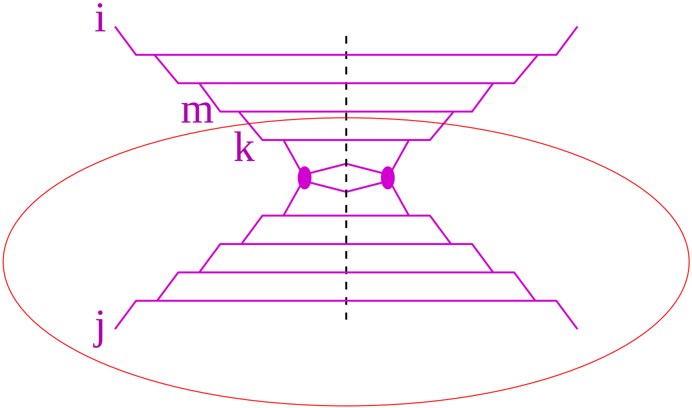

$$prob(\xi, Q^2) = d\xi \frac{dQ^2}{Q^2} \Delta^m(Q_1^2, Q^2) \frac{\alpha_s}{2\pi} P_m^k(\xi) \sigma_{\mathrm{hard}}^{kj}(\xi \hat{s}, Q^2, Q_2^2)$$

No conceptual, **but technical difficulties**.

Sofar we had only 4 classes of parton pairs, namely (with q meaning light (anti)quark)):

- □ gg, gq, qg, qq
- □ where masses are ignored (prob$(u) = $prob$(q)/(2N_f)$)

used in many places.

Now we have for the parton pairs i,j :

(q=light, c=charm,b=bottom)

- **gg, gg, gq, qg, qq, gc, cg, qc, cq, gb, bg, qb, bq, cc, bb, cb, bc**
- **with c and b being different from q (masses and thresholds)**

where in addition one has to distinguish cc, $\bar{c}\bar{c}$ from $c\bar{c}$, $\bar{c}c$.

- **All these cross sections have to be**
  - **computed,**
  - **tabulated.**
- **The interpolation function have to be updated**
- **The calculation of the Pomeron amplitudes have to be updated**

4.8 From partons to strings:

For $t > 0$, a (cut) Pomeron represents actually a (mainly) **longitudinal color field**,

where the ladder rungs (gluons) represent small transverse momentum components[(1)].

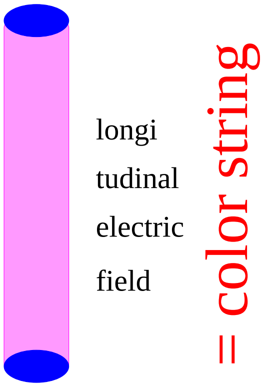

[(1)] Lund model idea, first e+e-,
then generalized to pp, see also CGC

Realization:

One-dimensional character of the fields

=> classical string theory
(which does not use much more than some general symmetries)

- **Mapping: parton ladders -> kinky strings**
  (parton momentum = kink)

- **Classical string evolution + decay via area law**

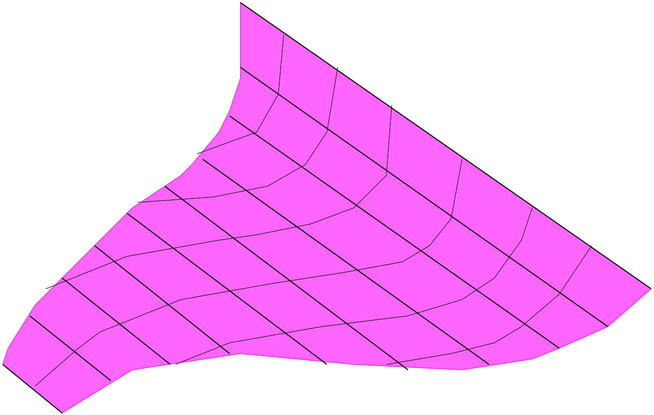

String:

two-dimensional surface

$$x(\sigma, \tau)$$

in Minkowski space

Break probability :

$$dP = p_B \, dA,$$

In detail: The string surface is given as

$$x^{\mu}(\sigma,\tau) = x_0 + \frac{1}{2}\int_{\sigma-\tau}^{\sigma+\tau} g^{\mu}(\xi)d\xi,$$

so it is completely given in terms of some function $g^{\mu}(\xi)$ with

$$g^{\mu}(\sigma) = \dot{x}^{\mu}(\sigma,\tau=0).$$

We consider only strings with a piecewise constant initial velocity g, which are called kinky strings.

- **This string is characterized by a sequence of σ intervals $[\sigma_k, \sigma_{k+1}]$, and the corresponding constant values (say v_k) of g in these intervals.**

Such an interval with the corresponding constant value of g is referred to as “kink”.

A parton ladder represents a **sequence of partons** of the type $q - g ... - g - \bar{q}$, with soft "end partons" q and $\bar{q}$, and hard inner gluons g.

The mapping "partons →string" is done such that we **identify a parton sequence with a kinky string**

by requiring "parton = kink",

$$\textbf{with} \quad \sigma_{k+1} - \sigma_k = \textbf{energy of parton } k$$

$$\textbf{and } v_k = \textbf{momentum of parton } k \,/\, E_k.$$

What is really done (PR 232, pp 87-299, 1993, PR 350, pp 93-289, 2001):

A string represents a two-dimensional surface in Minkowski space

$$x = x(\sigma, \tau),$$

with σ being a space-like and τ a time-like parameter.

In order to obtain the equations of motion, we need a Lagrangian. It is obtained by demanding the invariance of the action with respect to gauge transformations. This way one finds the Lagrangian of Nambu-Goto:

$$L = -\kappa\sqrt{(x'\dot{x})^2 - x'^2\dot{x}^2},$$

with “dot” and “prime” referring to the partial derivatives with respect to σ and τ, and with κ being the string tension.

With this Lagrangian we get the Euler-Lagrange equations of motion:

$$\frac{\partial}{\partial \tau}\frac{\partial L}{\partial \dot{x}_\mu} + \frac{\partial}{\partial \sigma}\frac{\partial L}{\partial x'_\mu} = 0.$$

We use the gauge fixing

$$x'^2 + \dot{x}^2 = 0 \text{ and } x'\dot{x} = 0,$$

which provides a very simple equation of motion, namely a wave equation,

$$\frac{\partial^2 x_\mu}{\partial \tau^2} - \frac{\partial^2 x_\mu}{\partial \sigma^2} = 0,$$

with the boundary conditions:

$$\partial x_\mu / \partial \sigma = 0, \; \sigma = 0, \pi.$$

The solution of the equation of motion (with initial extension zero) is

$$x^{\mu}(\sigma,\tau)=x_0+\frac{1}{2}\left(\int_{\sigma-\tau}^{\sigma+\tau}g^{\mu}(\xi)d\xi\right),$$

where g is the initial velocity, $g(\sigma)=\dot{x}(\sigma,\tau)_{\tau=0}$.

Strings are classified according to the function g. Strings with piecewise constant g are called kinky strings, each segment being called kink, finally identified with perturbative partons.

In the following figure, we show the evolution of a string generated in electron-positron annihilation (4 internal kinks).

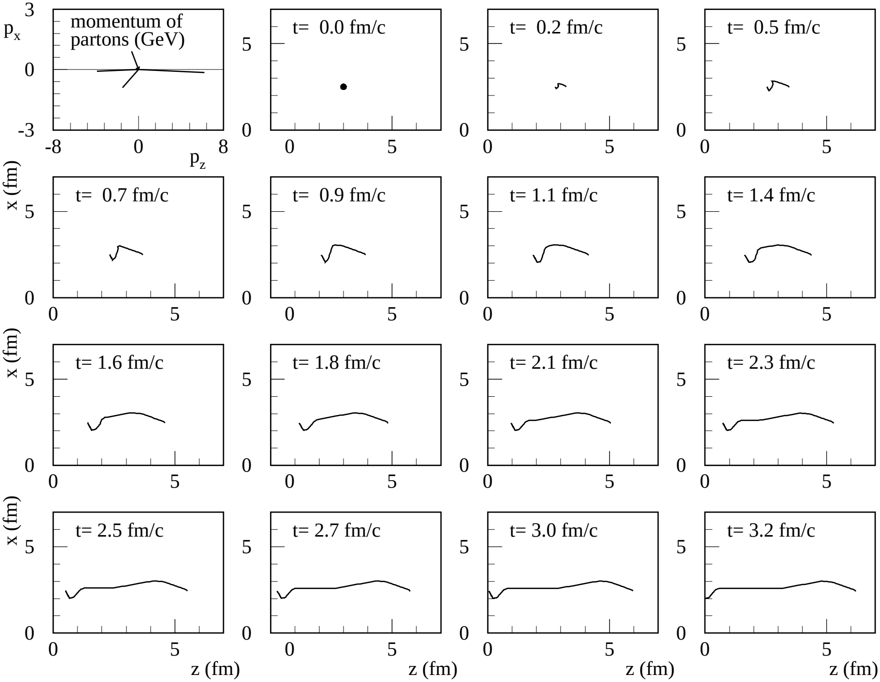
momentum of partons (GeV)
p_x
p_z
t= 0.0 fm/c
t= 0.2 fm/c
t= 0.5 fm/c
t= 0.7 fm/c
t= 0.9 fm/c
t= 1.1 fm/c
t= 1.4 fm/c
t= 1.6 fm/c
t= 1.8 fm/c
t= 2.1 fm/c
t= 2.3 fm/c
t= 2.5 fm/c
t= 2.7 fm/c
t= 3.0 fm/c
t= 3.2 fm/c
x (fm)
z (fm)

4.9 Hadron production

is finally realized via string breaking, such that string fragments are identified with hadrons.

Hypothesis: the string breaks within an infinitesimal area dA on its surface with a probability which is proportional to this area,

$$dP = p_B \, dA,$$

where p_B is the fundamental parameter of the procedure. [1]

[1] Elegant realization, making use of the dynamics of strings with piecewise constant initial conditions.

A string break is realized via **quark-antiquark** or **diquark-antidiquark** pair production with probability

$$p_{i(j)} = \frac{1}{Z} \exp\left(-\pi \frac{M_{i(j)}^2}{\kappa}\right)$$

with

$$M_{ij} = M_i + M_j + c_i c_j M_0$$

Transverse momenta $\vec{p}_t$ and $-\vec{p}_t$ are generated at each breaking, according to

$$f(k) \propto e^{-|\vec{p}_t|/2\bar{p}_t}\,, \tag{1}$$

with a parameter $\bar{p}_t$.

Jets:

Parton ladder = color flux tubes = **kinky strings**

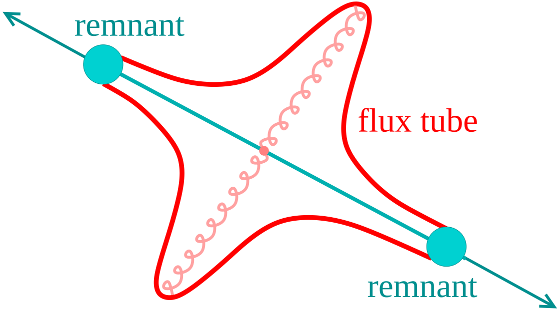

(here no IS radiation, only hard process producing two gluons)

which expand and break
via the production of quark-antiquark pairs
(Schwinger mechanism)

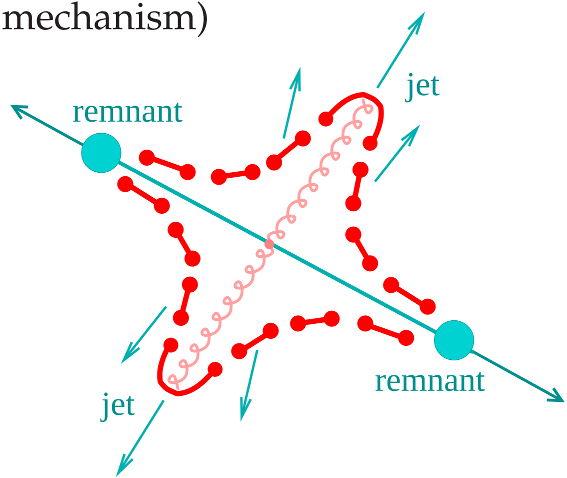

String segment = hadron. Close to “kink”: jets

Check: jet production in pp at 7 TeV

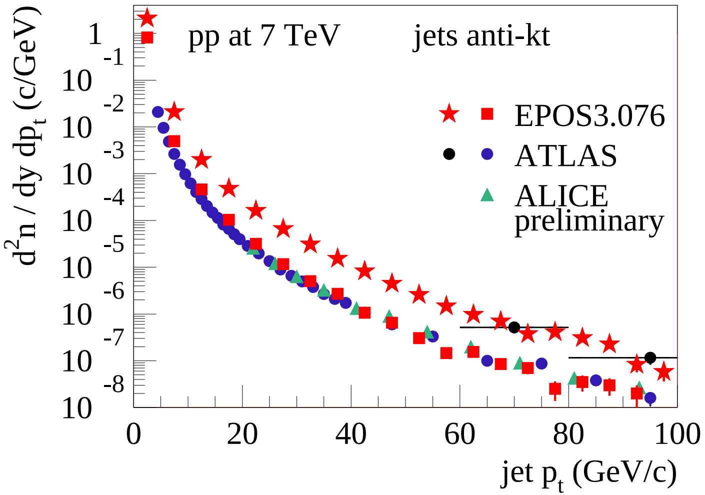

Comparison with parton model calculation using CTEQ PDFs for pp at 7 TeV

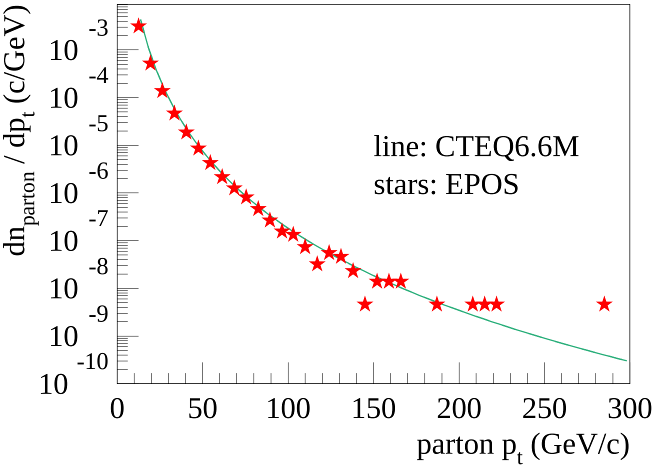

5 Collectivity in EPOS

5.1 Core-corona procedure

Heavy ion collisions
or high energy & high multiplicity pp events:

- ☐ the usual procedure has to be modified, since the density of strings will be so high that they cannot possibly decay independently

Some string pieces will constitute bulk matter,
others show up as jets

These are the same strings (all originating from hard processes at LHC) which constitute BOTH jets and bulk !!

again: single scattering => 2 color flux tubes

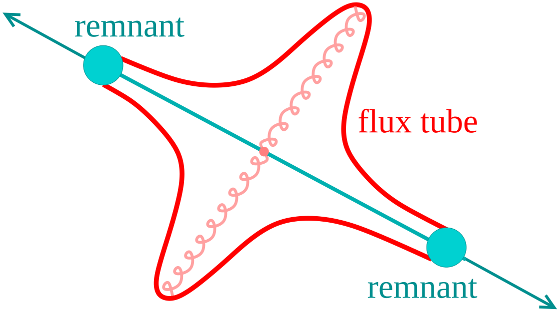

... two scatterings => 4 color flux tubes

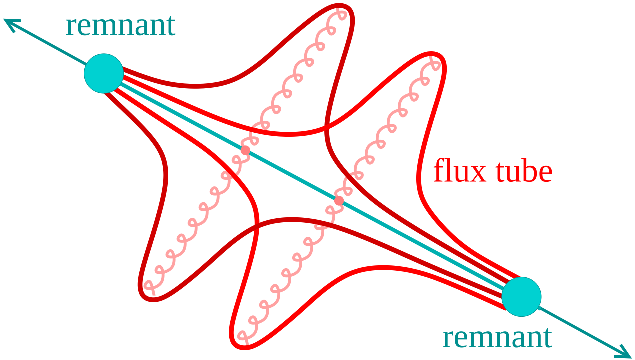

... many scatterings (AA) => many color flux tubes

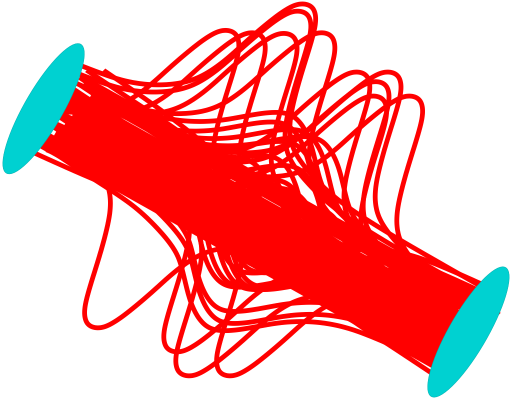

=> matter + escaping pieces (jets)

Core-corona procedure (for pp, pA, AA):

Pomeron => parton ladder => flux tube (kinky string)

String segments with high pt escape => **corona**,
the others form the **core** = initial condition for hydro
depending on the local string density

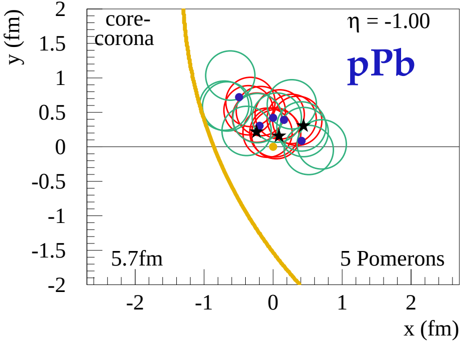

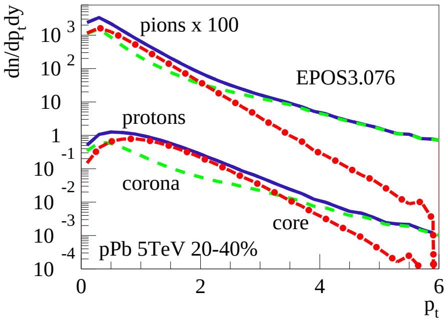

Core:

(we use α and β rather than σ and τ)

We split each string into a sequence of string segments, corresponding to widths $\delta\alpha$ and $\delta\beta$ in the string parameter space

Picture is schematic: the string extends well into the transverse dimension, correctly taken into account in the calculations

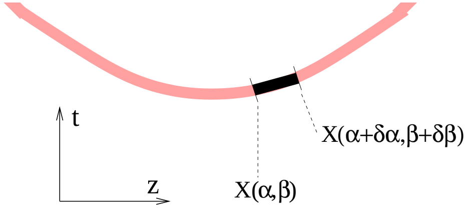

Energy momentum tensor and the flavor flow vector at some position x at initial proper time $\tau = \tau_0$:

$$T^{\mu\nu}(x) = \sum_i \frac{\delta p_i^\mu \delta p_i^\nu}{\delta p_i^0} g(x - x_i),$$

$$N_q^\mu(x) = \sum_i \frac{\delta p_i^\mu}{\delta p_i^0} q_i \, g(x - x_i),$$

$q \in u, d, s$: net flavor content of the string segments

$\delta p = \left\{ \frac{\partial X(\alpha,\beta)}{\partial \beta} \delta\alpha + \frac{\partial X(\alpha,\beta)}{\partial \alpha} \delta\beta \right\}$: four-momenta of the segments.

g: Gaussian smoothing kernel with a transverse width $\sigma_\perp$

The Lorentz transformation into the comoving frame provides the energy density ε and the flow velocity components v^i.

5.2 Hydrodynamic evolution

The evolution of the system for $\tau \geq \tau_0$ treated **macroscopicly**, solving the equations of **relativistic hydrodynamics**:

Three equations concerning conserved currents:

$$\boldsymbol{\partial_\nu N_q^\nu = 0}$$

with

$$N_q^\nu = n_q\, u^\nu$$

and n_q ($q = u, d, s$) representing (net) quark densities, u^ν is the velocity four vector.

Four equations concerning energy-momentum conservation:

$$\partial_\nu T^{\mu\nu} = 0.$$

The energy-momentum tensor $T^{\mu\nu}$ is

- the flux of the μth component of the momentum vector
- across a surface with constant ν coordinate (using four-vectors)

$\boldsymbol{T^{00}}$: **Energy density** $dE/dx^1dx^2dx^3$ (x^0 const)

$\boldsymbol{T^{01}}$: **Energy flux** $dE/dx^0dx^2dx^3$ (x^1 const)

$\boldsymbol{T^{i0}}$: **Momentum density**

$\boldsymbol{T^{ij}}$: **Momentum flux**

The equation

$$\partial_\nu T^{\mu\nu} = 0$$

is very general, no need for thermal equilibrium, no need for particles.

The energy-momentum tensor is

the **conserved Noether current**

associated with **space-time translations**.

- □ We have $4 + n_f$ equations, so we should express T in terms of 4 quantities (unknowns)
- □ and/or find additional equations
- □ which means additional assumptions

First approach: **Ideal Fluid**

In the local rest frame of a fluid cell:

- ☐ $T^{00} = \varepsilon$ (energy density in LRF)
- ☐ $T^{0i} = 0$ (no energy flow)
- ☐ $T^{0i} = 0$ (no momenum in LRF)
- ☐ $T^{ij} = \delta_{ij} p$ (p = isotropic pressure)

In arbitrary frame:

$$T^{\mu\nu} = (\varepsilon + p)u^{\mu}u^{\nu} - pg^{\mu\nu}$$

+ Equation of state $p = p(\varepsilon)$ of QGP from lQCD

=> 4 equations for 4 unknowns (ε, velocity)

Other way of writing T:

$$\boxed{T^{\mu\nu} = \varepsilon u^\mu u^\nu - p\Delta^{\mu\nu}}$$

with Δ being the projector $\perp$ to u ($\Delta^{\mu\nu} u_\nu = 0$):

$$\Delta^{\mu\nu} = g^{\mu\nu} - u^\mu u^\nu$$

Including viscous effects, following Landau:

Navier Stokes equations (with shear and bulk viscosity η, ζ):

$$\boxed{\begin{aligned} T^{\mu\nu} &= \varepsilon u^\mu u^\nu - (p+\Pi)\,\Delta^{\mu\nu} + \pi^{\mu\nu} \\ \pi^{\mu\nu} &= \pi^{\mu\nu}_{NS} = 2\eta\,\nabla^{\langle\mu}u^{\nu\rangle}, \\ \Pi &= \Pi_{NS} = -\zeta\,\nabla_\alpha u^\alpha \end{aligned}}$$

$$A_{\langle\mu}B_{\nu\rangle} = \frac{1}{2}\left(\Delta^\alpha_\mu\Delta^\beta_\nu + \Delta^\alpha_\nu\Delta^\beta_\mu - \frac{2}{3}\Delta^{\alpha\beta}\Delta_{\mu\nu}\right)A_\alpha B_\beta,\ \nabla^\mu = \Delta^{\mu\nu}\partial_\nu$$

$\pi^{\mu\nu}$, Π shear stress tensor, bulk pressure

NS does not work:

□ instabilities due to acausal behavior

□ Solution : Mueller-Israel-Steward (MIS) approach

Some math: Covariant derivative $\partial_{;i}$

Scalar function: $\partial_{;i} f = \partial_i f$

Basis vectors $\boldsymbol{e}_j$:

$$\partial_{;i} \boldsymbol{e}_j = \Gamma^k_{\ ij} \boldsymbol{e}_k$$

Any vector (using product law):

$$\begin{aligned} \partial_{;i} \left(u^j \boldsymbol{e}_j \right) &= \left(\partial_{;i} u^j \right) \boldsymbol{e}_j + u^j \partial_{;i} \boldsymbol{e}_j \\ &= \left(\partial_i u^j \right) \boldsymbol{e}_j + u^j \Gamma^k_{\ ij} \boldsymbol{e}_k \\ & \quad \underbrace{\left(\partial_i u^j + \Gamma^j_{\ ik} u^k \right)}_{\partial_{;i} u^j} \boldsymbol{e}_j \end{aligned}$$

Tensor rank 2 :

$$\partial_{;i}\left(t^{mn}\boldsymbol{e}_m\boldsymbol{e}_n\right)$$

$$= \left(\partial_{;i}t^{mn}\right)\boldsymbol{e}_m\boldsymbol{e}_n + t^{mn}\left(\partial_{;i}\boldsymbol{e}_m\right)\boldsymbol{e}_n + t^{mn}\boldsymbol{e}_m\left(\partial_{;i}\boldsymbol{e}_n\right)$$

$$= \left(\partial_{i}t^{mn}\right)\boldsymbol{e}_m\boldsymbol{e}_n + t^{mn}\left(\Gamma^k_{\ im}\boldsymbol{e}_k\right)\boldsymbol{e}_n + t^{mn}\boldsymbol{e}_m\left(\Gamma^k_{\ in}\boldsymbol{e}_k\right)$$

$$= \underbrace{\left(\partial_i t^{mn} + \Gamma^m_{ik}t^{kn} + \Gamma^n_{ik}t^{mk}\right)}_{\partial_{;i}t^{nm}}\boldsymbol{e}_m\boldsymbol{e}_n$$

Mueller-Israel-Steward (MIS) approach

(second order + π and Π dynamical quantities, governed by relaxation equations)

$$\partial_{;\nu} T^{\mu\nu} = \partial_\nu T^{\mu\nu} + \Gamma^\mu_{\nu\lambda} T^{\nu\lambda} + \Gamma^\nu_{\nu\lambda} T^{\mu\lambda} = 0$$

(Christoffel symbols: $\Gamma^\lambda_{\mu\nu} = \frac{1}{2} g^{\lambda\rho} (\partial_\mu g_{\rho\nu} + \partial_\nu g_{\rho\mu} - \partial_\rho g_{\mu\nu})$)

The energy-momentum tensor may be expressed via a systematic expansion in terms of gradients (of $\ln \varepsilon$ and u):

$$T^{\mu\nu} = T^{\mu\nu}_{(0)} + T^{\mu\nu}_{(1)} + T^{\mu\nu}_{(2)} + ...,$$

with the "equilibrium term" $T^{\mu\nu}_{(0)} = \epsilon u^\mu u^\nu - p\Delta^{\mu\nu}$, where $\Delta^{\mu\nu} = g^{\mu\nu} - u^\mu u^\nu$ is the projector orthogonal to u^μ.

One usually writes

$$T^{\mu\nu} = T^{\mu\nu}_{(0)} - \Pi\Delta^{\mu\nu} + \pi^{\mu\nu}. \tag{2}$$

(shear stress tensor, bulk pressure). Mueller-Israel-Steward (MIS) theory: Promote π and Π to dynamical quantities, governed by relaxation equations

$$\pi^{\mu\nu} = \pi^{\mu\nu}_{\mathrm{NS}} + \tau_\pi \left(-D\pi^{\mu\nu} + I^{\mu\nu}_\pi\right),$$

$$\Pi = \Pi_{\mathrm{NS}} + \tau_\Pi \left(-D\Pi + I_\Pi\right)$$

with $D = u^\mu \partial_\mu$. Details concerning second order expressions see Paul Romatschke and Ulrike Romatschke, arXiv:1712.05815. Different choices for the I.

EPOS implementation (Yuri Karpenko)

Milne coordinates:

$$\begin{aligned} \eta &= \frac{1}{2}\ln\frac{t+z}{t-z} \\ \tau &= \sqrt{t^2 - z^2} \end{aligned}$$

Metric tensor:

$$g^{\mu\nu} = \mathrm{diag}(1, -1, -1, -1/\tau^2).$$

Nonzero Christoffel symbols:

$$\Gamma^{\eta}_{\tau\eta} = \Gamma^{\eta}_{\eta\tau} = 1/\tau, \quad \Gamma^{\tau}_{\eta\eta} = \tau.$$

($\Gamma^{\lambda}_{\mu\nu} = \frac{1}{2} g^{\lambda\rho}(\partial_\mu g_{\rho\nu} + \partial_\nu g_{\rho\mu} - \partial_\rho g_{\mu\nu})$). The hydrodynamic equations (using covariant drivatives):

$$\partial_{;\nu} T^{\mu\nu} = \partial_\nu T^{\mu\nu} + \Gamma^{\mu}_{\nu\lambda} T^{\nu\lambda} + \Gamma^{\nu}_{\nu\lambda} T^{\mu\lambda} = 0$$

Freeze out

happens at a hypersurface defined by $T = T_H$ (for given T_H).

Hyper-surface: $x^\mu = x^\mu(\tau, \varphi, \eta)$:

$$x^0 = \tau \cosh \eta,\ x^1 = r \cos \varphi,\ x^2 = r \sin \varphi,\ x^3 = \tau \sinh \eta,$$

with $r = r(\tau, \varphi, \eta)$.

The hypersurface element is

$$d\Sigma_\mu = \varepsilon_{\mu\nu\kappa\lambda} \frac{\partial x^\nu}{\partial \tau} \frac{\partial x^\kappa}{\partial \varphi} \frac{\partial x^\lambda}{\partial \eta} d\tau d\varphi d\eta,$$

(with $\varepsilon^{0123} = 1$)

Computing the derivatives, one gets:

$$
\begin{aligned}
d\Sigma_0 &= \left\{ -r\frac{\partial r}{\partial \tau}\tau \cosh\eta + r\frac{\partial r}{\partial \eta}\sinh\eta \right\} d\tau d\varphi d\eta, \\
d\Sigma_1 &= \left\{ \frac{\partial r}{\partial \varphi}\tau \sin\varphi + r\,\tau \cos\varphi \right\} d\tau d\varphi d\eta, \\
d\Sigma_2 &= \left\{ -\frac{\partial r}{\partial \varphi}\tau \cos\varphi + r\,\tau \sin\varphi \right\} d\tau d\varphi d\eta, \\
d\Sigma_3 &= \left\{ r\frac{\partial r}{\partial \tau}\tau \sinh\eta - r\frac{\partial r}{\partial \eta}\cosh\eta \right\} d\tau d\varphi d\eta.
\end{aligned}
$$

Cooper-Frye hadronization amounts to calculating

$$E\frac{dn}{d^3p} = \int d\Sigma_\mu p^\mu f(up),$$

with u being the flow four-velocity in the global frame, related to Milne fram via

$$\begin{aligned} u^0 &= \tilde{u}^{\,0}\cosh\eta + \tilde{u}^{\,3}\sinh\eta\,, \\ u^1 &= \tilde{u}^{\,1}\,, \\ u^2 &= \tilde{u}^{\,2}\,, \\ u^3 &= \tilde{u}^{\,0}\sinh\eta + \tilde{u}^{\,3}\cosh\eta\,. \end{aligned}$$

Similarly p expressed in terms of $\tilde{p}$ in the Milne frame.

f is the Bose-Einstein or Fermi-Dirac distribution.

Hadronic afterburner: UrQMD

After “hadronization” hadrons follow straight and may still interact via

$$h_1 + h_2 \to \sum_j h'_j$$

We use “UrQMD”.

M. Bleicher et al., J. Phys. G25 (1999) 1859;

H. Petersen, J. Steinheimer, G. Burau, M. Bleicher and H. Stocker, Phys. Rev. C78 (2008) 044901

5.3 New trends on the foundations of hydrodynamics

- **A systematic way get the equations of relativistic hydrodynamics is via a formal gradient expansion of $T^{\mu\nu}$** (in terms of gradients (of $\ln\varepsilon$ and u)

- **The hydrodynamic gradient expansion has (probably) a vanishing radius of convergence**

- **Good news: There are tools to deal with that. Need to go beyond perturbative expansions.**

New trends :

- **Resurgence theory => go beyond the case of "small gradients" (close to equilibrium).**
- **Systematic treatment of divergent power series, methods to include exponential corrections ("instantons"). Jean Ecalle (1981)**
- **Applied to hydrodynamics by several authors** (Michal P. Heller, Michal Spalinski, Phys. Rev. Lett. 115, 072501 (2015); Paul Romatschke and Ulrike Romatschke, arXiv:1712.05815; Buchel, Michal P. Heller, Jorge Noronha Phys. Rev. D 94, 106011 (2016))

Truncated conformal Bjorken hydrodyn.

Mueller-Israel-Steward (MIS) approach

(second order + shear stress tensor π and bulk pressure Π dynamical quantities, governed by relaxation equations)

+ imposing scale and boost invariance,

Michal P. Heller, M. Spalinski, Phys. Rev. Lett. 115, 072501 (2015)

$$\tau\dot{\epsilon} = -\frac{4}{3}\epsilon + \phi, \quad \tau_\pi\dot{\phi} = \frac{4\eta}{3\tau} - \frac{\lambda_1\phi^2}{2\eta^2} - \frac{4\tau_\pi\phi}{3\tau} - \phi,$$

with $\phi = -\pi_y^y$ shear stress.

Equation considered (per def.) complete (not expansion), but one is investigating perturbative solutions.

With $\epsilon = T^4$, $\tau_\pi = C_{\tau\pi}/T$, $\lambda_1 = C_{\lambda_1}\eta/T$, $\eta = C_\eta s$, defining w and f as

$$w(\tau) = \tau T, \quad f(w) = \tau\frac{\dot{w}}{w}$$

=> diff. equation (DE) for $f(w)$

$$\boxed{\begin{gathered} C_{\tau\pi} w f f' + 4C_{\tau\pi} f^2 + \left(w - \frac{16C_{\tau\pi}}{3}\right) f \\ -\frac{4C_\eta}{9} + \frac{16C_{\tau\pi}}{9} - \frac{2w}{3} = 0. \end{gathered}}$$

$w = \tau^{2/3}$ for ideal hydro.

Perturbative solution: series in powers of w^{-1}

$$f = \sum_{n=0}^{\infty} a_n w^{-n},$$

called **hydrodynamical expansion** for large w (large times), coefficients obtained from DE:

$$a_n \sim n!$$

so the series is divergent.

Solving the equation numerically => **attractor**

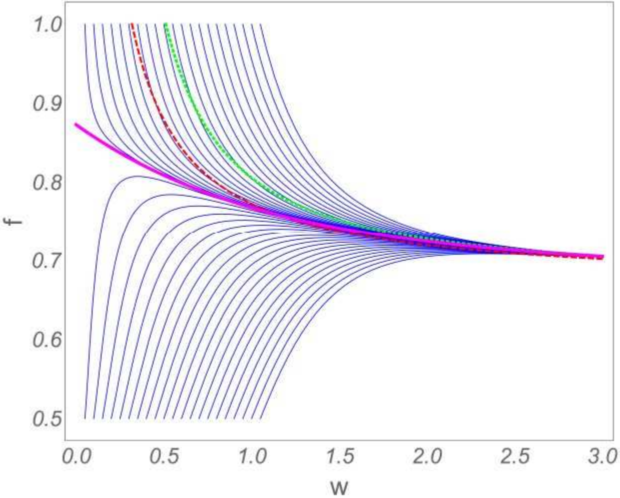

Picture from Heller, M. Spalinski.

well defined solutions even at small w (small times),

contrary to the perturbative expansion.

=> well defined solutions "far off equilibrium"

Resummation

(a very systematic approch for divergent series)

$$f = \sum_{n=0}^{\infty} a_n w^{-n},$$

(computed up to $n = N = 200$) is **Borel transformed**

$$f_B(x) = \sum_{n=0}^{\infty} a_n \frac{x^n}{n!} = \sum_{n=0}^{\infty} B_n x^n,$$

has a finite radius of convergence.

The **inverse Borel transform** is

$$f_{iB}(w) = w \int_0^\infty f_B(x) e^{-wx} dx.$$

Analytic continuation of f_B via **Padé approximants** having a sequence of singularities

$$f_{PB}(x) = h_0(x) + (a-x)^\gamma h_1(x) + (2a-x)^{2\gamma} h_1(x) + ...$$

These branch-cut singularities

=> **ambiguities** (for large w) of the form

$$\boldsymbol{w^{-m\gamma} e^{-maw}}$$

This ambiguity = feature of the hydrodynamic series

indication of physics outside the grad expansion.

The solution should have the form of a trans-series

$$f(w) = \sum_{m=0}^{\infty} c^m \, \boldsymbol{w}^{-m\gamma} \boldsymbol{e}^{-maw} f_m(w)$$

with perturbative series f_m,
get coeficients by substituting the trans-series into the DE, then same procedure

=> **unique result called "resummation result"**

One finds (on percent level):

Resummed result

= Hydrodynamical attractor

both being in general quite different compared to the perturbative expansions

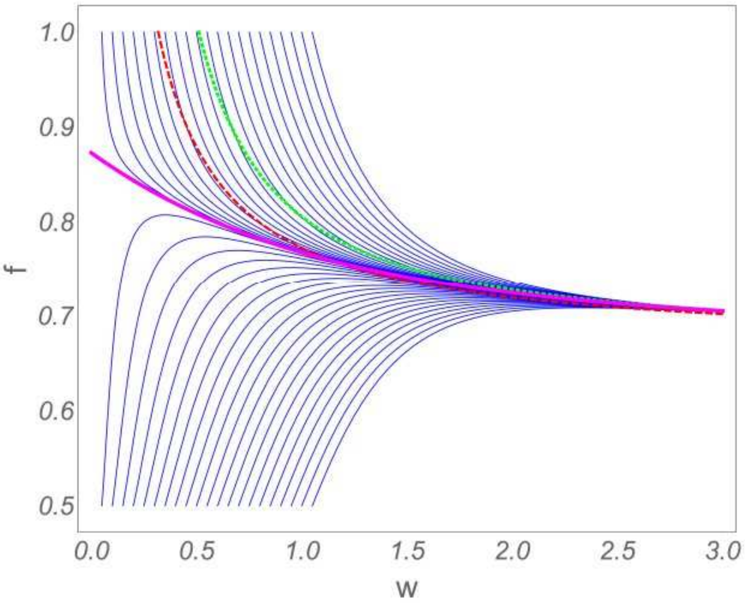
1.0
0.9
0.8
0.7
0.6
0.5
f
0.0
0.5
1.0
1.5
2.0
2.5
3.0
w

What do these "resummation" results tell us?

- Hydro may be applicable even far off equilibrium (in particular relevant for small systems)

- => True solution : Hydrodynamic attractor
  Accessible (in principle) via resummation

- Frequently asked question:
  "Why do small systems thermalize so quickly?"
  Maybe they simply don´t ...

5.4 Microcanonical hadronization

- No need to match dynamical part
- Energy and flavor conservation for small systems
- Needed to “unify” EPOSLHC and EPOS3

Grand canonical decay, T = 130 MeV

V=50 fm^3; V=1000 fm^3

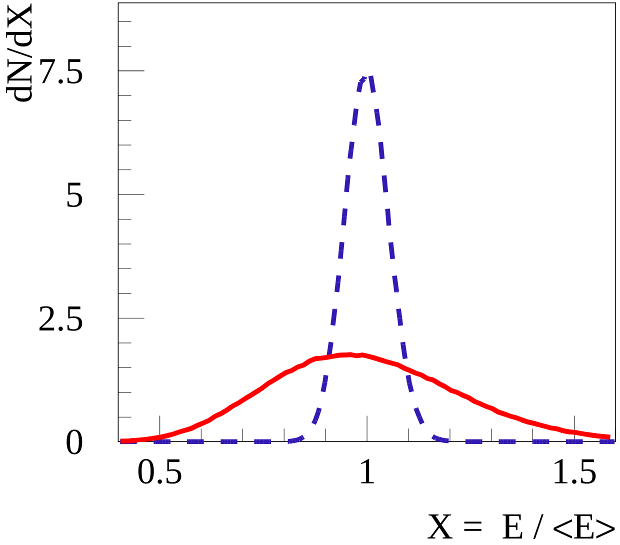

Microcanonical hadronization in EPOS

(very preliminary)

Hadronization hyper-surface $x^\mu(\tau, \varphi, \eta)$:

$$\boxed{\begin{aligned} x^0 &= \tau \cosh \eta, \\ x^1 &= r \cos \varphi, \\ x^2 &= r \sin \varphi, \\ x^3 &= \tau \sinh \eta \end{aligned}}$$

with $r = r(\tau, \varphi, \eta)$, representing the **FO condition**.

Hypersurface element:

$$\boldsymbol{d\Sigma_\mu = \varepsilon_{\mu\nu\kappa\lambda}\frac{\partial x^\nu}{\partial\tau}\frac{\partial x^\kappa}{\partial\varphi}\frac{\partial x^\lambda}{\partial\eta}\,d\tau\,d\varphi\,d\eta.}$$

$$\begin{aligned}
d\Sigma_0 &= \left\{-r\frac{\partial r}{\partial\tau}\tau\cosh\eta + r\frac{\partial r}{\partial\eta}\sinh\eta\right\}d\tau d\varphi d\eta,\\
d\Sigma_1 &= \left\{\frac{\partial r}{\partial\varphi}\tau\sin\varphi + r\,\tau\cos\varphi\right\}d\tau d\varphi d\eta,\\
d\Sigma_2 &= \left\{-\frac{\partial r}{\partial\varphi}\tau\cos\varphi + r\,\tau\sin\varphi\right\}d\tau d\varphi d\eta,\\
d\Sigma_3 &= \left\{r\frac{\partial r}{\partial\tau}\tau\sinh\eta - r\frac{\partial r}{\partial\eta}\cosh\eta\right\}d\tau d\varphi d\eta.
\end{aligned}$$

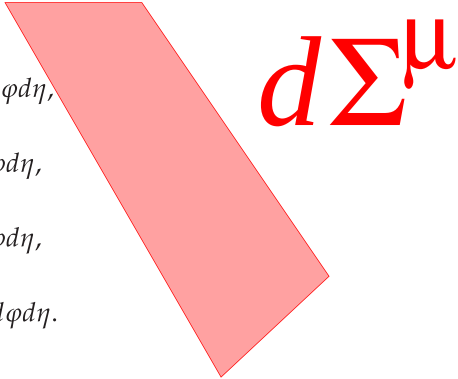

GC particle production via Cooper-Frye

$$E\frac{dn}{d^3p} = \int d\Sigma_\mu p^\mu f(up),$$

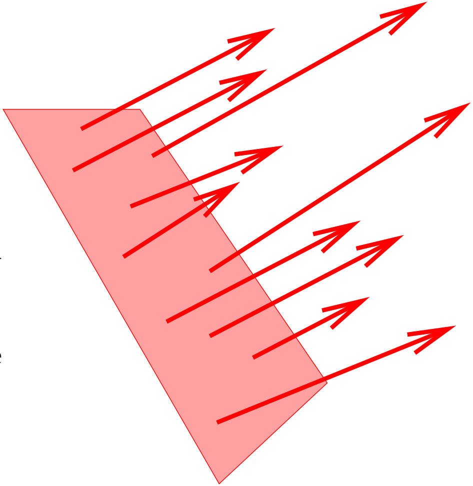

assuming that "matter" is a thermalized resonance gas

(adding δf for viscous hydro, close to equilibrium)

More general:

Flow of momentum vector dP^{μ} and conserved charges dQ_A through the surface element:

$$
\begin{aligned}
dP^{\mu} &= T^{\mu\nu} d\Sigma_{\nu}, \\
dQ_A &= J_A^{\nu} d\Sigma_{\nu}.
\end{aligned}
$$

Momentum and charges are conserved :

$$\int_{\Sigma_{\mathrm{FO}}} dP^{\mu} = P^{\mu}_{\mathrm{ini}},$$
$$\int_{\Sigma_{\mathrm{FO}}} dQ_A = Q_{A\,\mathrm{ini}}$$

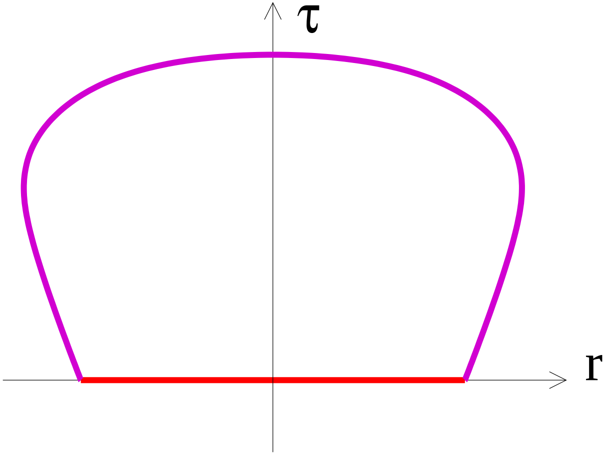

Construct an **effective mass** by summing surface elements:

$$M = \int_{\text{surface area}} dM,$$

with

$$dM = \sqrt{dP^\mu dP_\mu},$$

knowing for each element four-velocity and volume element

$$U^\mu = dP^\mu / dM,$$

$$dV = u^\mu d\Sigma_\mu.$$

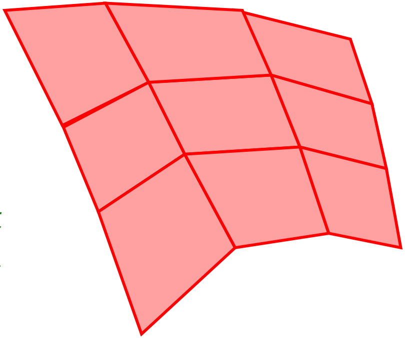

The four-velocity U^μ is NOT equal to the fluid velocity u^μ!
(Only in case of zero pressure)

These effective masses we **decay microcanonically**:

$$
\begin{aligned}
dP &= C_{\mathrm{vol}}\, C_{\mathrm{deg}}\, C_{\mathrm{ident}} \\
&\quad \times \delta(E - \Sigma E_i)\, \delta(\Sigma \vec{p}_i) \prod_A \delta_{Q_A, \Sigma q_{A\,i}} \prod_{i=1}^{n} d^3 p_i,
\end{aligned}
$$

$$
C_{\mathrm{vol}} = \frac{V^n}{(2\pi\hbar)^{3n}}, \quad C_{\mathrm{deg}} = \prod_{i=1}^{n} g_i, \quad C_{\mathrm{ident}} = \prod_{\alpha \in \mathcal{S}} \frac{1}{n_\alpha!},
$$

(n_α is the number of particles of species α, $\mathcal{S}$ is the set of particle species)

then **boost the particles** according to velocities U^μ.

Microcanonical decay

$$dP \propto d\Phi_{\mathrm{NRPS}} = \delta(M - \Sigma E_i)\,\delta(\Sigma \vec{p}_i)\,\prod_{i=1}^{n} d^3 p_i$$

- □ Hagedorn 1958 methods to compute Φ_{NRPS}
- □ Lorentz invariant phase space (LIPS) (James 1968)
- □ Hagedorn methods used for decaying QGP droplets (Werner, Aichelin, 1994, Becattini 2003)
- □ 2012 (Bignamini,Becattini,Piccinini) compute Φ_{NRPS} via the Lorentz invariant phase space (LIPS)

- ☐ **Hagedorn integral method can be made very efficient at large n,** but becomes VERY time consuming at small n

- ☐ **LIPS method very fast for small n,** gets time consuming at large n

- ☐ **around $n \approx 30 - 40$ both methods work (=> checks)**

Hagedorn integral method, optimized

The phase-space integral:

$$\phi_{\mathrm{NRPS}}(M, m_1, \ldots, m_n)$$
$$= (4\pi)^n \int \prod_{i=1}^{n} p_i^2 \, \delta(E - \sum_{i=1}^{n} E_i) \, W(p_1, \ldots, p_n) \prod_{i=1}^{n} dp_i,$$

with the “random walk function” W given as

$$W(p_1, \ldots, p_n) := \frac{1}{(4\pi)^n} \int \delta(\sum_{i=1}^{n} p_i \times \frac{\vec{p}_i}{p_i}) \prod_{i=1}^{n} d\Omega$$

We obtain (Werner, Aichelin 94)

$$\phi(M, m_1, \ldots, m_n) = \int_0^1 dr_1 \ldots \int_0^1 dr_{n-1} \psi(r_1, ..., r_{n-1})$$

$$\psi = \frac{(4\pi)^n \, T^{n-1}}{(n-1)!} \prod_{i=1}^{n} p_i \, E_i \, W(p_1, \ldots, p_n),$$

with $z_i = r_i^{1/i}$, $x_i = z_i x_{i+1}$, $s_i = x_i T$, $t_i = s_i - s_{i-1}$,
$E_i = t_i + m_i$, $T = M - \sum_{i=1}^{n} m_i$

Suitable for MC

The random walk function may be written as

$$W(p_1,\ldots,p_n) = \frac{1}{(4\pi)^n}\frac{1}{(2\pi)^3}\int\int e^{-i\vec{\lambda}\Sigma p_j\hat{p}_j}\,\prod_{j=1}^{n} d\Omega_j\, d^3\lambda,$$

which gives $W = \int_0^\infty F(\lambda)\,d\lambda$ with

$$F(\lambda) = \frac{1}{2\pi^2}\,\lambda^2\prod_{j=1}^{n}\frac{\sin p_j\lambda}{p_j\lambda}.$$

For small λ :

$$\prod_{j=1}^{n}\frac{\sin p_j\lambda}{p_j\lambda} \approx \exp\left(-P^2\lambda^2\right), \quad P = \sqrt{\frac{1}{6}\sum_{j=1}^{n} p_j^2}$$

Approximation is stricly true for small λ, but for large n it provides a good approximation over the whole range of λ

=> estimate $W \approx \left(4\pi P^2\right)^{-3/2}$

In order to get more precise results, we define

$$F_0(\lambda) = F(\lambda) \times \exp\left(P^2\lambda^2\right),$$

with F_0/λ^2 being a slowly varying function of λ.

This allows to use the Gauss-Hermite formula

$$W = \frac{1}{P}\int_0^\infty F_0\left(\frac{x}{P}\right)\times \exp\left(-x^2\right)\,dx$$

$$\approx \frac{1}{P}\sum_{k=1}^{K} w_j^{GH} F_0\left(\frac{x_j^{GH}}{P}\right),$$

with Gauss-Hermite nodes and weights x_j^{GH} and w_j^{GH} found in text books.

With only six nodes we get excellent results.

Sampling via Markov chains

To generate $K = \{h_1, \ldots, h_n; r_1, ...r_m\}$ $(m = 3n - 1 \text{ or } m = 3n - 4)$ according to $\Omega(K)$, consider random configurations

$$K_0\,,\ K_1\,,\ K_2, ...$$

with Ω_t being the law for K_t. Per def

$$\Omega_{t+1}(B) = \sum_A \Omega_t(A)\, p(A \to B)$$

Convergence in case of detailled balance:

$$\Omega(A)\, p(A \to B) = \Omega(B)\, p(B \to A)$$

Use

$$p(A \to B) = w_{AB} \times u_{AB} \,,$$

with a so-called proposal matrix w and an acceptance matrix u. Detailed balance now reads

$$\frac{u_{AB}}{u_{BA}} = \frac{\Omega_B}{\Omega_A}\frac{w_{BA}}{w_{AB}} \,,$$

which is fulfilled for

$$u_{AB} = \min\left(\frac{\Omega_B}{\Omega_A}\frac{w_{BA}}{w_{AB}}, 1\right)$$

(more generally using some function F fulfilling $F(z) \,/\, F(z^{-1}) = z$)

Grand canonical limit

For very large M we should recover the “grand canonical limit” for single particle spectra:

$$f_k = \frac{g_k V}{(2\pi\hbar)^3} \exp\left(-\frac{E_k}{T}\right),$$

The average energy is

$$\bar{E} = \frac{g_k V}{(2\pi\hbar)^3} \sum_k \int_0^\infty E_k \exp\left(-\frac{E_k}{T}\right) 4\pi p^2 dp$$

Changing variables via $E_k dE_k = p dp$, and using $K_1(z) = z \int_1^\infty \exp(-zx)\sqrt{x^2-1}\,dx$, and $3\,K_2(z) = z^2 \int_1^\infty \exp(-zx)\sqrt{x^2-1}^3\,dx$,

=>

$$\bar{E} = \frac{4\pi g_k V}{(2\pi\hbar)^3} m^2 T \left(3TK_2(\frac{m}{T}) + mK_1(\frac{m}{T}) \right).$$

The microcanonical decay of an object of mass M and volume V should converge (for $M \to \infty$) to the GC single particle spectra

with T obtained from $M = \bar{E}$.

We consider a complete (?) set of hadrons ($\approx$ 400, PDG list)

Comparing GC et MiC decay, we check effect of

- **energy conservation**
- **flavor conservation**

GC decay, E/V= 0.333 GeV/fm^3 T=164 MeV

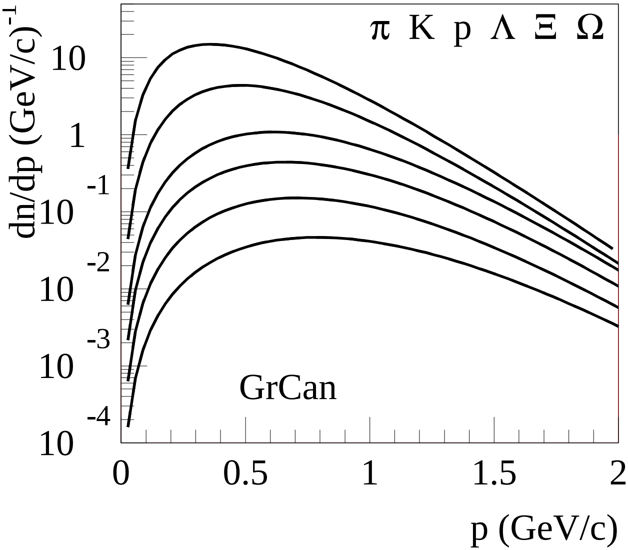

V=150 fm^3

GC+MiC decay, E/V= 0.333 GeV/fm^3 M=200 GeV

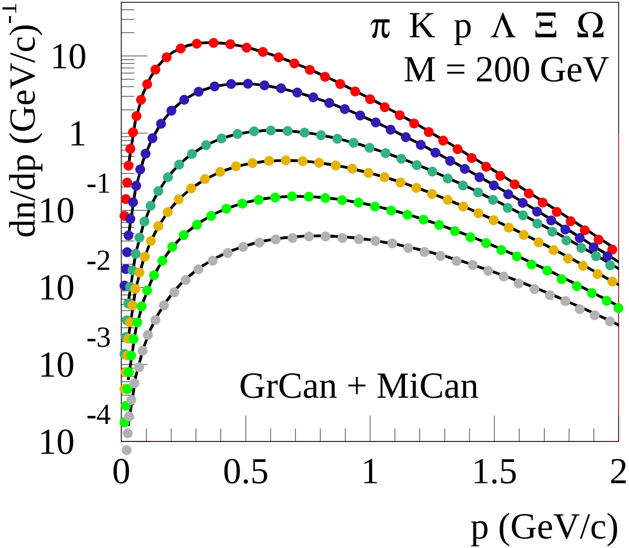

V=600 fm^3

$\times \frac{1}{4}$

good test for
Metropolis proposal

GC+MiC decay, E/V= 0.333 GeV/fm^3 M=100 GeV

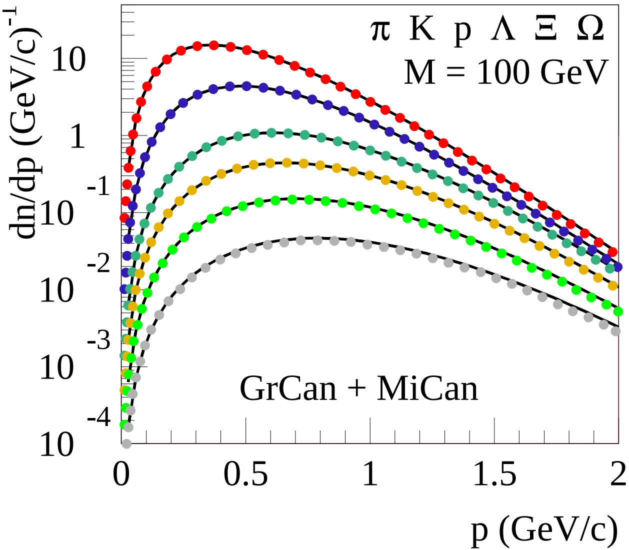

V=300 fm^3

$\times \frac{1}{2}$

GC+MiC decay, E/V= 0.333 GeV/fm^3 M=50 GeV

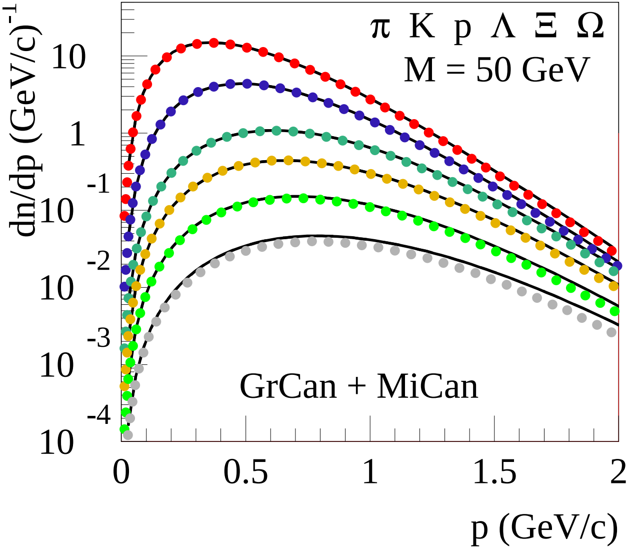

V=150 fm^3

$\times 1$

GC+MiC decay, E/V= 0.333 GeV/fm^3 M=25 GeV

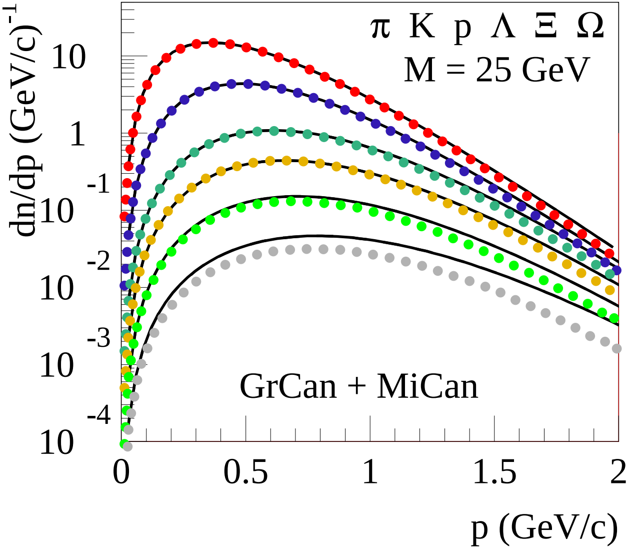

V=75 fm^3

×2

GC+MiC decay, E/V= 0.333 GeV/fm^3 M=12.5 GeV

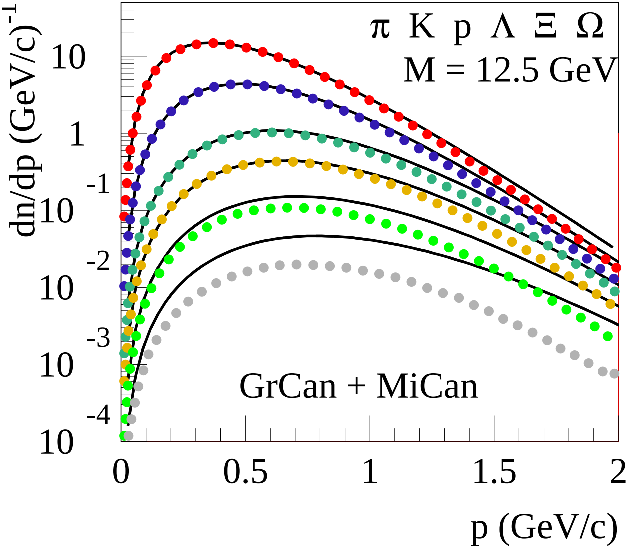

V=37.5 fm^3

$\times 4$

GC+MiC decay, E/V= 0.333 GeV/fm^3 M=6.25 GeV

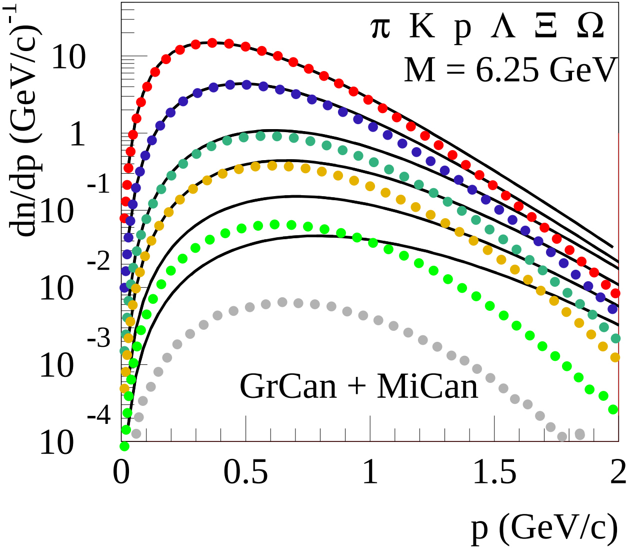

V=18.75 fm^3

$\times 8$

Status on microcanonical hadronization:

- Reliable and fast methods, even for large systems
- Very recently: works for complete hadron set
- Todo:
  - Implementation to do hadronization for “flowing” plasma

6 Flow in small systems

=> comparing models

with / without collectivity built in

pPb results (more results: arXiv:1312.1233)

We will compare EPOS3 with data

and also with

EPOS LHC

LHC tune of EPOS1.99, :
same GR, but uses **parameterized flow**
T. Pierog et al, arXiv:1306.5413

AMPT

Parton + hadron cascade **-> some collectivity**
Z.-W. Lin, C. M. Ko, B.-A. Li, B. Zhang and S. Pal, Phys. Rev. C 72, 064901 (2005).

QGSJET

GR approach, **no flow**
S. Ostapchenko, Phys. Rev. D74 (2006) 014026

CMS: Multiplicity dependence of pion, kaon, proton pt spectra

CMS, arXiv:1307.3442

We plot 4 centrality classes:

$\langle N_{\mathbf{trk}}^{\mathbf{offline}} \rangle = 8, 84, 160, 235$ (in $|\eta| < 2.4$)

Multiplicity = centrality measure

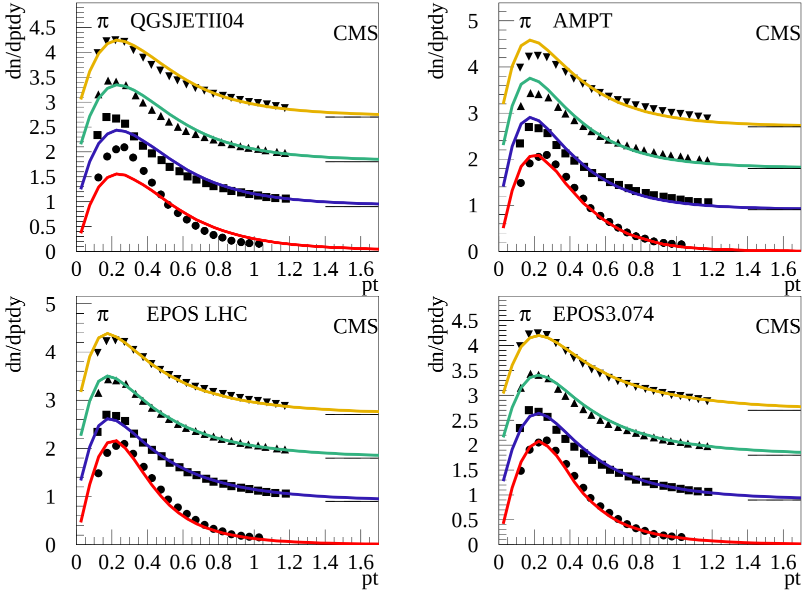

Little change with multiplicity for pions

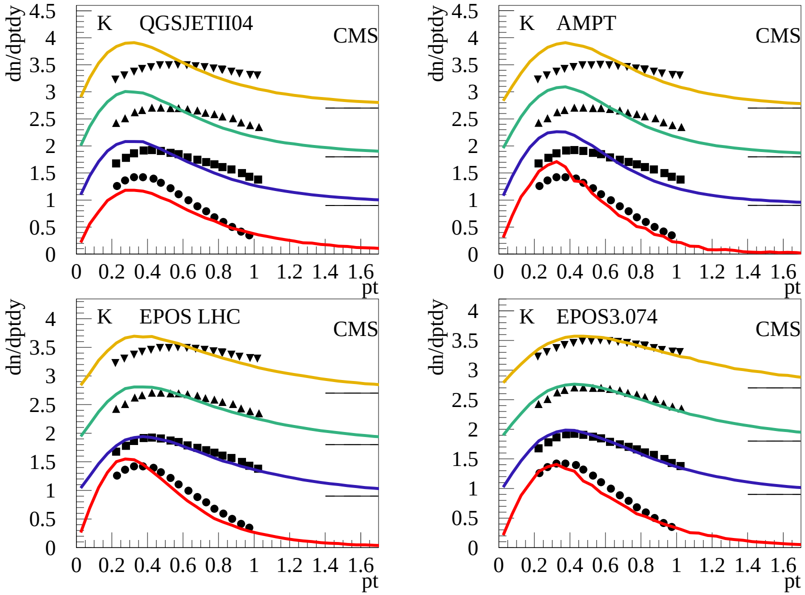

Kaon spectra change with multiplicity

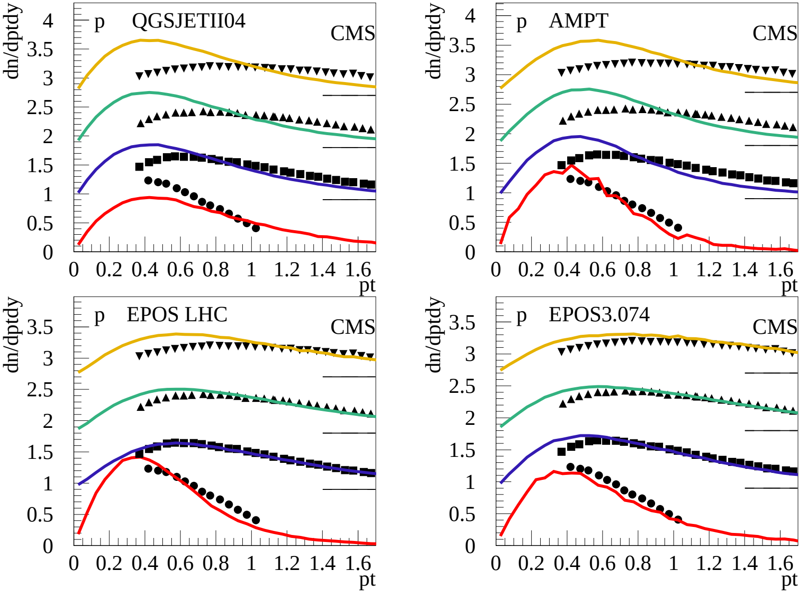

Strong variation of proton spectra => flow helps

ALICE: compare pt spectra for identified particles in different multiplicity classes: 0-5%,...,60-80%

(in $2.8 < \eta_{\rm lab} < 5.1$) From R. Preghenella, ALICE, talk Trento workshop 2013

Useful : ratios (K/pi, p/pi...)

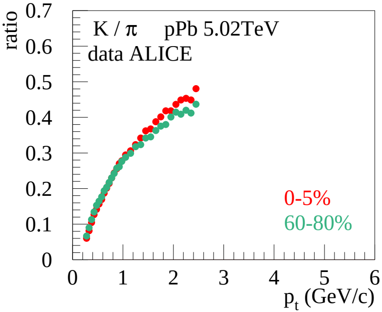

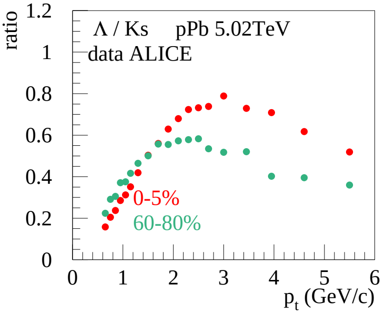

Significant variation of lambda/K – like in PbPb

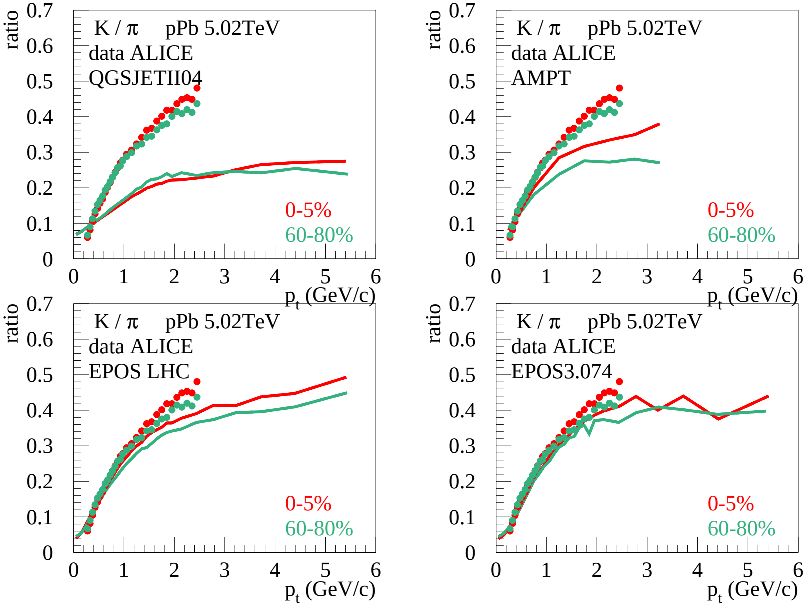

No multiplicity dependence (not trivial to get the peripheral right)

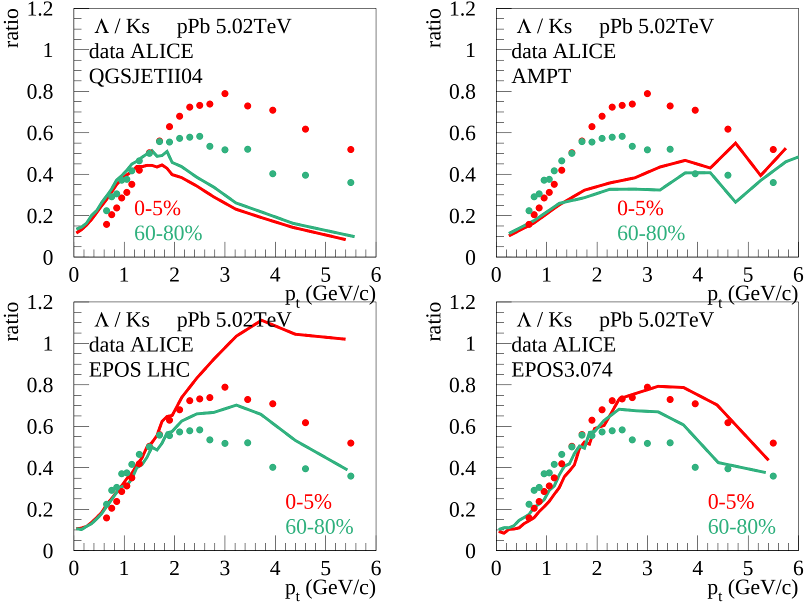

Significant multiplicity dependence. Flow helps

v_2 in PbPb

from central to peripheral

Changes smoothly towards peripheral

=> physics changes smoothly

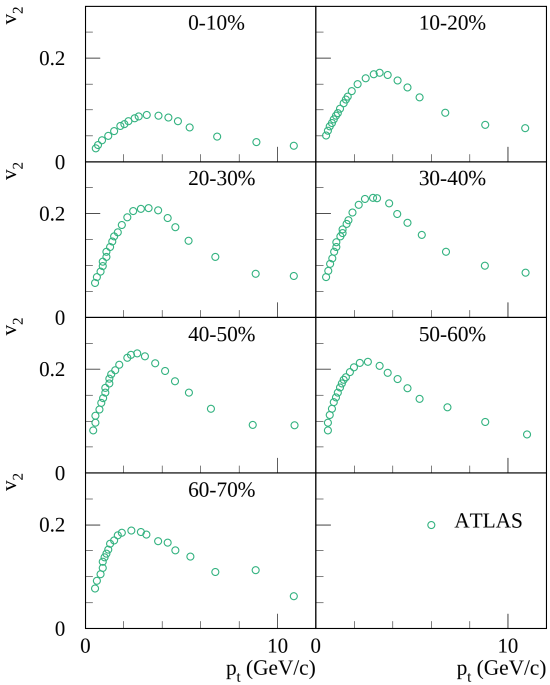

with EPOS simulations

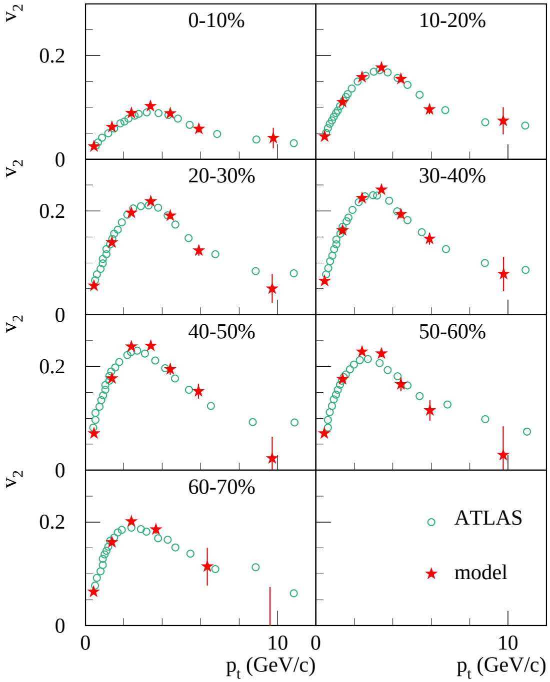

Flow is needed even for peripheral collisions!

“Ridges” in pA

ALICE, arXiv:1212.2001, arXiv:1307.3237

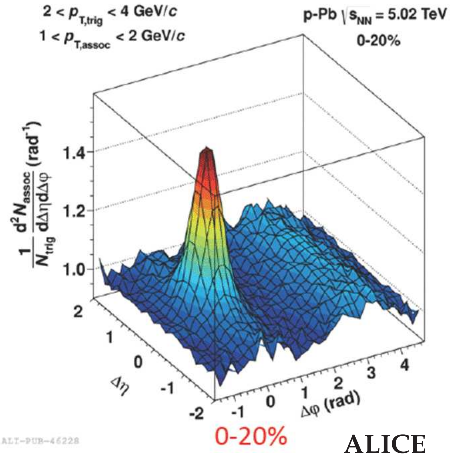

ALICE

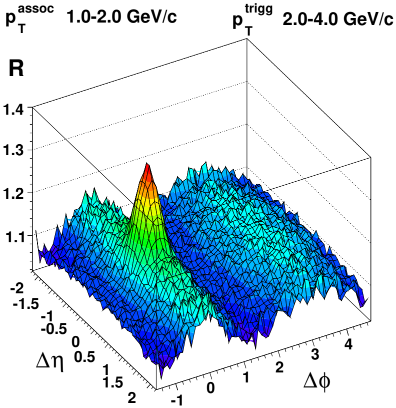

EPOS3.074

Central - peripheral (to get rid of jets)

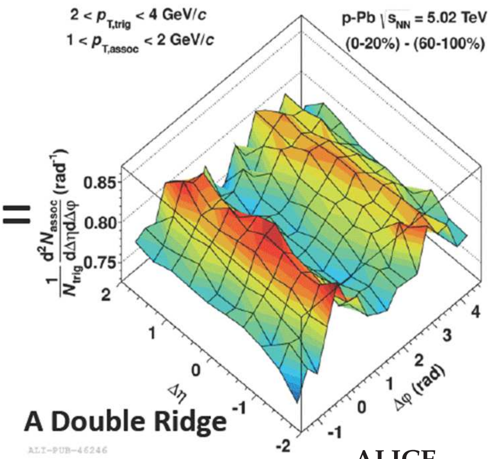

ALICE

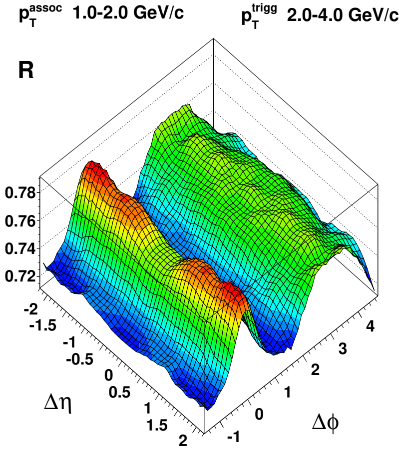

EPOS3.074

Identified particle v2

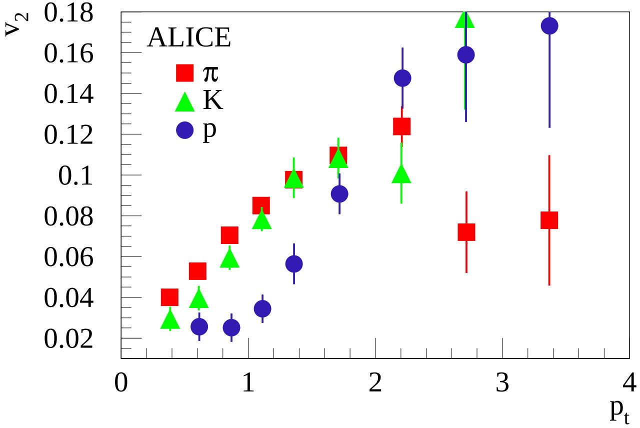

mass splitting, as in PbPb !!!

pPb in EPOS3:

Pomerons (number and positions)
characterize geometry (P. number $\propto$ multiplicity)

random
azimuthal
asymmetry
=>
asymmetric flow
seen at higher pt for
heavier ptls

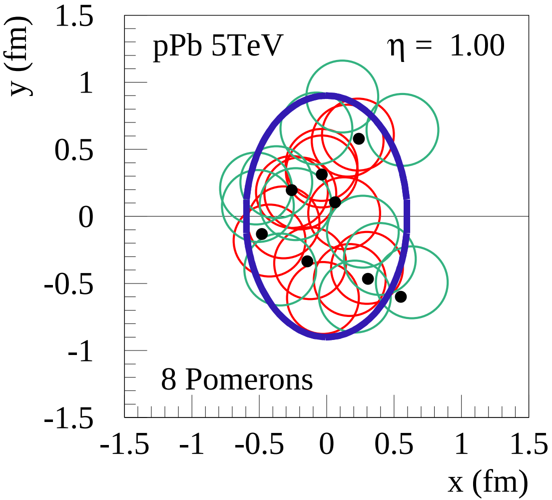

v2 for ß, K, p clearly differ

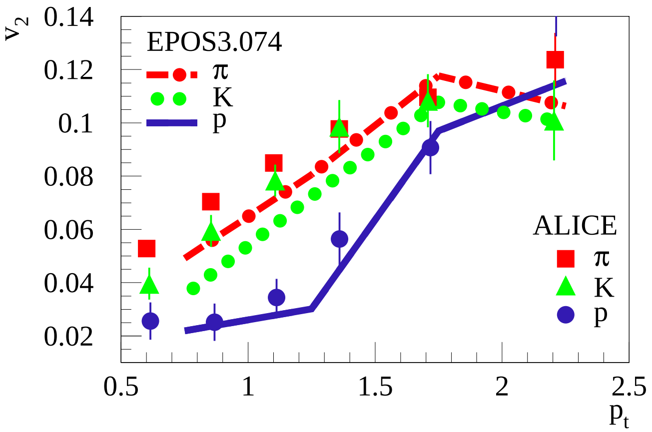

mass splitting, due to flow

7 Recent developments

(Saturation, strangeness and charm enhancement with multiplicity)

Reminder :

$$\sigma^{\mathrm{tot}} = \sum_{\mathrm{cut\,P}} \int \sum_{\mathrm{uncut\,P}} \int$$

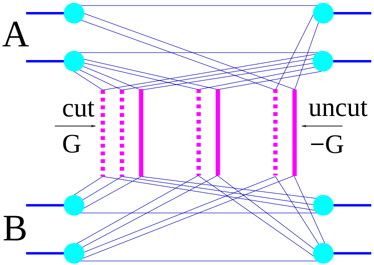

$$d\sigma_{\mathrm{exclusive}}$$

=

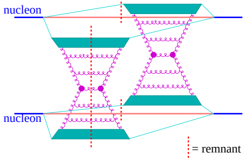

parton ladders

=> kinky strings

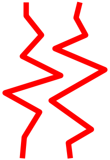

Non-linear effects

Computing the expressions G for single Pomerons:
A cutoff Q_0 is needed (for the DGLAP integrals).

Taking Q_0 constant leads to a power law increase of cross sections vs energy (=> wrong)

because non-linear effects like gluon fusion are not taken into account

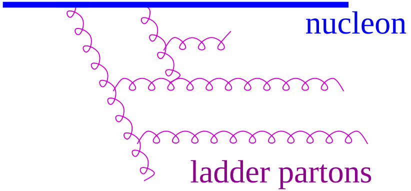

Solution: Instead of a constant Q_0, use a dynamical saturation scale for each Pomeron:

$$Q_s = Q_s(N_{I\!P}, s_{I\!P})$$

with

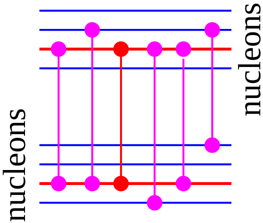

$N_{I\!P}$ = number of Pomerons connected to a given Pomeron (whose probability distribution depends on Q_s)

$s_{I\!P}$ = energy of considered Pomeron

We get $Q_s(N_{\mathbb{P}}, s_{\mathbb{P}})$ from fitting

- □ the energy dependence of elementary quantities (σ_{tot}, σ_{el}, σ_{SD}, $dn^{\mathrm{ch}}/d\eta(0)$) for pp
- □ the multiplicity dependence of dn^{π}/dp_t at large p_t for pp at 7 TeV

We find

$$\boldsymbol{Q_s \propto \sqrt{N_{\mathbb{P}}} \times (s_{\mathbb{P}})^{0.30}}$$

CGC for AA:

$$Q_s \propto N_{\mathrm{part}} \times (1/x)^{0.30}$$

Parton distributions

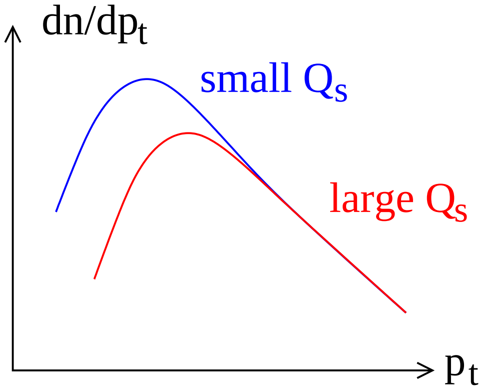

Increasing multiplicity

=> increasing $N_{\mathbf{Pom}}$

=> Increasing Q_s

=> harder Pomerons

=> harder strings

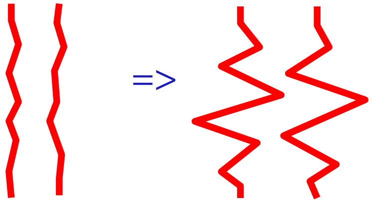

=> more high pt particles

=> Strong increase of $\langle p_t \rangle$ with multiplicity

These saturation effects concern the corona !

What about multiplicity dependence of core-corona separation ?

- **First check particle ratios**
  (core-corona)
- **Then mean pt vs multiplicity**
  (core-corona+saturation)

We compare simulations to ALICE data

Particle ratios to pions vs $\left\langle \frac{dn_{ch}}{d\eta}(0) \right\rangle$

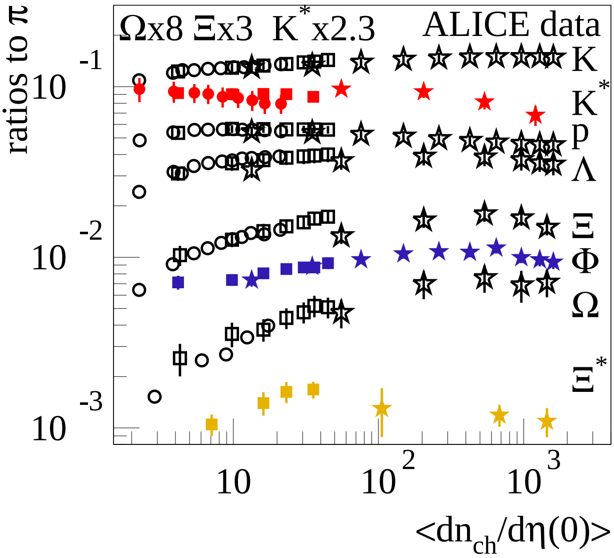

circles = pp (7TeV)

squares = pPb (5TeV)

stars = PbPb (2.76TeV)

Refs: next slide

Mean p_t vs $\left\langle \frac{dn_{ch}}{d\eta}(0) \right\rangle$

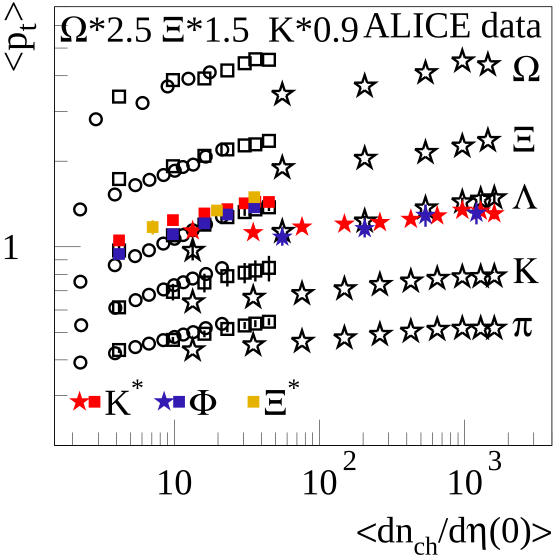

circles = pp (7TeV)

squares = pPb (5TeV)

stars = PbPb (2.76TeV)

Data partly collected by A. G. Knospe

Refs:
<dNch/deta> in Pb+Pb: Phys. Rev. Lett. 106 032301 (2011)
pi+-, K+-, and (anti)protons in Pb+Pb: Phys. Rev. C 88 044910 (2013)
Lambda in Pb+Pb: Phys. Rev. Lett. 111 222301 (2013)
Xi- and Omega in p+Pb: Phys. Lett. B 758 389-401 (2016)
pi+-, K+-, (anti)protons, and Lambda in p+Pb: Phys. Lett. B 728 25-38 (2014)
<dNch/deta> in p+Pb: Eur. Phys. J. C 76 245 (2016)
Xi- and Omega in p+Pb: Phys. Lett. B 758 389-401 (2016)
<dNch/deta> in p+p 7 TeV: Eur. Phys. J. C 68 345-354 (2010)
pi+-, K+-, and (anti)protons in p+p 7 TeV: Eur. Phys. J. C 75 226 (2015)
Xi- and Omega in p+p 7 TeV: Phys. Lett. B 712 309 (2012)
and data points from Rafael Derradi de Souza, SQM2016

D or J/Ψ multiplicity vs $\frac{dn_{ch}}{d\eta}(0)$ in pp

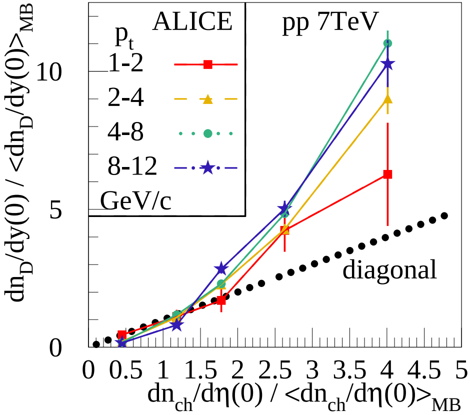

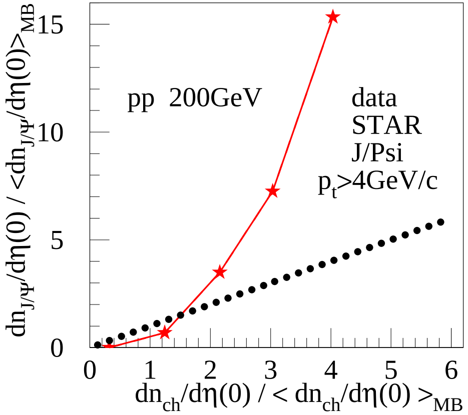

ALICE JHEP 09 (2015) 148, arXiv:1505.00664v1

STAR, shown at MPI2016

strongly nonlinear increase

Core-corona picture in EPOS

Gribov-Regge approach => (Many) kinky strings
=> core/corona separation (based on string segments)

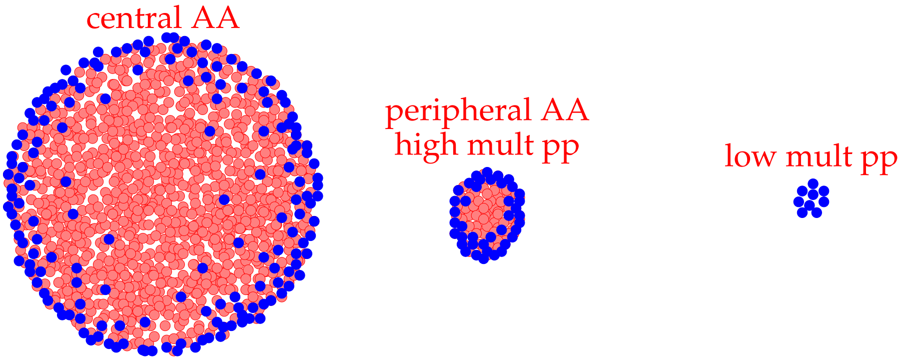

core => hydro => statistical decay ($\mu = 0$)
corona => string decay

Pion yields: core / corona contribution

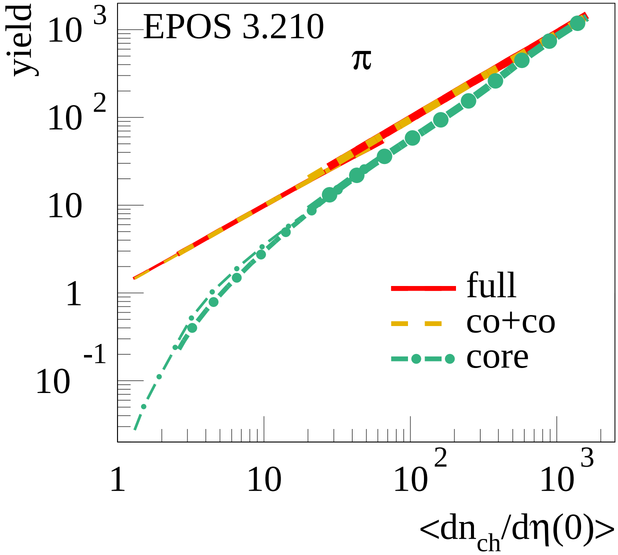

thick lines

= pp (7TeV)

thin lines
= pPb (5TeV)

hc = hadronic cascade

(UrQMD)

Proton to pion ratio

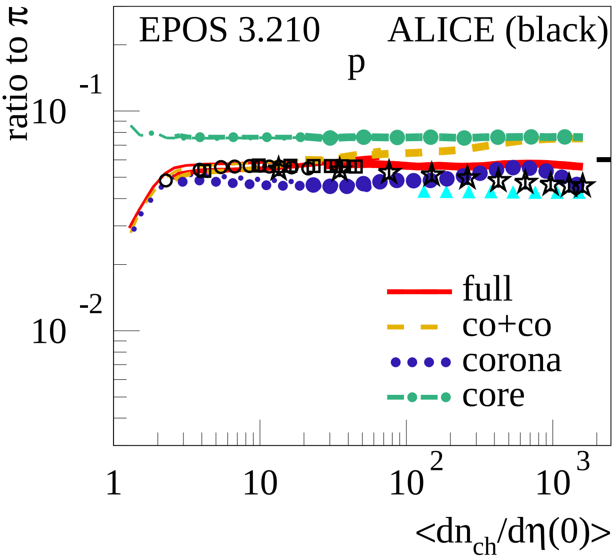

core hadronization:
$T = 164\,\mathrm{MeV},\ \mu_B = 0$

statistical model fit
(horizontal black line)
A. Andronic et al.,
arXiv:1611.01347
$T = 156.5\,\mathrm{MeV}, \mu_B = 0.7\,\mathrm{MeV}$

thick lines = pp (7TeV)
thin lines = pPb (5TeV)

circles = pp (7TeV)
squares = pPb (5TeV)
stars = PbPb (2.76TeV)

Omega to pion ratio

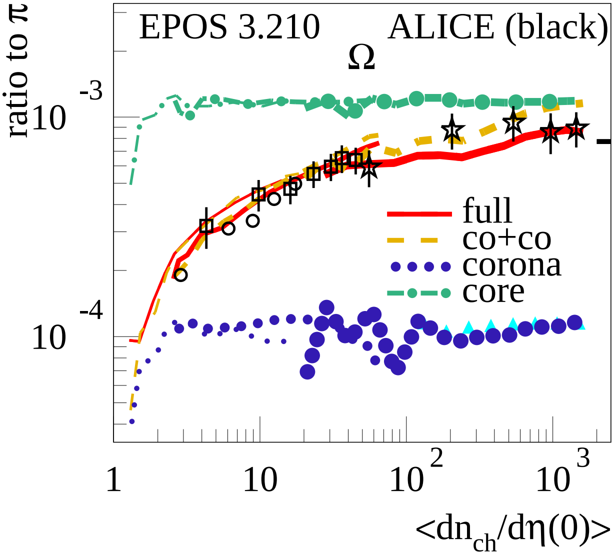

thick lines = pp (7TeV)
thin lines = pPb (5TeV)

circles = pp (7TeV)
squares = pPb (5TeV)
stars = PbPb (2.76TeV)

Kaon to pion ratio

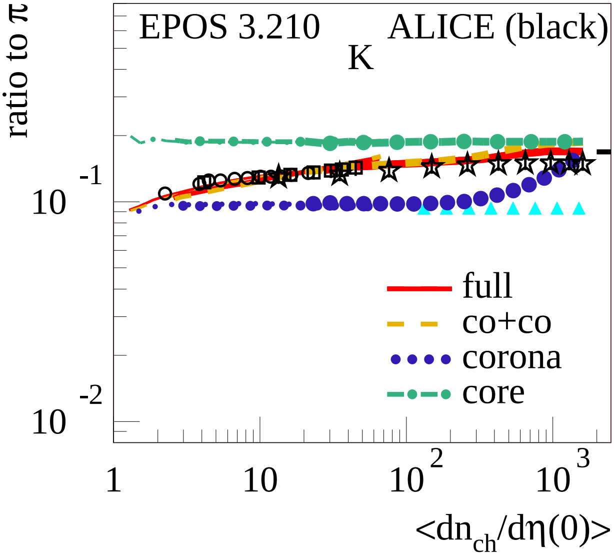

thick lines = pp (7TeV)
thin lines = pPb (5TeV)

circles = pp (7TeV)
squares = pPb (5TeV)
stars = PbPb (2.76TeV)

Lambda to pion ratio

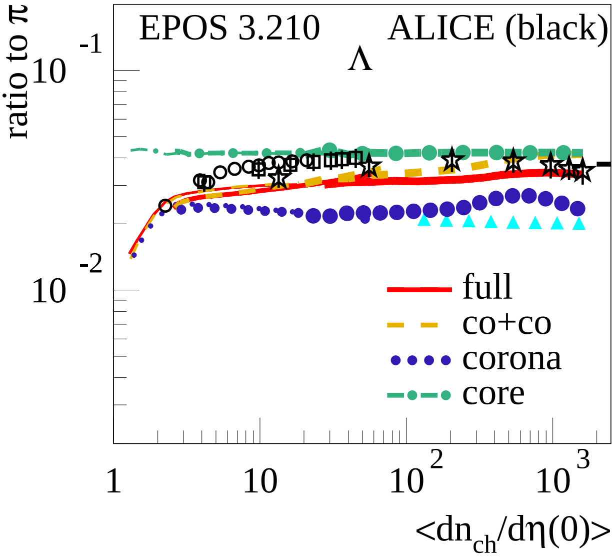

thick lines = pp (7TeV)
thin lines = pPb (5TeV)

circles = pp (7TeV)
squares = pPb (5TeV)
stars = PbPb (2.76TeV)

Xi to pion ratio

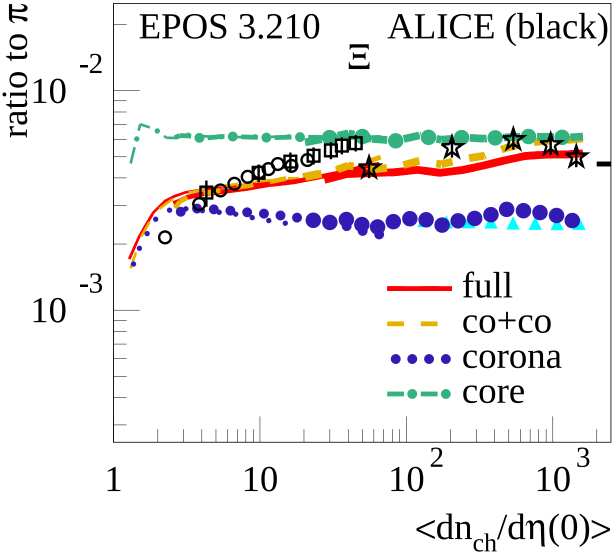

thick lines = pp (7TeV)
thin lines = pPb (5TeV)

circles = pp (7TeV)
squares = pPb (5TeV)
stars = PbPb (2.76TeV)

Ratios h/π for $h = p, K, \Lambda, \Xi, \Omega$ vs $\left\langle \frac{dn}{d\eta}(0) \right\rangle$:

Core and corona contributions separately roughly constant

Difference (core - corona) increasing for $p \to K \to$

=> inceasing slope
(not enough for Ξ, Ω)

Average p_t of protons

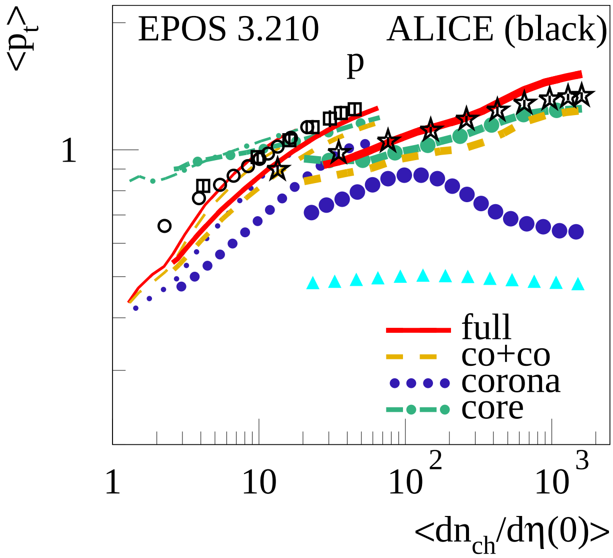

thin lines = pp (7TeV)
intermediate lines = pPb (5TeV)
thick lines = PbPb (2.76TeVVV)
circles = pp (7TeV)
squares = pPb (5TeV)
stars = PbPb (2.76TeV)

Average p_t of Omegas

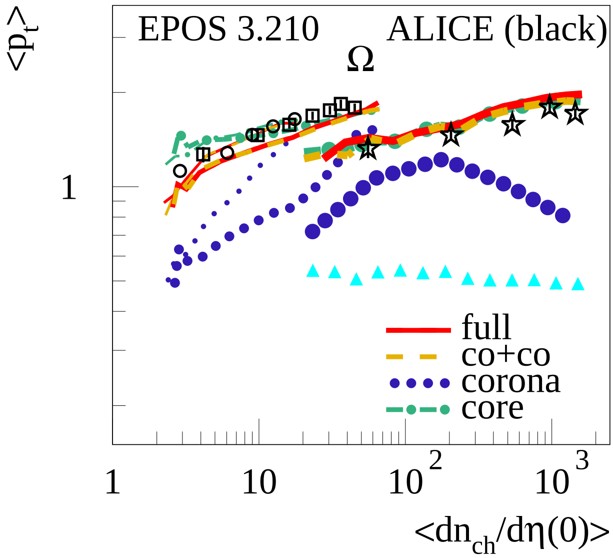

thin lines = pp (7TeV)
intermediate lines = pPb (5TeV)
thick lines = PbPb (2.76TeVVV)
circles = pp (7TeV)
squares = pPb (5TeV)
stars = PbPb (2.76TeV)

Average p_t of lambdas

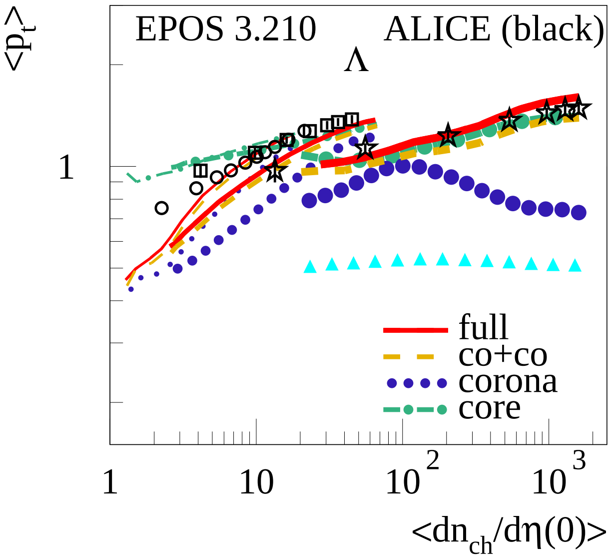

thin lines = pp (7TeV)
intermediate lines = pPb (5TeV)
thick lines = PbPb (2.76TeVVV)
circles = pp (7TeV)
squares = pPb (5TeV)
stars = PbPb (2.76TeV)

Average p_t of kaons

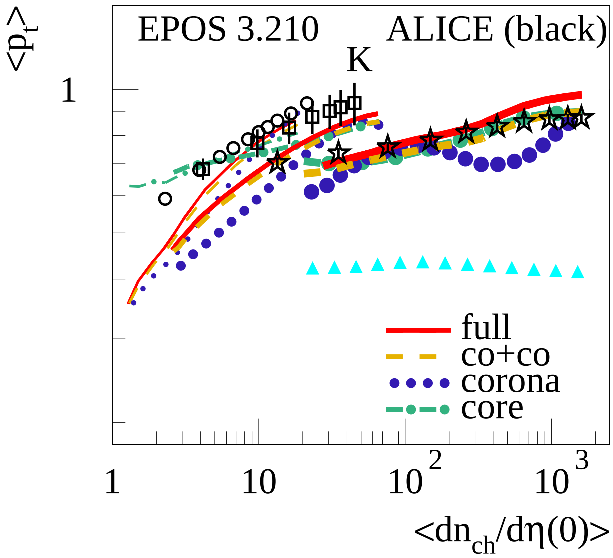

thin lines = pp (7TeV)
intermediate lines = pPb (5TeV)
thick lines = PbPb (2.76TeVVV)
circles = pp (7TeV)
squares = pPb (5TeV)
stars = PbPb (2.76TeV)

Average p_t of $K, p, \Lambda, \Xi, \Omega$ vs $\left\langle \frac{dn}{d\eta}(0) \right\rangle$:

Moderate increase of core contribution
(same for pp and pPb, similar to PbPb)

Strong increase of corona contribution
(stronger for pp than for pPb, much stronger than for PbPb)

Slope(pp) > slope(pPb) >> slope(PbPb)

K, π : pp-pPb splitting

The multiplicity dependence of the corona contribution is crucial

Very closely related to this discussion:

The multiplicity dependence of charm production (D, J/Ψ,...)

The "ultimate tool" to test multiple scattering (and the implementation of Q_S)

EPOS 3 compared to ALICE data

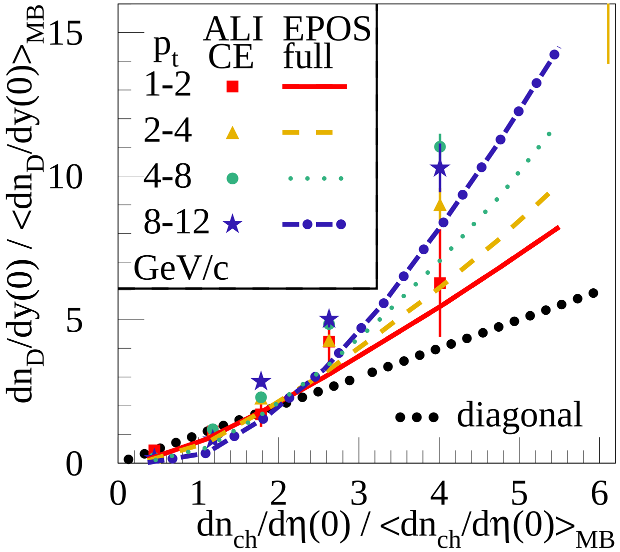

hadronic cascade on/off has no effect

hydro on/off has small effect

EPOS 3 compared to RHIC data

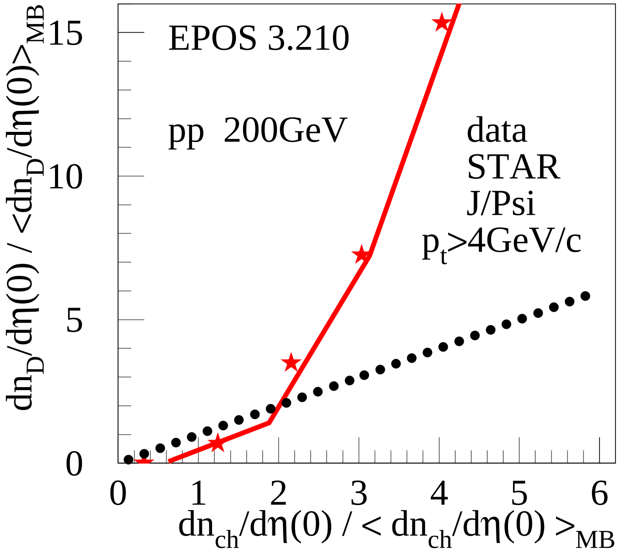

Calculations:
D mesons

Data: J/Ψ

Increase stronger than at LHC

Multiplicity at FB rapidity (LHC)

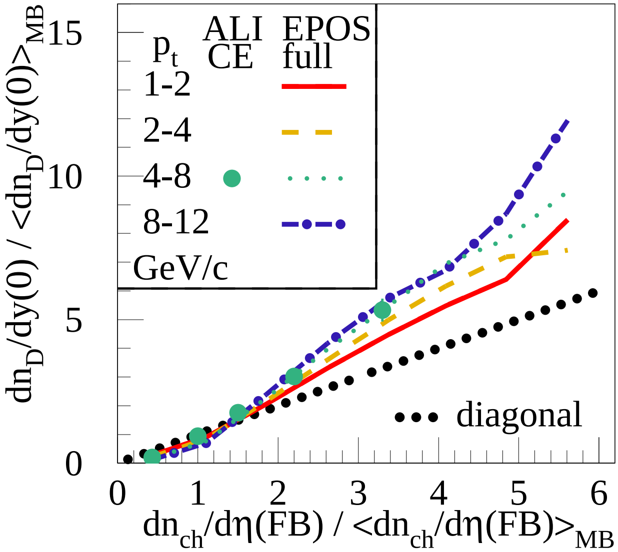

FB = forward/backward rapidity range:

$$2.8 < \eta < 5.1$$
and
$$-3.7 < \eta < -1.7$$

Smaller increase

Low multi-plicity (LM)

Small N_{Pom}

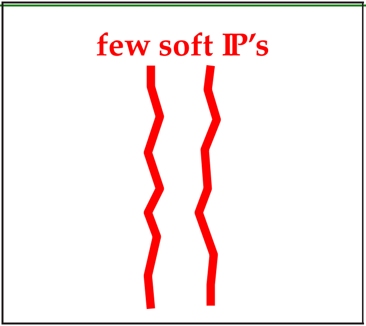

$\mathbb{P}$ = Pomeron

"Hardness" increases with N_{Pom}

(larger Q_s)

High multi-plicity (HM)

many hard $\mathbb{P}$'s on avg

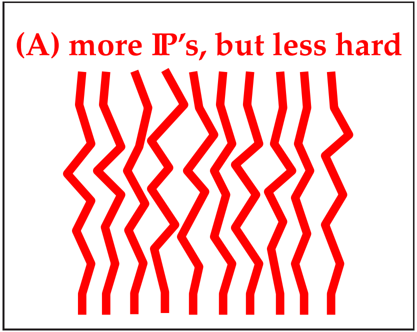

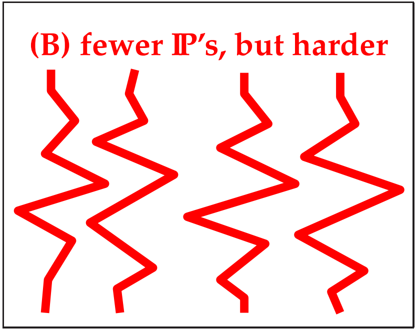

LM $\rightarrow$ HM:

Pomerons get harder (larger Q_s)

$\rightarrow$ favors high pt or large masse production

in particular due to case B (fewer IP's, but harder)
for highest pt bins !

Bigger effect at RHIC due to much narrower N_{Pom} distribution (harder IP's are needed)

Smaller effect for $\frac{dn}{d\eta}(FB)$ as multipl. variable

(case B is replaced by case C: fewer IP's, but more covering the FB rapidity range)